

The Science of Nuclear Energy: Fission and Fusion

Robert J. Goldston

Dedicated to my wife Ruth, my sons Josh and Jake,
my daughter-in-law Katie, and especially to my grandsons, Max and Ezra,
who will have to live with all the decisions we make and do not make.

Preface



Lise Meitner, circa 1930

At this point we both sat down on a tree trunk, and started to calculate on scraps of paper. ... When the two drops separated they would be driven apart by their mutual electric repulsion and would acquire a very large energy, about 200 MeV in all; where would that come from? Fortunately Lise Meitner remembered how to compute the masses of nuclei from the so-called packing fraction formula, and in that way she worked out that the two nuclei formed by the division of a uranium nucleus would be lighter than the original uranium nucleus by about one-fifth the mass of a proton. Now whenever mass disappears energy is created, according to Einstein's formula $E = mc^2$, and one-fifth of a proton mass was just equivalent to 200 MeV. So here was the source for that energy; it all fitted!

Otto Frisch

The science of nuclear energy can be viewed from two different perspectives, and we will explore both of them: the beauty and grace of the underlying science, and the scientific underpinnings of the implications for society

of the resulting technology. This dual perspective is unusual for a textbook like this.

First, the underlying science is beautiful. We will sit on the tree trunk with refugee Lise Meitner and her nephew Otto Frisch in the snowy woods in Sweden in December 1938. We will share their “Aha!” experience as we understand when they find – and then explain to the world – that nuclear fission has been observed for the first time. The measurements had been taken on Meitner’s insistence in the laboratory in Germany she had been forced to abandon in July, and she was the first to interpret them. We will also follow Enrico Fermi in discovering the subtle – but ultimately simple and beautiful – physics of neutron thermalization and diffusion, required to design a self-sustaining chain reaction. Amazingly, he achieved this goal only four years later, in December 1942.

We will also study the new science of plasma physics, the physics of ionized gases, developed in large part to make fusion energy possible. We will have eyewitness access to the development of the experimental and theoretical understanding of the macroscopic stability limits of fusion plasmas, of the micro-scale turbulent processes that govern how heat is transported across magnetic fields in macroscopically stable plasmas, and the physics that determines the narrow layer through which heat escapes from a plasma.

Throughout this book you will be sharpening, deepening, and extending your understanding of concepts that are useful in many areas of the physical sciences and technology. The midterm projects include fun options to develop a simple, but powerful, Monte Carlo computational simulation to test some of the analytic theories we will develop.

Looked at from the second perspective, nuclear energy is a low-carbon source of electrical energy and process heat, and so can contribute to the advancement of global development without adding to climate change. However, it also brings with it risks associated with safety, waste and nuclear proliferation. We will stand next to the operators of the Fukushima Daiichi nuclear power station and understand their actions as they carefully switch on and off the emergency core cooling system to control the cool-down of Unit 1 – until the tsunami hits and they lose control. We will also probe the aftermath, and the root causes of the accident. We will see why it has been so hard to open a geological repository for civilian nuclear waste in the U.S. or elsewhere. We will also sit with U.S. Secretary of Energy Ernie Moniz and understand as he negotiates the scientific aspects of the recent Iran agreement with his counterpart, Ali Akbar Salehi. Finally, we will peek under the hood of future technologies for nuclear fission.

We will learn about the great successes and tough challenges facing the

development of practical fusion energy. We will talk about the scientific progress and prospects for the massive collaborative international fusion energy experiment in France, ITER, which involves China, the European Union, India, Japan, Russia, South Korea, and the U.S. We also look at the scientific issues that remain before fusion can be commercialized.

With the understanding we will develop, you will be able to form your own considered opinions about the important policy issues surrounding nuclear energy. Society grants scientists the privilege and great pleasure of studying and learning; it is only fair that we give back to society our best, honest understanding of the societal issues on which we are well informed.

What background do you need to benefit from this book? The science and mathematics we use should be familiar to third-year university students in the physical sciences and engineering. However very well prepared first-year students and interested fourth-year students, also graduate students, have benefited from this course. We use vector calculus extensively, for example Gauss's and Stokes's theorems, and we will solve together the partial differential heat equation, which arises in a number of contexts. We will use elementary thermodynamics and quantum mechanics. We will present basic nuclear physics in the context of non-relativistic quantum mechanics.

Scientists and engineers from other fields of research who want to understand the ideas behind nuclear energy may find that this book gives them a useful perspective. It should be particularly helpful to those interested in arms control and nuclear non-proliferation, which we cover in some depth. Policymakers with a technical bent may not want to follow all of the derivations (nor do all of the exercises!), but they may be able to glean enough useful technical perspective on key issues to orient themselves, and to ask the right questions of experts.

You can use this book as an introduction to the science of nuclear fission by reading chapter 1 and all of part I. Section 1.2 will give you a helpful self-contained perspective on fusion energy. If instead you are looking for an introduction to nuclear fusion science, you can read all of chapter 1, getting a quick perspective on fission, sections 2.1 - 2.3 to understand reaction rates, 4.1 - 4.5 to understand the diffusion equation, and all of part II.

At Princeton we have 12-week semesters, and I have taught the course associated with this book in two 80 minute sessions per week, plus one evening precept for Q&A. Chapter 1 is longer than most; I don't cover section 1.2.3 in class, since these topics are covered more deeply later. It is included here to provide an overview of fusion for those primarily interested in fission. Chapters 3, 4, 5, 6 and 10 have about twice the content of the

others. These longer chapters each form a logical unit, and are covered in two lectures each. I have used the last lecture period for student presentations.

A comment about the questions that appear in the text: I find that it is a good idea to break up lectures every ~ 15 minutes with Q&A following the concept of “think-pair-share.” Groucho Marx’s duck from “You Bet Your Life” comes down on one of my slides and presents the students with a question. They gather together in small groups and work on answers to share with the whole class. Meanwhile I get a few sips of soda. Then we have a lively discussion for a few minutes. The questions every few pages in the text are an attempt at reproducing the spirit of this in book form.

All units are SI, unless otherwise specified with a subscript. We frequently use a unit of energy that is common in both fission and fusion research, the “electron volt,” or eV. 1 eV equals the energy that an electron gains when it is accelerated across a potential difference of 1 V in free space, e Joules. Here e is the magnitude of the electron charge in Coulombs, $1.602 \cdot 10^{-19} C$. Thus energy expressed in eV, E_{eV} , and energy expressed in the SI energy unit, Joules, E , are related by $E = eE_{eV} = 1.6021 \cdot 10^{-19} E_{eV}$.

I would like to thank all of the clever and energetic students who have taken this course over the last eight years, asked great questions that helped deepen my understanding and clarify my explanations, completed innumerable exercises, some of which really needed the clarification that is included here, and wrote overwhelmingly thoughtful essays. I would also like to thank my dedicated Assistants in Instruction, Tyler Abrams, Abraham Fetterman, Laura Berzak Hopkins, Sébastien Philippe, Jacob Schwartz and David Turnbull, who helped with the teaching, with the precepts, and with developing and grading the exercises.

I would particularly like to thank Prof. Alex Glaser, with whom I shared this course for the first three years, and from whom I have learned a great deal about nuclear fission energy and nuclear proliferation.

Rob Goldston
November 1, 2017



Groucho Marx’s Duck

Contents

Preface	<i>page</i> iii
1 Fission and Fusion	1
1.1 Fission	3
1.1.1 Self-sustaining fission reactions	3
1.1.2 Safety, waste, nuclear proliferation	9
1.1.3 Past may be prologue, but what is it telling us?	16
1.1.4 Prospects	19
1.2 Fusion	20
1.2.1 Self-sustaining fusion reactions	20
1.2.2 Why fusion?	27
1.2.3 Scientific progress	30
1.2.4 Prospects	47
Review	48
Resources	48
Exercises	49
 PART ONE FISSION	51
2 Neutron Interactions with Matter	53
2.1 Cross-sections	54
2.2 Beam attenuation and mean free path	55
2.3 Reaction rates	56
2.4 Elements of non-relativistic quantum mechanics	57
2.5 Elements of nuclear physics	59
2.6 Fission	67
2.7 Radiative Absorption	72
2.8 Elastic and Inelastic Scattering	75
2.9 Try This at Home	77
Review	78
Resources	78
Exercises	79
3 Neutron Energy Distribution	81
3.1 Energy change in elastic scattering	82
3.2 Logarithmic energy decrement	87
3.3 Slowing Down Time	90
3.4 Neutron flux vs. energy, $\phi(E)$, and vs. lethargy, $\phi(u)$	91
3.5 Fast energy region $\phi_F(E)$	93

	<i>Contents</i>	ix
3.6	Intermediate energy region $\phi_I(E)$	100
3.7	Thermal energy region $\phi_T(E)$	107
3.8	Visualizing the four-factor formula	113
3.9	Fast reactors	114
	Review	119
	Resources	119
	Exercises	119
4	Neutron Spatial Distribution	121
4.1	Neutrons as a one-speed gas	122
4.2	The one-speed neutron diffusion equation	125
4.3	1-D δ -function initial condition without boundaries	129
4.4	Statistical interpretation of the neutron diffusion equation	130
4.5	1-D δ -function steady source without boundaries	132
4.6	Boundary conditions	134
4.7	Bounded Systems	137
4.8	Non-leakage probability	147
4.9	Spatial diffusion in thermal reactors	148
4.10	Spatial diffusion in fast reactors	150
4.11	Integrated numerical modeling	151
	Review	151
	Resources	151
	Exercises	151
5	Safety	152
5.1	The neutron “kinetic” equation	152
5.2	Including delayed neutrons	152
5.3	Consequences for reactor stability	152
5.4	Behavior over longer time scales	152
5.5	Chernobyl	152
5.6	Fukushima	152
5.7	Regulatory response	152
5.8	Effects of radiation on human health	152
5.9	Impacts of Chernobyl and Fukushima	152
	Review	152
	Resources	152
	Exercises	152
6	The Nuclear Fuel Cycle	153
6.1	Mining	153
6.2	Enrichment	153
6.3	Burnup	153

6.4	Interim storage	153
6.5	Geological repository	153
6.6	Reprocessing for thermal reactors	153
6.7	Fast reactors and reprocessing	153
	Review	153
	Resources	153
	Exercises	153
7	Nuclear Weapons and Nuclear Proliferation	154
7.1	How nuclear weapons work	155
7.2	History of nuclear proliferation	155
7.3	Proliferation risks going forward	155
7.4	Means to manage risks	155
	Review	155
	Resources	155
	Exercises	155
8	Advanced Reactors	156
8.1	Generation III and III+ reactors	156
8.2	Generation IV reactors	156
8.3	Thorium cycle	156
8.4	Breed and burn in Place	156
	Review	156
	Resources	156
	Exercises	156
	PART TWO FUSION	157
9	Power and Particle Balance	159
9.1	Fusion reactions	159
9.2	Plasma heating	159
9.3	Heat loss	159
9.4	Energy gain!	159
9.5	Particle balance	159
	Review	159
	Resources	159
	Exercises	159
10	Particle Motion	160
10.1	Uniform electric and magnetic fields	160
10.2	Curved magnetic field	160
10.3	Perpendicular gradient in magnetic field strength	160

	<i>Contents</i>	xi
10.4	Parallel gradient in magnetic field strength	160
10.5	Drifts in toroidal magnetic field	160
10.6	Passing particle orbits	160
10.7	Trapped particle orbits	160
10.8	Bootstrap current	160
	Review	160
	Resources	160
	Exercises	160
11	Plasmas as Fluids	161
11.1	Plasmas as fluids?	161
11.2	Equilibrium in a cylinder	161
11.3	Plasma control	161
11.4	Stellarators	161
11.5	2-fluid model and parallel force balance	161
	Review	161
	Resources	161
	Exercises	161
12	Macroscopic Stability	162
12.1	Ideal MHD stability	162
12.2	Interchange and ballooning modes	162
12.3	Kink modes	162
12.4	Plasma shaping	162
12.5	Stellarators	162
	Review	162
	Resources	162
	Exercises	162
13	Collisions and their Effects	163
13.1	Coulomb collisions	163
13.2	Debye shielding	163
13.3	Small-angle scattering	163
13.4	Collisional cross-field transport	163
13.5	Other collisional effects	163
	Review	163
	Resources	163
	Exercises	163
14	Turbulent Transport	164
14.1	Bohm and GyroBohm	164
14.2	Turbulence and flows – simulation	164
14.3	Turbulence and flows – measurement	164

14.4	Transport barriers	164
14.5	Global scaling	164
	Review	164
	Resources	164
	Exercises	164
15	Divertors, Scrape-off layers, and Plasma-Facing Components	165
15.1	Divertors	165
15.2	Scrape-off layers	165
15.3	Transient events	165
15.4	Plasma-facing components	165
	Review	165
	Resources	165
	Exercises	165
16	Neutron Interactive Materials, Blankets; Safety, Waste and Proliferation	166
16.1	Neutron interactive materials	166
16.2	Blanket designs	166
16.3	Safety	166
16.4	Waste	166
16.5	Nuclear proliferation	166
	Review	166
	Resources	166
	Exercises	166
17	Inertial Fusion Energy	167
17.1	Vision and status	167
17.2	Batch burn vs. hot-spot ignition	167
17.3	Drivers	167
17.4	Targets and chambers	167
	Review	167
	Resources	167
	Exercises	167
18	Power Plant Concepts, Development Path and Deployment	168
18.1	Power plant concepts	168
18.2	Development path	168
18.3	Deployment	168
	Review	168
	Resources	168

<i>Contents</i>	xiii
Exercises	168

Chapter 1

Fission and Fusion



what's past is prologue; what to come,
In yours and my discharge

The Tempest, William Shakespeare

In this opening chapter we will explore some of the general features of fission and fusion. We will first address the basic physical requirements for sustainment of both reactions. Next we will take a first look at the societal issues that are driven by the underlying technologies of fission and fusion, and then we will review progress and prospects for each. All of this, of course, will be covered more thoroughly in the chapters that follow, but here we will get an overview, and develop a sense of what's to come.

As shown in figure 1.1, the mass-energy of most nuclei is 8 ± 1 MeV/nucleon below the mass-energy of the free nucleons, protons and neutrons, that came together to form them. This nuclear potential energy is the negative of the conventional “Curve of Binding Energy,” or “packing fraction” curve. It better expresses the analogy to the lower gravitational potential energy of a ball at the bottom of a well as compared with at the top. The nucleons have, in effect, “fallen” together, because the strong short-range nuclear force of attraction has overcome the average long-range mutual electrostatic repulsion, and created a deep potential well that contains the nucleons. The potential energy per nucleon is evidently lower near the bottom of the curve and if a group of nucleons move from either end towards the lowest point, their nuclear potential energy drops. This reduction in potential energy makes

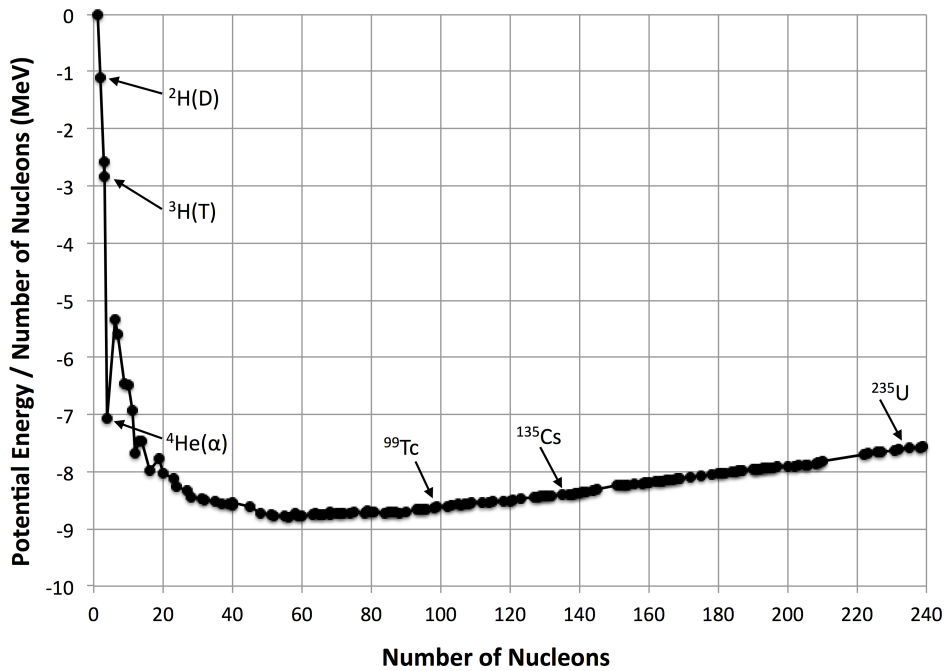


Figure 1.1 Curve of potential energy per nucleon. Average mass-energy (mc^2) per nucleon of selected isotopes less the average mass-energy per nucleon of the free protons and neutrons (~ 950 MeV each) from which they are formed. Some nuclei are tagged that participate in fusion (to the left) or fission (to the right) as reactants or products. When an energy is specified in eV, “electron volts,” the stated value, E_{eV} , is the electric potential difference, in volts, that would accelerate a stationary, singly charged particle such as an electron to the energy being specified. Stated in joules, this energy is eE_{eV} J.

energy available to take other forms, in particular the kinetic energy of the reaction products.

Warm-up Question: Why is the ^1H nucleus at zero potential energy?

Figure 1.1 shows that if a heavy nucleus, such as uranium, fissions into two nuclei averaging about half its weight, a bit less than 1 MeV per nucleon is freed up for a total of ~ 200 MeV. On the other hand, if we can arrange for two light nuclei to fuse together to form a heavier nucleus (helium looks like a particularly promising candidate) then something like 5 MeV is freed up per nucleon, for a total of ~ 20 MeV. *And so our story begins . . .*

1.1 Fission

1.1.1 Self-sustaining fission reactions

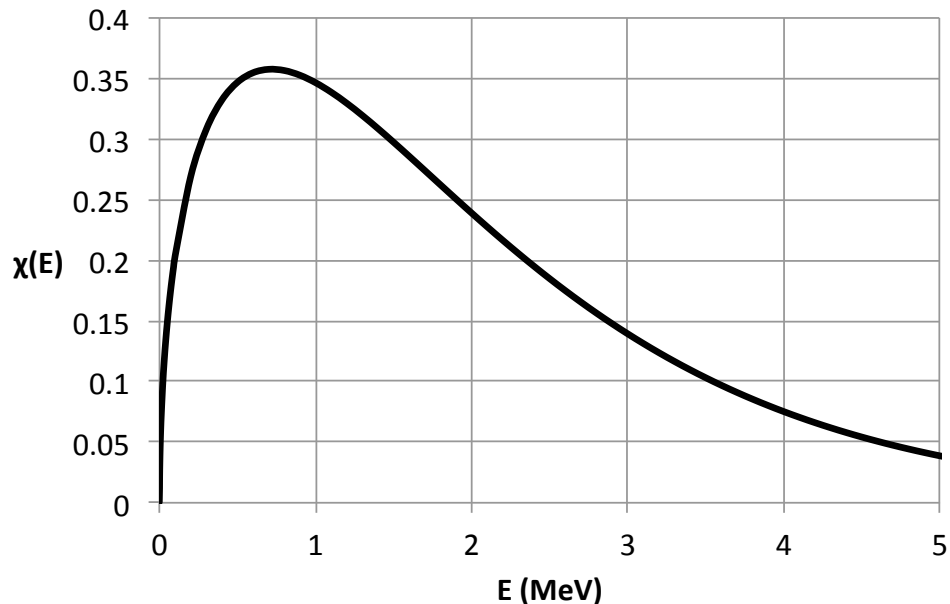


Figure 1.2 Probability distribution of neutrons produced by fission

Figure 1.2 shows the probability distribution of neutrons that emerge from fission of ^{235}U . Evidently neutrons boil out of the fission process with energies in the general range of the released binding energy per nucleon, but also below and significantly above. Note that the spectrum has been normalized such that $\int_0^\infty \chi(E)dE_{\text{MeV}} = 1$, where the subscript “MeV” indicates that E is measured in MeV. This means, for example, that about 1/3 of the neutrons are emitted with energies in the 1 MeV wide range from 0.5 MeV to 1.5 MeV, and about 1/2 of the neutrons are emitted in the 2 MeV wide range from 1 MeV to 3 MeV.

The speed of a non-relativistic neutron is $1.383 \cdot 10^7 \sqrt{E_{\text{MeV}}} \text{ m/sec}$. We will be studying neutrons up to at most 14.1 MeV, and since relativistic effects scale as $(v/c)^2$, we can safely treat neutrons as non-relativistic. Another way to see this is to note that the rest mass of the neutron is about 940 MeV, so we are making errors in the range of $10^{-3} - 10^{-2}$ by ignoring relativistic effects. The other simplifying approximations we will make to understand the basic physics will exceed this one.

While the neutrons from various fusion reactions are born at energies of up

to 14.1 MeV, and fission neutrons are born generally in the low MeV range, we will also be interested in the behavior of neutrons as they lose energy and ultimately thermalize with their surroundings. In addition we will be interested in hot fusion fuel in the ionized state, with electrons stripped from nuclei, called “plasma.” You should be familiar with the fact that the average kinetic energy of a molecule in a gas of temperature, T_K (temperature expressed in kelvins), is given by

$$\langle E \rangle = (3/2) kT_K = 1.5 \cdot 1.381 \cdot 10^{-23} T_K \quad (1.1)$$

This is $(1/2)kT_K$ for each of the three degrees of freedom of motion. In fusion plasma physics, we tend to subsume Boltzmann’s constant into the definition of temperature, expressing temperature, T , directly in energy units, joules, in our equations. We then proceed to *talk* about temperature in units of eVs, T_{eV} (temperature expressed in electron volts). Since T_{eV} is the electrical potential required to accelerate a unit charge to the energy under discussion, the temperature expressed in Joules that corresponds to T_{eV} is $T = eT_{eV}$, and the average particle kinetic energy equals $(3/2)eT_{eV}$. Now we can derive the relationship between T_{eV} and T_K :

$$\frac{3}{2}kT_K = \frac{3}{2}eT_{eV} \quad (1.2)$$

$$\frac{T_K}{T_{eV}} = \frac{e}{k} = \frac{1.602 \cdot 10^{-19}}{1.381 \cdot 10^{-23}} = 11,600 \quad (1.3)$$

It is instructive to survey some energies and temperatures we will be studying:

- Birth energy of neutrons from the ${}^2\text{H} + {}^3\text{H}$ (deuterium + tritium) reaction: $14.1 \text{ MeV} = 2.259 \cdot 10^{-12} \text{ J}$, $v_n = 5.193 \cdot 10^7 \text{ m/s}$.
- Average birth energy of neutrons from thermal fission of ${}^{238}\text{U}$: $2 \text{ MeV} = 3.204 \cdot 10^{-13} \text{ J}$, $v_n = 1.956 \cdot 10^7 \text{ m/s}$.
- Temperature of a fusion plasma: $10 \text{ keV} = 116 \text{ M}^\circ \text{ K}$. Average ion or electron energy = $15 \text{ keV} = 2.403 \cdot 10^{-15} \text{ J}$.
- Temperature of a weakly ionized plasma: $1 \text{ eV} = 11,600^\circ \text{ K}$. Average ion or electron energy = $1.5 \text{ eV} = 2.403 \cdot 10^{-19} \text{ J}$.
- Room temperature: $293^\circ \text{ K} = 0.0253 \text{ eV}$, $v_n = 2200 \text{ m/s}$.

Now we are prepared to consider how to sustain a fission reaction in uranium. By definition a uranium nucleus contains 92 protons. The two predominant isotopes found in nature are ${}^{238}\text{U}$ and ${}^{235}\text{U}$, which have abundances of 99.29% and 0.71% respectively, by mass. A nucleus of ${}^{238}\text{U}$ contains 146 neutrons, while a nucleus of ${}^{235}\text{U}$ contains, evidently, 143. As we will

understand in Chapter 2, ^{235}U fissions nicely when struck by a neutron of any energy, but especially when struck by a thermal or near-thermal neutron. ^{238}U , on the other hand, only fissions with significant probability when struck by neutrons above about 1.4 MeV, and then the reaction probability is only about 40% of that of ^{235}U . The good news is that when either of them fission, while they consume a neutron, they produce, on average, 2 – 3 neutrons.

This could also be considered the bad news. When neutron emission during fission was discovered in 1939, soon after fission itself was discovered, some physicists deduced immediately that an explosive chain reaction, on an energy scale $\sim 10^6$ times greater than that of chemical explosions, might be possible. Nuclear energies are measured in MeV, chemical energies in eV. Nuclear fission disappeared from open physics journals, but not before the critical measurement of neutron production was published.

Question: What effects, both positive and negative, could this silence have had on the Axis powers' efforts to develop a nuclear weapon? On balance, was it a good idea?

To get a first look at how much the neutron population in a fission reactor changes from one generation to the next, consider neutron balance in a very simple situation. Imagine that there are neutrons present at only one specified energy in a large mass of pure uranium, containing a specified percentage of ^{235}U . In this situation the fraction of this first generation of neutrons that drive fission, rather than become absorbed without fission, is defined by the underlying nuclear physics. A fission event provides a gain of about 2.5:1. (In general a little higher for energetic neutrons than for thermal ones, and a little higher for plutonium than for uranium.) If the fraction of fission events divided by all events, fission plus absorption without fission, is greater than $\sim 40\%$, then the neutron gain at the specified energy, $\eta(E)$, is greater than unity, and sustained fission might be possible. Not surprisingly, the neutron gain will always be higher with uranium more enriched in ^{235}U , as can be seen in figure 1.3.

To get more insight from this figure, we need to recognize that in the real world there will always be other losses from the neutron population than fission-less absorption by uranium nuclei. Most prominently, the coolant that is needed in a real power plant will absorb neutrons, as we will discuss in Chapters 2 and 3, and some neutrons will escape from the reactor, as discussed in Chapter 4, so $\eta(E) > 1$ represents a bare minimum requirement.

Self-sustainment in the range of 100's of keV requires fuel enriched to about 20%. This is the energy range of "fast reactors", FRs, so named be-

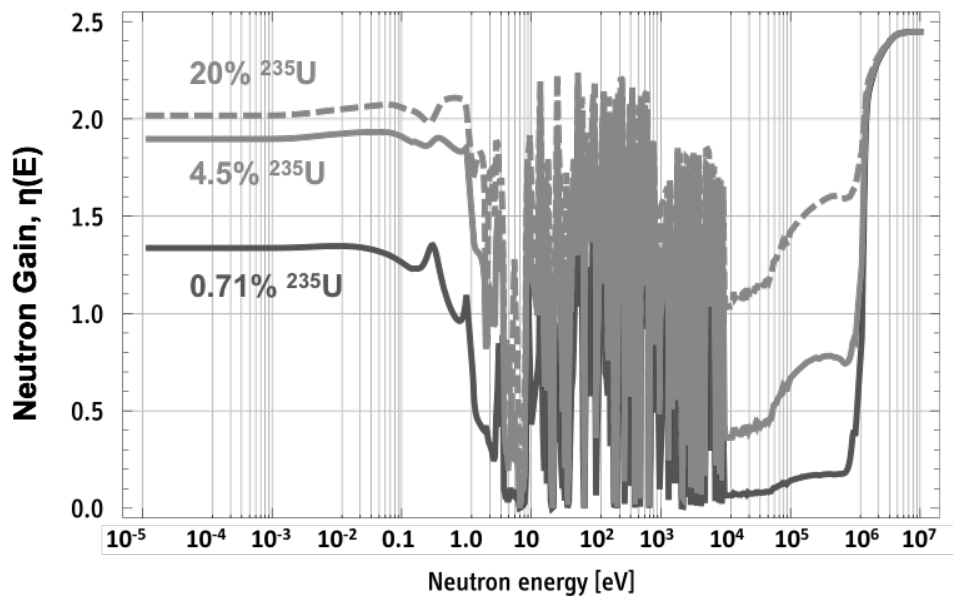


Figure 1.3 Gain in number of neutrons from one generation to the next at a specified energy in a specified mixture of ^{238}U and ^{235}U , with no other materials present.

cause they utilize energetic and therefore fast neutrons. These reactors need coolant that neither absorbs fast neutrons significantly nor slows them down too quickly past a few 100 keV into the “no-man’s land” of the very large spikes, called “resonances.” Neutrons that spend any appreciable amount of time in this intermediate energy region are eaten up mercilessly by absorbing resonances of ^{238}U , a process we will study in Chapters 2 and 3. Liquid sodium is currently being used in the few operational fast reactors, but other coolants such as lead, lead-bismuth and helium gas, which is basically transparent to neutrons, are being considered, as discussed in Chapter 8. One potential advantage of fast reactors, discussed in Chapter 6, is that they can in principle produce more fission fuel than they consume, because most of the absorption of neutrons can be by ^{238}U . In this case as much as $\sim 50\%$ more ^{238}U can be converted to Pu than $^{235}\text{U} + \text{Pu}$ is burned. By reprocessing the fuel and extracting the fissile material, most of the natural uranium dug from the earth can in principle be burned, stretching by a factor ~ 60 the amount of energy that can be extracted from a given amount of natural uranium. The reprocessing step, however, is expensive and messy, and presents a serious nuclear proliferation risk, as described in Chapter 7.

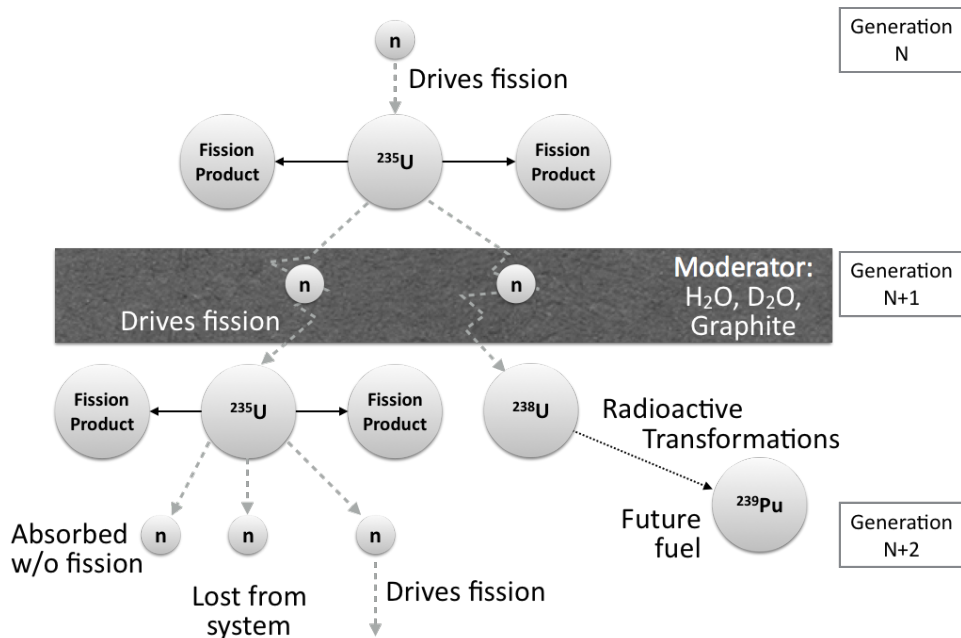


Figure 1.4 Fission, moderation and Pu production in a thermal reactor. Generations of neutrons are indicated.

The other energy range that is practicable is the thermal range. In this case while neutrons are born in the MeV range, they are very rapidly slowed down past the resonances to 1 eV and below, in order to minimize the chance of being absorbed in the resonance region. Ultimately they drive fission in the thermal energy region, where ^{235}U is very reactive. Figure 1.4 illustrates a chain reaction in a thermal reactor. The key, as with FRs, is that the number of fissions must stay very precisely constant from one generation to the next.

As discussed in Chapter 3, the best materials for causing rapid slowing-down, or “moderation,” of neutrons, with very little absorption of the slowed-down neutrons, are pure graphite and heavy water, D_2O . (D represents deuterium, ^2H , the isotope of hydrogen with one proton and one neutron.) In fact graphite and heavy-water systems are so efficient in their neutron economy that reactors that use them can fission natural uranium. They can also be prodigious producers of weapon-grade plutonium as we will learn in Chapter 7. The great majority of the world’s fission reactors are “light-water reactors,” LWRs. In this case regular water, H_2O , is used both to moderate the neutrons and to carry away the nuclear heat, a great simplification. LWRs, however, do require uranium to be enriched, because while the pro-

tons in H₂O are excellent at slowing down neutrons, even better than the deuterons in D₂O and C in graphite, they compete with the uranium fuel in absorbing thermalized neutrons. Because of this absorption, there is less production of Pu in LWRs, but it is still significant. Over time as it builds up and fissions it adds to the total energy that is extracted from the fuel. In fact about as much Pu has burned as ²³⁵U has not burned, ~1% out of ~4.5% ²³⁵U, by the time fuel is unloaded from an LWR.

Question: If each succeeding generation makes 1% more neutrons than the one before it, how many generations does it take to double the power being produced? And if 2% more are produced? 7%? (In finance, this pattern is called the rule of 70.)

There are two kinds of LWRs, pressurized water reactors, PWRs, shown in figure 1.5, and boiling water reactors, BWRs. The majority of operating fission reactors, and most new designs, are PWRs (see table 1.1), in which the cooling water that passes through the reactor core is highly pressurized, and so does not boil. A secondary cooling loop, in which the water is allowed to boil and form steam, provides extra isolation from the reactor, but adds complexity. In a boiling-water reactor the water boils in the reactor core itself, and the resulting steam is transported directly to the turbines that generate electricity. Both of these reactor designs deliver electrical efficiency in the range of 33%, so about 3000 MW of thermal power, 3000 MW(th), is required to generate 1000 MW(e) of electricity, 1000 MW(e) = 1 GW(e).

The neutron-absorbing control rods that are used to regulate the fission reaction are inserted from the top in PWRs (and from the bottom in BWRs). These rods, which can be of various shapes, penetrate into the core region occupied by the reacting fuel, as shown in figure 1.5. Figure 1.6 shows a PWR fuel assembly. Thin fuel pins, or rods, ~1 cm in diameter and ~4 m in length, hold ceramic pellets of UO₂ within zirconium-alloy cladding that is nearly transparent to neutrons. The fuel pins are bound together into fuel assemblies of perhaps 250 pins. Water flows freely between the individual fuel pins and fuel assemblies, both moderating (rapidly slowing down) the MeV neutrons that easily escape from the thin fuel pins and also carrying off the heat emanating from the fuel pellets.

The distribution of types of nuclear plants that are currently operating is shown in table 1.1.

Question: What are some reasons why water is such a commonly used coolant in different technologies, from the little heat pipes in your laptop, to automobiles, to coal-fired power plants?

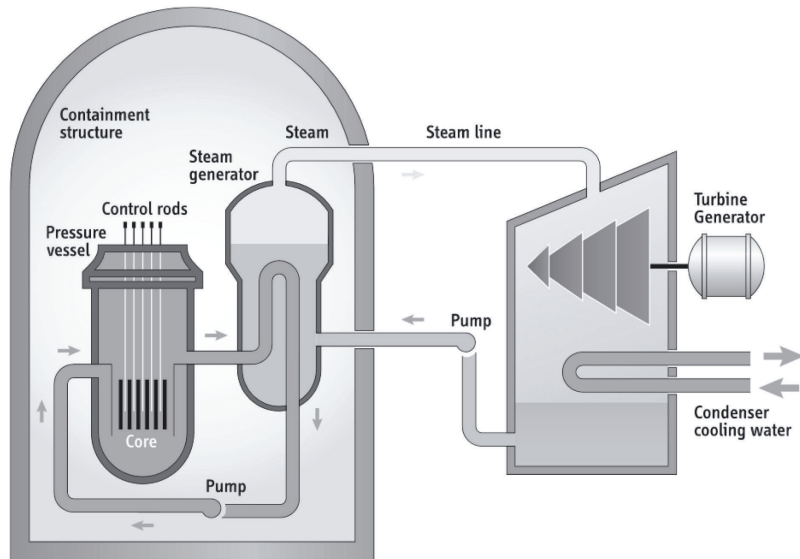


Figure 1.5 Diagram of a pressurized water reactor, PWR.

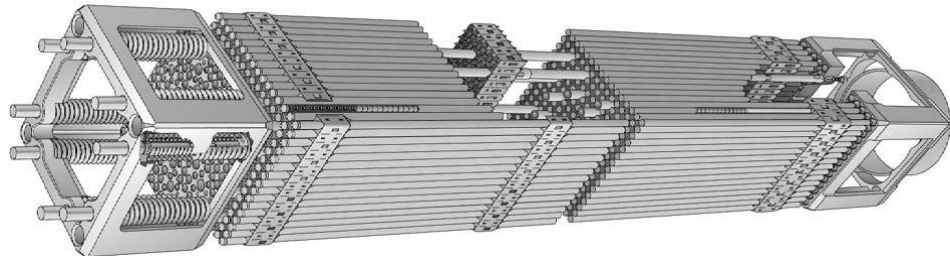


Figure 1.6 PWR fuel assembly (set sideways).

1.1.2 Safety, waste, nuclear proliferation

There are three issues that have dogged nuclear fission power throughout its development. The first is safety, discussed in Chapter 5, which is headlined by the major (“Level 7”) accidents at Chernobyl in 1986 and at Fukushima in 2011. Each of these resulted in the dispersal of large amounts of radioactivity and the long-term evacuation of large areas of land. The second is waste, discussed in Chapter 6, which is headlined in the U.S. by the failure to open a geological repository for long-lived civilian nuclear waste despite almost 60 years of effort. The third is the link between the technologies of peaceful nuclear energy and nuclear weapons, discussed in Chapter 7, which has been

Table 1.1 *Current distribution of reactor types.*

Source: IAEA Technology Review, 2015

%		Type of Reactor
63.2	PWR	Pressurized (Light) Water Reactor
16.3	BWR	Boiling (Light) Water Reactor
11.2	PHWR	Pressurized Heavy Water Reactor
11.2	LWGR	Light Water Cooled Graphite Moderated Reactor
3.4	GCR	Gas Cooled Reactor
0.5	FR	Fast Reactor

headlined recently by the difficult agreement reached between China, France, Germany, Great Britain, Russia, the U.S. and Iran to verifiably limit Iran's nuclear program to energy applications.

Safety

The proximate cause of the Chernobyl accident was "prompt criticality." Each nuclear fission reaction, as we discussed, emits roughly 2.5 neutrons. It is crucial to the controllability of the fission chain reaction that a small fraction, $\beta \sim 0.65\%$ for uranium, of these neutrons are emitted with an average delay of 12.9 seconds, again for uranium. The delayed neutrons are emitted in the decay chains of the fission products, which naturally begin rich in neutrons. In Chapter 5 we will see that a nuclear reactor is controllable only for very small values of positive reactivity $\rho \equiv (k - 1)/k$, where k is the gain from generation to generation of the neutron population. The ratio ρ/β is so important to nuclear engineers that it is measured in dollars (\$), as shown in figure 1.7. If $\rho/\beta > \$1.00$ a reactor has gone into "prompt criticality," meaning that its power production can take off without waiting for any delayed neutrons, running away on the "prompt" neutrons alone, and so extremely rapidly. The reactor time, T , represents the characteristic time over which the power changes. In the course of disassembling itself, Chernobyl reactor #4 reached at least 10x its normal operating power. We will discuss the root causes that allowed this to happen, but most people think that prompt criticality can be avoided in light water reactors. Water-cooled graphite moderated reactors like Chernobyl, and fast reactors, can be more susceptible to this failure mode.

A failure mode that light water reactors still face, however, is associated

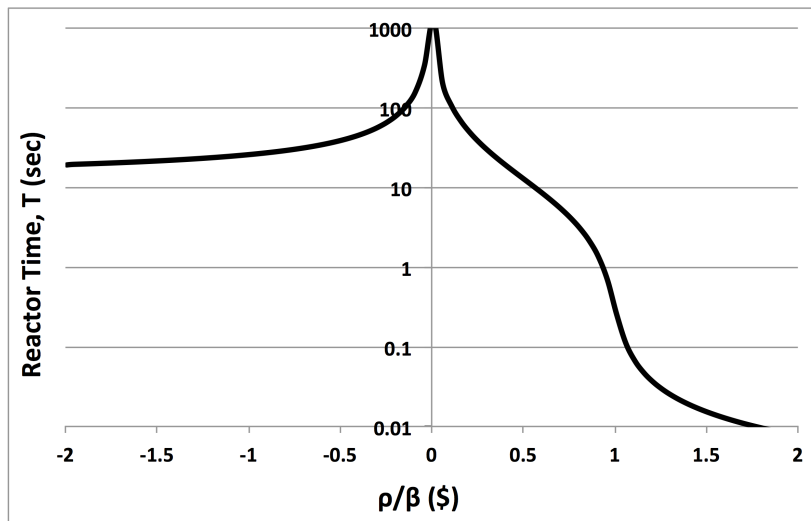


Figure 1.7 Characteristic reactor response time vs. reactivity divided by delayed neutron fraction.

with the decay heat from fission. About 94% of the power from uranium fission is emitted promptly; radioactive decay of the fission products emits the remaining 6%. As shown in figure 1.8, the decay heat power drops to about 2% by 15 minutes after all fission reactions have stopped, but then decays quite slowly. Nothing can prevent this heat from being emitted. If the heat is not removed, in about five hours all of the water will have boiled away, and the overheated fuel assemblies that make up the core of the reactor will begin to melt and slump down in the reactor vessel. This happened at the three reactors in Fukushima which lost core cooling. It was the proximate cause of the Level 7 accident, the highest level in the international system. Again we will discuss the root causes that allowed this to happen. Reducing the risk of a core meltdown due to decay heat is a major focus of new LWR fission reactor designs. In general fast reactors are believed to be even more difficult to protect against core meltdown and its consequences.

Questions: What was your response to the Fukushima accident? What did you expect to be the near-term consequences for nuclear power? What is your impression of what actually happened?

Waste

The second tough problem faced by nuclear fission is the disposal of long-lived, high-level nuclear waste, which requires geological storage. The mass

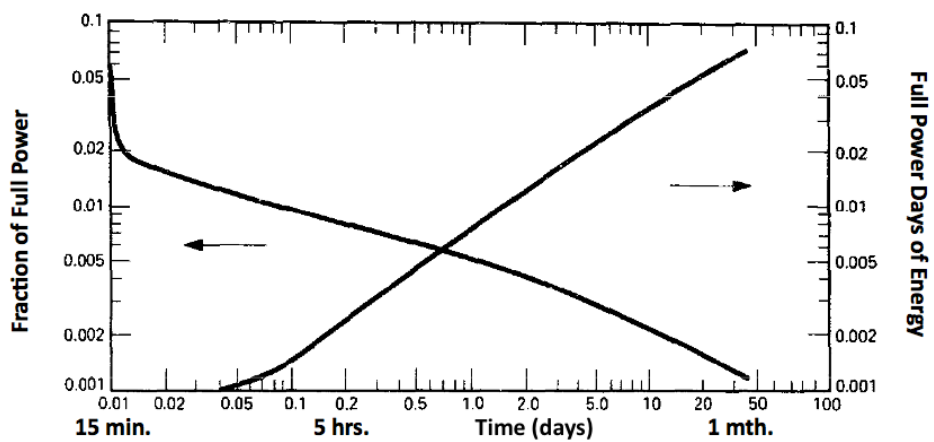


Figure 1.8 Decay power on left axis, decay energy on right axis vs. time in days.

and volume of high-level nuclear waste is small compared with those of waste from, for example, coal, but it is lethally radioactive for a very long period of time. Human society has never had to deal with a problem of this nature, and we have not developed a consensus on how to balance risks to our current citizens vs. risks to those living 10,000 or even 100,000 years from now. On the one hand, we are unable to justify burdening many future generations with the risks associated with waste created during the next few generations. On the other hand, at the rate of scientific progress we see today, it seems likely that we will have a cure for radiation-induced cancers and/or much more sophisticated ways of dealing with environmental contaminants 10,000 years from now. Another societally difficult balancing act, and in practice the most *politically* toxic one, is tied to the question, “Why should the citizens of one region be required to live in the near vicinity of the nuclear waste produced by a whole nation?” As we will discuss in Chapter 6, there is some progress being made, particularly in Finland and Sweden, by redefining the selection process and providing rewards to communities offering to host waste facilities.

Currently, spent fuel is first stored in cooling pools, for a period of at least five years. As more waste is produced these pools are being modified to accommodate more spent fuel assemblies. Eventually the spent fuel is transferred to dry storage casks (figure 1.9). Each cask can handle about 10 t of spent fuel, which comes to about two casks per reactor-year. These are now building up at reactor sites, as there is no agreement on what to do with them. They are stable, and believed to be safe from theft – in part because



Figure 1.9 Dry cask storage facility near a nuclear power plant.

if they were broken open the radiation levels would be very high. They are generally licensed for 50 years. However no long-term geological storage facility has been licensed anywhere in the world to isolate commercial nuclear waste from the environment, so the ultimate fate of this waste is uncertain.

In principle fast reactors, FRs, can reduce the burden of nuclear wastes. Most, but not all, of the longest-lived waste products are actually not the products of fission, but rather nuclei that have absorbed neutrons and transmuted to plutonium ($Z=94$) and other members of the actinide family, neptunium ($Z=93$), americium ($Z=95$) and curium ($Z=96$). In principle these can be fissioned in an FR. If fuel is removed from a thermal or fast reactor, it can be reprocessed to extract the actinides, including ^{238}U , for later burning in an FR. This can greatly increase the utilization of the nuclear energy in the original uranium, which is normally less than 1%, since it is basically the ^{235}U and the small fraction of ^{238}U transmuted to Pu that is fissioned in a thermal reactor. (Actually reprocessed Pu can be fissioned for one cycle even in a thermal reactor, but this only increases the energy utilization by $\sim 1/6$.) FR's have proven difficult to build, reprocessing has proven to be very expensive, and it is not clear that the advantages of removing actinides from the waste stream are as high as originally believed. Furthermore, the price of uranium has remained low, so there is little economic incentive now to extract energy from it more efficiently. A central problem with reprocess-

ing is that the Pu in the fuel that is produced is easily chemically separated, and is usable, if not ideal, in nuclear weapons.

Question: Why is element 94 called plutonium? (Hint: It is not named after the Roman god of the underworld.)

Nuclear proliferation

A final, but very important, problem that needs to be considered is nuclear proliferation. Nuclear fission was discovered in 1938, and its first application was in the form of nuclear weapons in 1945. Nuclear weapons run on fast, prompt neutrons, and at very high fractions of ^{235}U and/or ^{239}Pu , in order to maximize the increase of the fission rate from generation to generation, resulting in a powerful explosion. Processes for the enrichment of uranium in ^{235}U and the production of nearly pure ^{239}Pu in nuclear reactors were developed to provide the immensely powerful explosive materials for nuclear weapons. Unfortunately, much of the technology that is used for nuclear energy production is “dual-use,” applicable both for civilian and military purposes. Most troubling, the scale of facilities for uranium enrichment or extraction of plutonium from spent fuel needed for energy production is much greater than that needed to produce nuclear weapons. For example we will see in Chapter 7 that a commercial enrichment plant sized to provide the fuel needs for ten LWRs, if redirected to making weapons material, can produce enough highly enriched uranium for 70 weapons per month. The trick for doing this so quickly is to start from reactor fuel. We will show, surprisingly, that 4% enriched uranium is 2/3 of the way to 90%, in terms of the required enrichment work.

This scale difference introduces three problems. First, as just mentioned, a large enrichment or reprocessing facility if redirected to military application can produce weapons material quickly. This is called “breakout.” Second, a clandestine facility that produces enough material for a few weapons per year can be much smaller than a commercial facility, and can be difficult to detect. A hall containing centrifuges for uranium enrichment only 1600 m^2 in area, and consuming only 300 kW of power, can be disguised as a commercial facility while producing enough highly-enriched uranium for one weapon per year. This option of clandestine nuclear materials production has recently been dubbed, “sneakout.” Finally, in a “diversion” scenario, a small fraction of the production of a declared and safeguarded facility, is covertly diverted, providing material for bomb production. In all of these cases, breakout, sneakout, and diversion, the actions can be taken by a nation-state, and in



Figure 1.10 Centrifuge hall in commercial-scale enrichment plant. Source: URENCO

the latter two cases one has to consider non-state actors, perhaps working in collusion with insiders.

If some of the safeguards innovations in the recent Iran Agreement (The Joint Comprehensive Plan of Action, JCPOA) can be applied more broadly, it will help with the problem of nuclear proliferation based on uranium enrichment. Misuse of declared facilities will be rapidly detectable using real-time monitoring, and the supply of uranium and centrifuges that could be diverted to clandestine facilities will be tracked. A complementary approach is to encourage multi-national enrichment facilities, where the multiple parties will provide brakes on each other. On the other hand it is not clear what technical or organizational mechanism can be used to assure that owners of reactors that burn Pu in their fuel do not use this Pu for weapons, so non-proliferation concerns weigh heavily against reprocessing.

It will remain a large challenge to avoid the proliferation of nuclear weapons capability to many more countries if nuclear energy spreads and grows significantly. Countries actively engaged with the International Atomic Energy Association (IAEA) in planning for new nuclear power programs include Bangladesh, Belarus, Egypt, Jordan, Kenya, Morocco, Nigeria, Poland, Turkey and Viet Nam. The IAEA reports that others, including Azerbaijan, Bangladesh, Belarus, Bolivia, Kuwait, Mongolia, Nigeria, South Africa, Su-

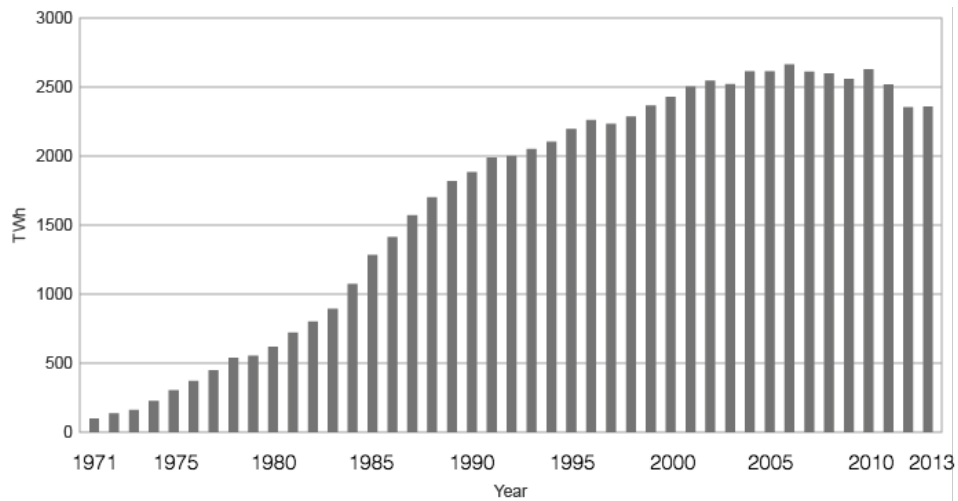


Figure 1.11 TW-hrs of nuclear electricity produced per year. 1 GWe-yr = 8.766 TW-hr.

dan, Thailand, Tunisia and the United Republic of Tanzania, are considering building new research reactors.

1.1.3 Past may be prologue, but what is it telling us?

The history of nuclear fission power is unusual. Figure 1.11 shows that electricity production rose very rapidly from 1971 to 1990. During that period it increased from 2% to 16% of world electrical power production. After 1990, however, growth slowed, peaking at 18% of world production in 1996. Some of the slowing may have been driven by the Chernobyl accident in 1986, but a larger factor was likely rising costs and longer construction times. Since 1990 a large part of the growth in nuclear electrical energy production has come from better operation of the existing power plants. For example, in the U.S. the nuclear power plant capacity factor (yearly average power production divided by name-plate rating) has risen from 65% to 90% since 1990. After the accident at Fukushima in 2011, absolute world nuclear energy production fell and it now constitutes only 11% of world electricity production. On the other hand, as shown in tables 1.2 and 1.3 some 70 new nuclear power reactors are currently under construction, adding to the ~390 currently operating.

The factors that drive a nation to construct nuclear power plants are complex. In the U.S. natural gas is so inexpensive that nuclear power cannot compete in unregulated electricity markets, and even some older operat-

Table 1.2 *Reactors under construction, by nation.*
Source: IAEA Technology Review, 2015

Country	Units	Total MWe
Argentine	1	25
Belarus	2	2218
Brazil	1	1245
China	26	25,756
Finland	1	1600
France	1	1630
India	6	3907
Japan	2	2650
S. Korea	5	6370
Pakistan	2	630
Russia	9	7371
Slovakia	2	880
Ukraine	2	1900
United Arab Emirates	3	4035
United States	5	5633

Table 1.3 *Reactors under construction, by year.*
Source: IAEA Technology Review, 2015

Year	2006	2007	2008	2009	2010	2011	2012	2013	2014
Units	28	35	45	57	68	65	66	72	70

ing nuclear power plants that are completely paid for are slated to be shut down. In many countries, however, fossil fuels, especially natural gas, are much more expensive than in the U.S., while the labor required to construct nuclear plants is less expensive. Furthermore, in most countries the electric power industry is less strongly driven by market forces, and more by government policies and direct or indirect government investment. Then society-wide issues like national energy security, including diversity and se-

curity of fuel supply, and/or limitation on CO₂ emission, play a stronger role. These factors have driven a significant increase in reactor construction over the last decade, particularly in the Far East, as shown in table 1.3.

The United Arab Emirates has contracted with South Korea to build four new LWRs. It has committed not to enrich uranium, nor to reprocess fuel, providing favorable assurances to the international community against nuclear proliferation risks, sometimes called the “gold standard.” A recent innovation is that Russia is offering, for example to Turkey, that it will build, own and operate new reactors, as well as provide fresh fuel and take back spent fuel, similarly mitigating proliferation risks. This “BOO” model may be an effective commercial approach in the future, since the capital cost of fission reactors is a major barrier to entry for many nations.

Question: What are the advantages and disadvantages, including risks, for the buyer and the seller in a “BOO” deal?

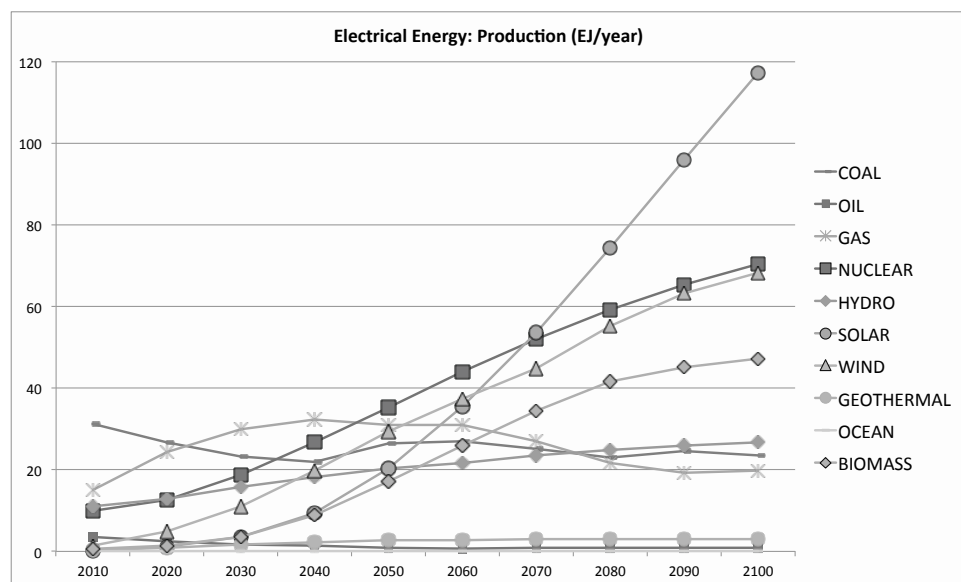


Figure 1.12 Mean electrical power production by technology, Energy Modeling Forum 27 model runs that limit global warming to 2 °C in 2100. 1 EJ = 31.7 GWe-yr.

Nuclear power may have an important role in mitigating climate change. The Intergovernmental Panel on Climate Change (IPCC) worked with energy/environment modeling groups to project the pathway to a world where global warming is constrained to no more than 2 °C above pre-industrial in the year 2100. Figure 1.12 shows the mean of the results from a set of

models, EMF-27, that succeed in constraining global warming to the IPCC target value. Nuclear power is one of the major technologies these models rely upon, and nuclear's market share increases moderately as its total yearly production rises a factor of seven by 2100. The values projected for the relatively near term, e.g., 2030, are near the high end of those projected by the IAEA and the World Nuclear association. The IAEA, in collaboration with the OECD-NEA, publishes estimates of world-wide uranium resources. These estimates have limitations, and certainly more uranium will be available at higher prices than considered in these reports, as discussed in Chapter 6. On the other hand, the nuclear energy scenario in figure 1.12 burns and commits to burn 100% of reported world-wide known and projected uranium resources, based on the sum of the IAEA/OECD categories of "Reasonably Assured," "Inferred," "Prognosticated," and "Speculative" resources, by 2055. Since uranium reserves are very unevenly distributed relative to human populations (there is much more U in Australia than in China), some nations will have more reason to be concerned about domestic reserves than others. These include China, India, Japan, South Korea, and countries in the Middle East. Concerns about national energy security, and concerns about waste storage, may lead to the adoption of fast reactors later in the century, in order to stretch uranium resources, creating a substantially increased risk of nuclear proliferation.

1.1.4 Prospects

The future of nuclear fission energy is uncertain. After the Fukushima accident Germany decided to phase out nuclear power, and only two of Japan's remaining 48 reactors are now in operation. On the other hand, after some review, China is continuing to build 26 new reactors and there appears to be growing interest in nuclear power in many areas of the world, as a form of secure domestic energy with low carbon emissions. In the U.S. and Europe the cost of nuclear power is a deterrent to its application. Progress is needed on safety, waste disposal, and the limitation of nuclear proliferation to reduce the risks associated with nuclear fission. In Chapter 8 we will examine designs of fission reactors that attempt to make progress against some or all of these goals, particularly "passively" safe LWRs, molten-salt-cooled reactors that use thorium to breed ^{233}U for fuel, and fast reactors that maximize the efficiency of breeding Pu without employing reprocessing.

Question: What do you now think is the future of fission power, considering

both the pro and con arguments? Perhaps your opinions will change as you learn more.

1.2 Fusion

1.2.1 Self-sustaining fusion reactions

For fusion, energy is extracted from the fusion of two light nuclei to form a heavier one. At distances large compared with a nuclear radius, even low-Z nuclei are kept apart by their electrostatic repulsion. If they approach closely enough, however, then the strong – but short-range – nuclear force dominates and the nuclei can be attracted together and fuse. There are multiple possible fusion reactions, but the easiest to access for energy applications is



Here D represents deuterium, the isotope of hydrogen containing one proton and one neutron, ${}^2\text{H}$. The nucleus of a deuterium atom is called a deuteron. T represents tritium, the isotope of hydrogen that contains one proton and two neutrons, ${}^3\text{H}$; its nucleus is called a triton. The advantage of fusing singly charged nuclei is that their electrostatic repulsion is minimized, so the kinetic energy required to overcome this repulsion is minimized as well. As can be seen in figure 1.1, the helium nucleus, or α particle, has a particularly low potential energy, making it attractive as a product. Starting from the isotopes of hydrogen, the only choice that allows an α particle as a product is $D + T$.

Of the 17.6 MeV from the reaction, $20\% = 3.5 \text{ MeV}$ goes to the α particle and $80\% = 14.1 \text{ MeV}$ goes to the neutron. This follows from momentum conservation. Ignoring the momentum of the incoming thermal D and T, the outgoing energetic particles must be oppositely directed, with equal mv , giving the neutron four times the speed of the α particle. The energy of the neutron then, $(1/2)mv^2/2 = (1/2)m\vec{v} \cdot \vec{v}$, is four times higher than the energy of the α particle, since mv is equal between the two.

To overcome the electrostatic repulsion between even singly-charged nuclei requires a great deal of kinetic energy. For a useful rate of reaction, this must be some 10's of keV. Such energies are easily achieved with simple electrostatic particle accelerators, but the scattering rate is much higher than the fusion rate, so we cannot simply fire beams of deuterons and tritons at each other. They would just scatter all over. What we need is a confined gas of these ions at a temperature in the range of 10 keV (116M K), so they

are constantly colliding with each other at energies in the range of 10's of keV.

Question: Suppose two deuterons, each with energy equal to the mean particle energy in a 10 keV plasma, collide head on. What is the energy of one of the deuterons in the frame of reference of the other?

Any cloud containing a useful density of ions would immediately blow itself apart from electrostatic repulsion, so we also need to include electrons at very, very nearly the same density. The electrons must also not be too much cooler than the ions, or the ions will lose too much energy as they thermalize collisionally with the electrons. The result is that we need a \sim 10 keV ion-electron gas, a high temperature plasma. The ionization potential of the hydrogen atom is 13.6 eV, so collisions between the free electrons in this plasma and the bound electrons in any hydrogenic atoms present will rapidly drive the system to full ionization.

Evidently, we need to heat this plasma to high temperature in the first place and then keep it hot to produce energy. We can start with externally supplied heating, but we would like the reaction largely to maintain itself, like logs in a fire, where all that is required is to throw new logs in as the old ones burn, and occasionally remove the ash. Neutrons produced by fusion immediately escape a magnetically-confined plasma without interacting, so are useless for plasma heating. Fortunately, however, the α particles from the DT reaction are born at 3.5 MeV and are themselves positively charged. So if our scheme for holding onto a DT plasma with charged particles at 10's of keV also holds onto MeV-energy charged α particles, then we can use those α particles to provide most or all of the power to maintain the temperature of the plasma, rather like the flame from one burning log lighting the next. If the heat is well enough contained, and the plasma is fueled steadily, and the He ash is removed, the plasma will maintain its high temperature and steady burn rate. To achieve all of this, we need to understand the physics of plasmas. The goal is to determine how to contain a hot, dense plasma that will make commercial amounts of fusion power, and at the same time leak heat at a slow enough rate, while remove helium at a fast enough rate, that it can sustain its own temperature largely by fusion, without too much power input from the outside. The requirements for this are addressed quantitatively in Chapter 9.

The most successful configuration to date at confining hot fusion plasma is called a “tokamak,” a Russian neologism for “toroidal chamber with magnetic coils.” In a uniform magnetic field, charged particles spiral along the field, as shown in figure 1.13. The circular motion across \vec{B} arises from the

$q\vec{v} \times \vec{B}$ Lorentz force. Since there is no force along \vec{B} , the velocity in that direction is constant, and the resulting total motion traces out a spiral along the magnetic field.

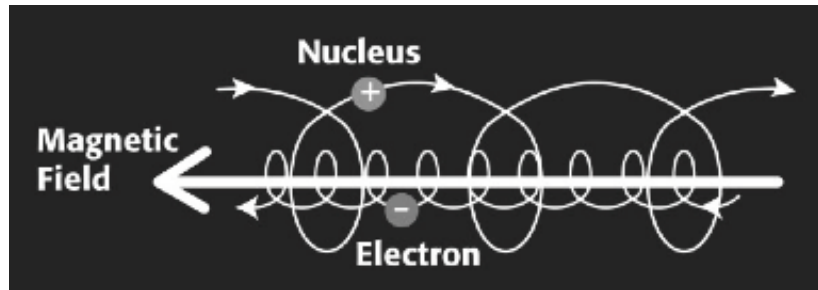


Figure 1.13 Charged particles spiraling along a uniform magnetic field.

If the magnetic field lines are then closed into a toroidal (doughnut-shaped) configuration, the particles largely spiral along the field lines, which face in the toroidal direction, the long way around the doughnut. However, as we will see in Chapter 10, a small vertical drift motion is induced by the curvature and gradient of a toroidal magnetic field. A twist, literally, needs to be added to the field as shown in figure 1.14, in order to confine the particle trajectories. With this twist, as a particle moves along a field line the vertical upward drift when it is at the top of the tokamak, taking the particle outward from the center of the plasma, is compensated by the vertical upward and inward drift when it is at the bottom. In a tokamak, the magnetic field that induces this twist is generated by an electrical current flowing in the plasma itself. This current makes a magnetic field that faces in the poloidal direction, the short way around the doughnut, and the sum of this field with the toroidal field from external magnets provides the overall twist. The poloidal field is much weaker than the toroidal magnetic field, so in tokamaks a field line makes more than one toroidal transit, or circumnavigation, per poloidal transit. Nonetheless, the result is remarkably well confined particle motion, and a plasma configuration that has already produced megawatts of fusion power, for pulses in the range of 0.5 to 5 seconds in laboratory experiments, but not yet self-sustained.

Tritium decays with a half-life of 12.3 years, meaning that one-half of any given quantity of tritium decays away after this time period, or about 5% decays away per year. Tritium does not exist in significant quantities in nature, and must be produced for fusion energy based on the DT reaction.

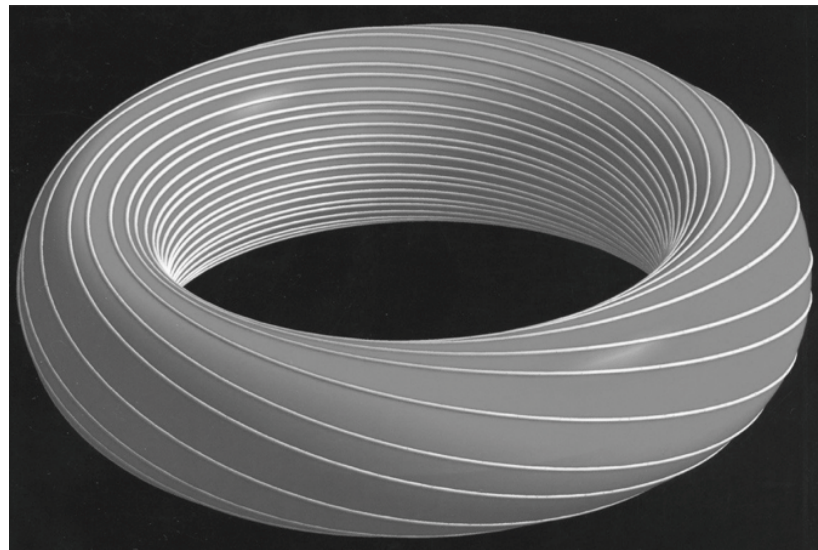


Figure 1.14 Twisted toroidal magnetic field to confine charged particles.
Source: Jeff Freidberg's book

The most efficient reaction for producing tritium is:



Tritium is also produced when neutrons interact with the deuterium in heavy-water reactors, by radiative capture with the emission of a gamma ray, an energetic photon.



The $n + {}^6Li$ and $n + D$ reactions can be used to produce tritium in fission reactors in order to start up a limited number of DT fusion systems, but the amount of tritium that will be burned in a fusion power system, $\sim 400\text{g/day}$, means that fission reactors are not a practical source for steady supply. The fusion neutrons themselves must be captured by 6Li to provide a steady supply of fuel. Since some neutrons will be absorbed by structural materials and coolant, it is necessary to include elements such as Pb or Be that function as neutron multipliers. When these nuclei are struck by an energetic neutron, two neutrons frequently emerge. Thus the first wall and blanket that surround a fusion plasma must not only capture the heat from the α particles and neutrons, but also multiply the neutrons and breed the tritium needed to keep the reaction going, as discussed in Chapter 16.

In sum, the α particles maintain the temperature of the plasma and the neutrons maintain the fuel supply.

Figure 1.15 illustrates a concept for a pilot fusion power plant based on the tokamak configuration. A vertically-elongated, toroidal plasma is held in the center of chamber. (We will see in Chapter 12 that vertical elongation improves a tokamak's ability to contain high pressure.) The plasma is largely surrounded by a first wall and blanket. Some of the heat from the plasma that originated from the fusion α 's is captured at the first wall, but the majority is channeled into the divertor region, a topic of much modern research, as discussed in Chapter 15. It is from this region that the He ash is pumped away as well. The neutrons are captured in the blanket for their heat and to breed tritium. The vacuum vessel separates the fusion fuel from contamination by the atmosphere, and vice-versa. The horizontal ports in the vessel provide access for heating and current drive systems, and for plasma measurement tools, called "diagnostics." The vertical ports provide access for maintenance. The TF (toroidal field) coils provide the main toroidally-directed magnetic field. The whole structure is contained in a cryostat, an excellent thermal insulator, to maintain the very low temperature ($\sim 4K$) of the superconducting coils. Superconductors are attractive for fusion magnets, because no energy is consumed in resistive dissipation of the coil current. They do, however, require impressive refrigerators. In the future, fusion systems may move to more advanced high-temperature superconductors.

The central solenoid, essentially a cylindrical magnet, is a key feature of a tokamak. It functions as the primary winding of a large transformer, driving up and sustaining the current in the plasma, which functions as a one-turn secondary winding. When, for example, the central solenoid's electrical current is reversed from clockwise to counter-clockwise, a substantial vertical $\partial B / \partial t$ is generated inside the cylinder, which causes a toroidally directed electric field. Hot plasmas are very good electrical conductors, so the electric field drives up millions of amperes of clockwise toroidally directed current. It is this plasma current that provides the necessary twist in the field lines. The magnetic fields created by the PF (poloidal field) coils interact with the plasma current to provide the desired plasma shape. The currents in the top and bottom PF coils attract the toroidal current flowing in the plasma towards the top and bottom, and so elongate the plasma. The resulting field pattern also directs plasma diffusing out from the core to flow into the divertor chambers.

Question: Where in Maxwell's equations does the toroidal electric field

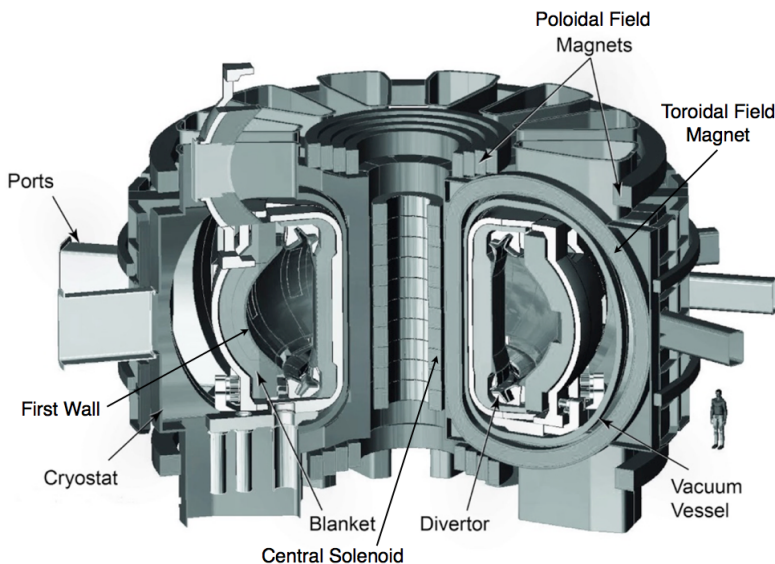


Figure 1.15 Concept for a fusion pilot plant, based on the tokamak magnetic configuration.

come from? What would happen if the sign in this equation were reversed? (This sign is Lenz's law.)

There are other toroidal configurations that are promising for fusion. The stellarator (or "star-maker," invented by Princeton astrophysicist Lyman Spitzer) takes a different approach to providing the necessary twist in the magnetic field. Rather than drive an electrical current through the plasma, it uses non-axisymmetric, distorted coils as can be seen in figure 1.16 to coax the magnetic field around in the poloidal direction. This trick, which appears to defy Ampere's law, but of course does not, provides a firmer cage around the plasma. After all, the poloidal field in a tokamak is primarily generated by the plasma's own current, so if the plasma moves it carries its magnetic cage with it! This is not the case for a stellarator. Such systems though difficult to build due to their lack of symmetry are less prone to macroscopic disturbances than tokamaks, and their fusion performance is in the same range for the same size of device, with the same magnetic field strength.

At the other extreme there are toroidal configurations with weaker toroidal magnetic fields, and even an example that in theory has only a poloidal magnetic field, created by a toroidal current. The plasmas in these configu-

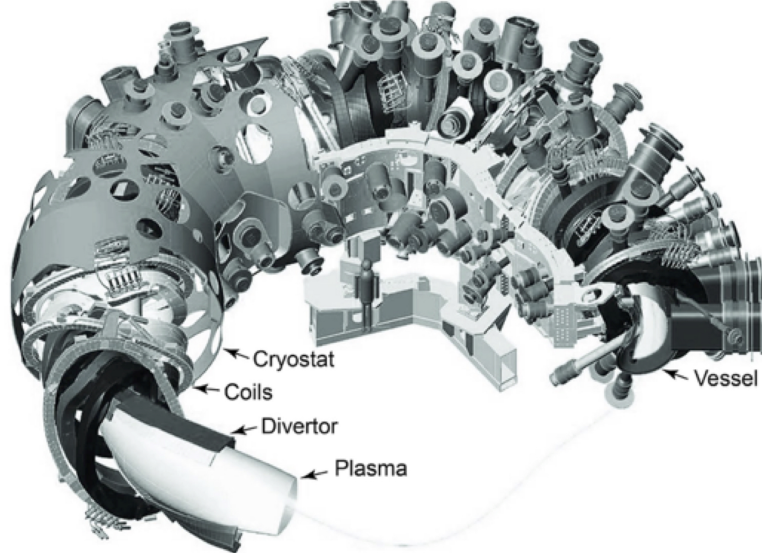


Figure 1.16 Cutaway drawing of the superconducting W7-X stellarator, which began operation in Germany in 2015.

rations are much more unruly, but without the massive toroidal field coils, they are less expensive to build. In some cases there are no magnet coils threading the center of the torus, and the heat flux from the plasma largely escapes along magnetic field lines that lead outside the magnet system, providing considerable engineering simplification. These latter configurations, however, do not even approach the tokamaks of the late 1960's in fusion performance. Nonetheless their advocates are hopeful that they will ultimately make more cost-effective fusion power systems. Some work in this area has attracted private financing, as opposed to the public funding that supports almost all fusion research.

Inertial confinement fusion, discussed in Chapter 17, is something completely different. Here the concept is to compress a ~ 5 mm diameter hollow sphere of frozen DT fuel very rapidly, using many powerful laser or particle beams. The center of the sphere is filled with DT gas, in equilibrium with the frozen fuel. When the inward motion, or implosion, stops at the center, kinetic energy is exchanged for heat and pressure, and a tiny, symmetrical, pure DT hot spot is formed at the center of the original sphere, largely from the gas that filled it. This hot spot, comprising only a few % of the fuel, is projected itself to burn vigorously and then ignite an outward propagating burn wave throughout the remainder of the fuel. The fuel is held in place

as it burns only by its own inertia, hence the name “Inertial Confinement Fusion,” or ICF. The most advanced approach to ICF at present is to use the intense heat from lasers to fill a small cavity with x-rays, and have the x-rays compress the sphere of fuel, in what is called “indirect drive.” If this sounds like something you have heard of (the hydrogen bomb) you are right. Inertial confinement fusion research is currently funded to help scientists understand the processes going on in nuclear weapons, on a very, very much smaller size and energy scale than an underground test of a nuclear weapon. This research has made progress in recent years, but it is still bedeviled by the challenge of getting the little shells to implode symmetrically. As we will discuss in Chapter 17, the implosion process is very unstable and hard to control. We will also discuss the energy application of ICF, which involves producing, targeting, imploding and cleaning up from 5 – 10 of these events per second, making 250 MJ to 600 MJ of fusion energy at each explosion.

Question: What might be the advantages and disadvantages of pursuing a form of fusion energy with close links to the physics of nuclear weapons?

1.2.2 Why fusion?

Harnessing fusion is clearly scientifically and technologically challenging. What makes fusion attractive as an energy source?

The basic fuels, deuterium and lithium, are abundant. Deuterium forms about 0.03% by mass of the hydrogen in seawater, and can be inexpensively extracted in effectively unlimited quantities. ^6Li forms about 6.5% of lithium by mass. Identified lithium reserves of 12 million tonnes would allow the full-power operation of 2000 1 GWe power plants for 1500 years, just burning the ^6Li and leaving the rest for applications such as automotive batteries. It should be economically practical to extract an additional 200 billion tonnes of lithium from seawater for fusion. There have been efforts to extract uranium from seawater; the energy density of lithium in seawater is 2800 times greater for fusion than is the energy density of uranium burned in LWRs.

The CO₂ emissions associated with fusion energy, like with fission, come dominantly from the construction process. This is similar to the levels needed for wind and solar construction, depending on the assumptions made.

Like fission, fusion is a baseload energy source that does not depend on space- and time-varying natural energy flows. Thus it does not incur the additional capital cost of extension of major components of the electrical grid to areas of low population density, where wind or solar power may be most efficiently harvested, nor does it suffer from power loss due to transmission

back from those areas. It does not require large-scale energy storage nor backup energy sources operated at low duty factor. It does not require large land use, as needed especially for biomass energy production. It also does not require carbon capture and storage as needed for the most effective use of biomass, and for coal, oil or gas.

There is no equivalent to prompt criticality for fusion. If the pressure in the plasma were to rise, causing increased power output, the system would naturally quench due to physical limits to the plasma pressure.

There is radioactive decay heat in a fusion system, due to radioactivity induced in the material surrounding the plasma. A loss of coolant could result in damage to such components, but could not result in a core meltdown nor the process of self-disassembly seen at Chernobyl and Fukushima.

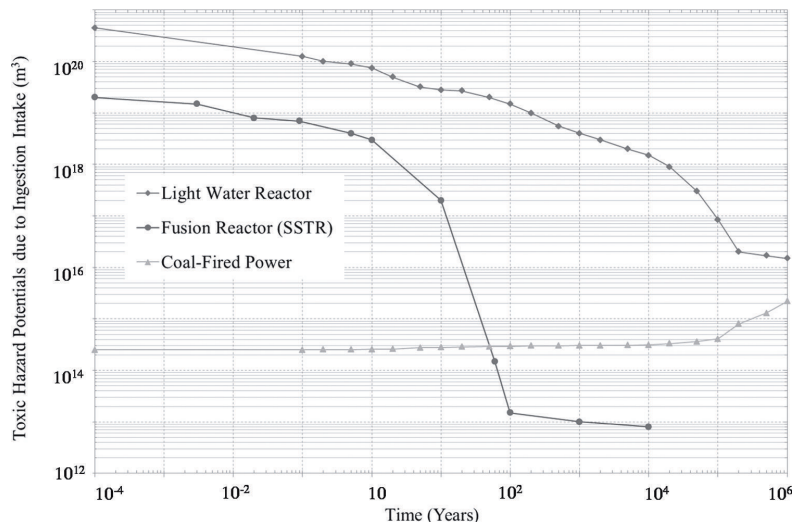


Figure 1.17 Toxic Hazard Potential from lifetime operation of 1 GWe fission LWR, a Japanese fusion power plant concept, SSTR, and coal power plant. Y-axis represents cubic meters of water in which system and waste must be dispersed to reach safe drinking level for all radioactive components. Source: Kikuchi and Inoue, 2002

The radioactive waste from fusion is much less dangerous than that from fission, and much less long-lived, as shown in figure 1.17. The y-axis of this figure, Toxic Hazard Potential, indicates the volume of water in which a ground-up power source and all of its waste would need to be dispersed so that the water would be considered drinkable. Fission reactors at Chernobyl and Fukushima have indeed exhibited the ability to distribute a significant

fraction of their radioactive constituents into the environment, in a manner that is impossible for fusion. After 50 years, fusion wastes drop below that associated with the waste from coal-fired plants, which is not considered a radiological hazard.

The proliferation risks associated with a safeguarded fusion power plant are qualitatively less than those associated with a safeguarded fission reactor. 14.1 MeV neutrons can be used to transmute ^{238}U to ^{239}Pu or ^{232}Th to ^{233}U , both of which are highly weapons-useable, but since these materials should not be present in any quantity in a fusion system, they should be straightforward to detect. It would be impossible to hide a “clandestine” fusion system capable of producing significant quantities of fissile material from 14.1 MeV neutrons. Finally, in a breakout scenario, it would be straightforward to disable a fusion power plant by military attack on any number of auxiliary systems, without risk of releasing radiation.

One can ask if fusion will be too late to contribute to constraining the maximum temperature rise to $< 2^\circ\text{C}$ above pre-industrial in the year 2100, as targeted by the IPCC. While near-term progress in controlling carbon emissions can be accomplished confidently with existing technologies, costs, risks of failure, and damaging side-effects may grow later in the century without the development of new technologies. Based on IPCC/EMF-27 projections (see figure 1.12), bio-energy plays a crucial role in the second half of the century since it serves as a net carbon sink. CO_2 absorbed by plants from the atmosphere is re-emitted when biomass is burned, but then most of it is captured and stored underground. However bio-energy is projected to require $\sim 40\%$ as much land area as is presently used for agriculture – in a world with growing population and per capita food demand. Carbon capture and storage (CCS), needed for both bio-energy and low-carbon energy production from other fossil fuels, is projected only to be adequate in volume and distribution if deep saline aquifers are employed later in the century. However R&D on CCS at the needed scale is only now beginning, and whether it will prove to be safe and effective is uncertain. Intermittent electricity sources, solar and wind, are projected to play a dramatically increasing role later in the century, but their effective cost increases as it becomes necessary to provide major enhancements to the electric grid, as well as large scale energy storage and/or large amounts of infrequently used highly dispatchable power. Substantial demand control is also required. Nuclear fission energy is projected to increase by a factor of about seven, but by mid-century will deplete known and projected reserves of uranium, especially in countries with high populations and low uranium reserves. This could lead to large-scale plutonium reprocessing, with its associated high nu-

clear proliferation risks. From this perspective, it is reasonable to conclude that while existing technologies are well suited to taking the near-term steps along the path to achieving the goals set out by the IPCC, R&D also needs to be aggressively pursued over a broad range of technologies, including fusion, for the longer term.

Question: The development of fusion, which may be needed in the second half of this century, is a long-term project that must be pursued today if the research investment is to “pay off” when it may be needed. How should we balance competition for government resources between projects like fusion R&D vs. loan guarantees and subsidies to support the near-term deployment of fission nuclear energy and renewables?

1.2.3 Scientific progress

Soon after WWII scientists and engineers began to consider non-explosive applications of nuclear power in earnest, including both fission and fusion. It is said that they considered magnetic confinement fusion in early meetings at Los Alamos, and Fermi proved that without the twist shown in figure 1.14 particles would not be confined by toroidal fields.

A period of innovation in magnetic confinement configurations followed, which was classified, because it was believed that fusion might be a means to provide the neutrons to produce large quantities of tritium for thermonuclear weapons, using $D + D \rightarrow T + n$. Soon, however, it became clear that large quantities of tritium were not needed, because, remarkably, equation 1.5 can be implemented inside of a thermonuclear weapon. The same heavy-water and graphite moderated fission reactors that were used to produce Pu could also produce the small amounts of T that were still required. Therefore the emphasis switched exclusively to power production and the $D + T$ reaction. In 1953 President Eisenhower announced the “Atoms for Peace” initiative, through which the US would share peaceful nuclear technology with the world. At the second Atoms for Peace conference, in Geneva in 1958, fusion energy research was declassified world-wide and an international collaborative (and sometimes competitive) effort to develop fusion energy began. Fusion provided one of the few channels of communication between Western and Soviet scientists during the Cold War.

A range of magnetic configurations was investigated, including not only toroidal configurations with much greater toroidal magnetic field than poloidal such as the tokamak, pursued in the USSR, and stellarator, pursued in the US, but also ones with higher poloidal field than toroidal, pursued mainly in

the US and in the UK. These are called “pinches” because the high plasma current is self-attracting (like currents attract) pinching the plasma together. A series of experiments at Los Alamos was whimsically named “Perhahpsatrons,” one of which is shown in figure 1.18. An alternative configuration, known as a “magnetic mirror” was also studied. Here the magnetic field was nearly linear, but higher in value at its two ends, to reflect particles back and forth, as will study in Chapter 10.

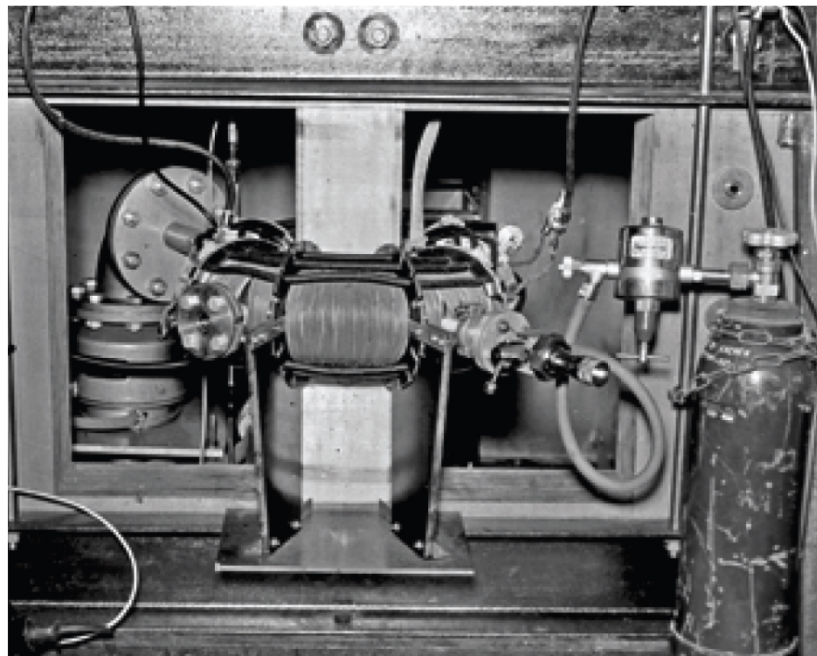


Figure 1.18 One of the early toroidal pinch experiments at Los Alamos, from the “Perhahpsatron” series.

The Soviets claimed that their tokamak plasmas were achieving much higher temperatures than the other configurations. In 1968 a British team visited the Kurchatov Institute in Moscow, bringing along a new plasma diagnostic that took advantage of the recently invented laser as an intense monochromatic and highly collimated light source. This technique, based on scattering laser light off of plasma electrons to measure their velocity distribution, was, and remains, the gold standard for measuring electron temperature. The British found that the Soviet T-3 tokamak achieved electron temperatures above 1 keV, with the very modest plasma heating power that resulted from resistive dissipation of the plasma current = $I_p^2 R$, where I_p is the plasma current and R the small electrical resistance of the plasma.

This was a better result than had been claimed by the Soviet team, and much better than had been achieved in stellarators, pinches and mirror machines.

After these results were reported, most fusion research programs around the world turned to the tokamak configuration. However significant stellarator programs were maintained in Germany and Japan, because the stellarator is a more natural configuration for steady-state operation, as it does not require a plasma current to be sustained with external power. Programs in mirrors and various types of pinches persisted as well, although ultimately at a lower level.

In the intervening decades tremendous progress has been made in the performance of fusion plasmas and in understanding the physics of magnetic confinement, particularly in the tokamak configuration. Experiments in the US and Europe have produced over 10 MW of thermal fusion power, and over 15 MJ of thermal fusion energy. This has led to the current construction of the international ITER (latin for “The Way”) tokamak in southern France. The goal of this project is to produce 100’s of MW of thermal fusion power for hundreds of seconds, at a gain (fusion power divided by external heating power) greater than 10. The entities participating in this project include China, Europe, India, Japan, South Korea, the Russian Federation, and the United States, representing more than one-half of the world’s population. If this project succeeds, it will demonstrate that fusion can be harnessed at the commercial scale. If enough physics and engineering research is performed in parallel with ITER, the nations that do this work will be positioned to construct pilot fusion energy projects capable of putting net electricity on the grid.

It is useful to briefly review the progress in fusion science and technology, and consider the remaining challenges. As an organizing principle, we will follow the power flow through a magnetically confined plasma, and then touch briefly on inertial confinement fusion.

Plasma heating and current drive

To achieve useful levels of fusion power density, plasmas must be heated to very high temperature, as shown in figure 1.19. This figure shows fusion power per cubic meter, p_{fus} , as a function of temperature. The pressure of pure fusion fuel plus charge-neutralizing electrons is set equal to 1 MPa. (This is very close to 10 atmospheres.) In computing the plasma pressure it is assumed that $T_e = T_i = T$. In addition to its variation with T shown in the figure, p_{fus} rises as the square of the particle density, at fixed temperature. This is because, again at fixed temperature, the rate of close encounters between reactants rises linearly with the density of each, which are assumed

to be proportional to the total density. Thus, at fixed and equal ion and electron temperatures, the fusion power density rises as the square of the pressure, and can be simply scaled by $(\text{Pressure}/1 \text{ MPa})^2$ from figure 1.19.

The center of the ITER plasma will be at a thermal pressure, $n_e T_e + n_i T_i$, of about 1 MPa, as used in the figure, but much of ITER's volume will be at lower pressure and temperature (see for example the temperature profiles shown in figure 1.20). The major radius, R_0 , the distance from the axis of symmetry to the center of the plasma, will be 6.2m. The horizontal minor radius, a , the distance from the plasma center to its inner and outer edges, will be 2m, and its vertical minor radius, b , the distance from the plasma center to its top and bottom will be about 3.4m, for a total plasma volume of 840 m^3 . Thus its volume average power density with 500 MW(th) fusion power production will be about 0.6 MW/m^3 .

Incidentally, figure 1.19 also illustrates why the DT reaction is the most likely candidate for producing practical fusion energy. For example, for the same plasma pressure, the $p - {}^{11}\text{B}$ reaction produces about 2400 times lower power density. Not surprisingly, as we will discuss below, this has severe consequences for the possibility of self-sustainment as well.

As a very first question, it is eminently reasonable to ask if the required temperatures, as indicated in figure 1.19, can be produced in the laboratory. Remarkably, the answer is yes. Figure 1.20 shows electron and ion temperatures achieved in the Joint European Torus experiment in England with a heating mechanism, neutral beam injection, that predominantly heats the ions. The electrons are subsequently heated by collisions with the hotter ions. This is a dramatic improvement beyond the $\sim 1\text{-}2 \text{ keV}$ temperatures achieved with Ohmic ($I_p^2 R$) heating alone.

Neutral beam heating involves the injection of high currents of neutral, typically D^0 , atoms. A single modern neutral beam might inject 20 amperes of 100 keV deuterium atoms into a tokamak plasma, providing 2 MW of heating. (The case shown in figure 1.20 had a total of 20 MW of heating power.) Neutral deuterium atoms travel easily across a magnetic field, and then are ionized by collisions with ions and electrons in the plasma. Now they are confined as charged deuterons, and transfer their energy to the bulk plasma. In general this occurs by simple binary collisions, but under some circumstances the fast ions can drive up instabilities. These conditions are now well understood, and even the nonlinear consequences of the fast ions interacting with the instabilities they drive have been characterized and compared successfully with theory. These experiments and the associated theory provide a basis for projecting that in most conditions ITER's injected fast ions and α particles from fusion will thermalize by binary collisions. We

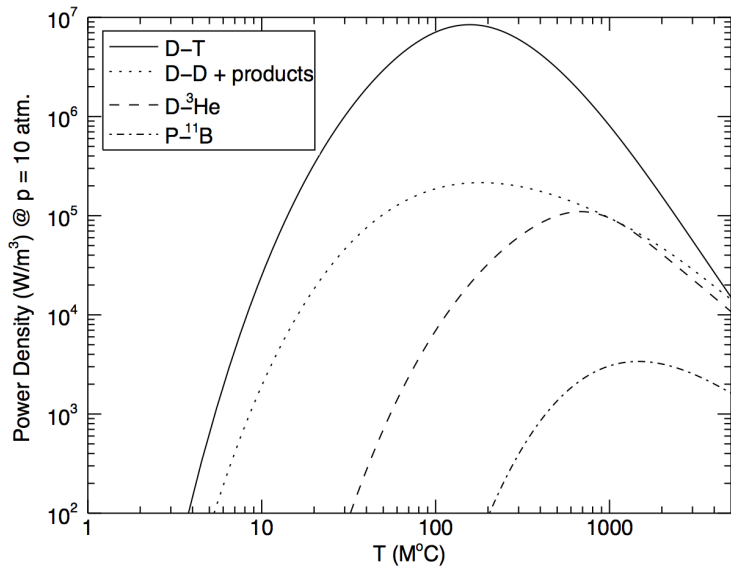


Figure 1.19 Fusion power density as a function of plasma temperature. In all cases the plasma particle kinetic pressure, $n_e T_e + n_i T_i$, is fixed at 1 MPa, about 10 atmospheres, and $T_i = T_e$ is assumed. For the DD reaction, it is assumed that the T and ^3He fusion products are burned as well.

will, however, be able to study conditions where instabilities are predicted to arise.

Other methods of plasma heating have also been developed, generally involving injecting radio waves that interact resonantly with the motion of the ions or the electrons, or even with a “hybrid” of the two motions. The interaction of these waves with the plasma, including how they heat the plasma electrons or ions preferentially and even drive current in the plasma, is well understood theoretically and confirmed experimentally. There are some challenges, however, in optimizing the efficiency of launching waves into the plasma, especially ones with large wavelength, so large launching structures. But the bottom line is that we are now quite confident that we will be able to drive ITER plasmas to the temperatures required for fusion.

Experiments on the Tokamak Fusion Test Reactor, TFTR and the Joint European Torus, JET, the two tokamaks which have operated in deuterium-tritium, have even shown the beginnings of heating by fusion alpha particles.

The current in the ITER plasma can be sustained by the electric field from the central solenoid for about 400 seconds, but then the solenoid will

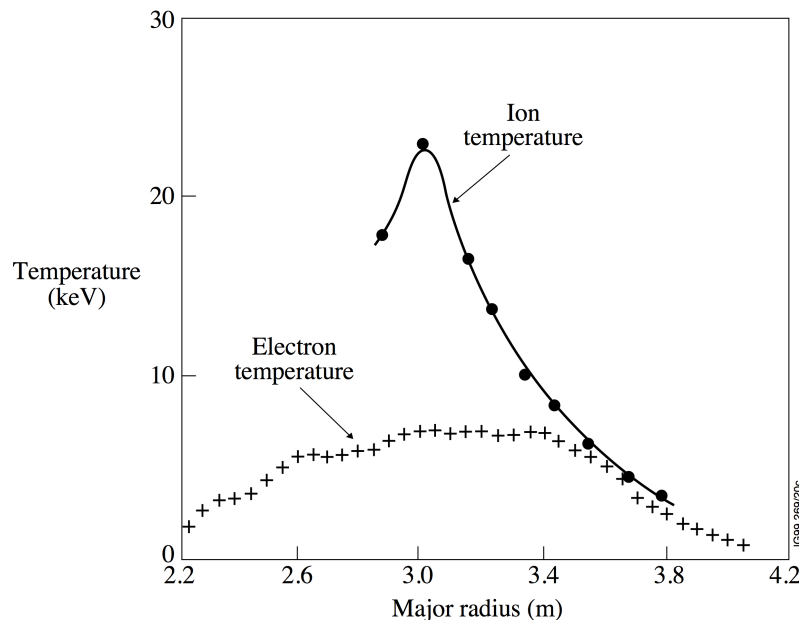


Figure 1.20 Measured ion and electron plasma temperature profiles in the Joint European Torus, across the horizontal midplane. Center of the plasma is at 3m major radius, horizontal minor radius is about 1.2m. (1 keV = 11.6M K).

reach its maximum current and magnetic field. No more dB/dt of the desired sign, so no more useful toroidal electric field, will be available. For the pulses of up to 3000 seconds planned for ITER, and even longer for a tokamak fusion power plant, it will be necessary to drive the current by external means. Getting the necessary efficiency of external current drive from radio waves and/or neutral beams, and taking advantage of the natural self-driven “bootstrap” current (see Chapter 10) in the tokamak, so that not too much fusion power needs to be siphoned off to sustain the plasma current, are challenges that will be studied using ITER and as well as smaller non-DT tokamak experiments. The stellarator, on the other hand, does not have this challenge and is being studied in parallel. Alternatively, one could operate a tokamak with long pulses, recharging the solenoid between pulses. This has the disadvantage of more frequent time-varying thermal and mechanical stresses.

Macroscopic Stability

Early in the study of fusion plasmas, the biggest challenge was holding the plasma from going macroscopically (large scale) unstable, in effect flinging itself to the walls of the vacuum chamber. Figure 1.21 shows an early British toroidal pinch plasma going unstable and doing exactly that, because of the very high energy in the poloidal field relative to that in the toroidal field. This results in a virulent “kink” instability, as we will study in Chapter 12. Tokamaks are much, much more kink-stable than pinches, because the strong toroidal field provides the plasma with the stiffness needed to resist bending or kinking. If the plasma current profile develops too strong a spatial gradient, however, this gradient can nonetheless drive significant macroscopic instabilities in tokamaks, even resulting in the rapid termination of the plasma, called a “disruption.” Disruptions can generally be avoided, but when they do occur they may damage internal components, particularly at the high plasma current, 15 MA, planned for ITER. This will be a very important area of study and – again – the backup is the stellarator, which can be designed to have no plasma current and, based on current understanding, no violent disruptions.

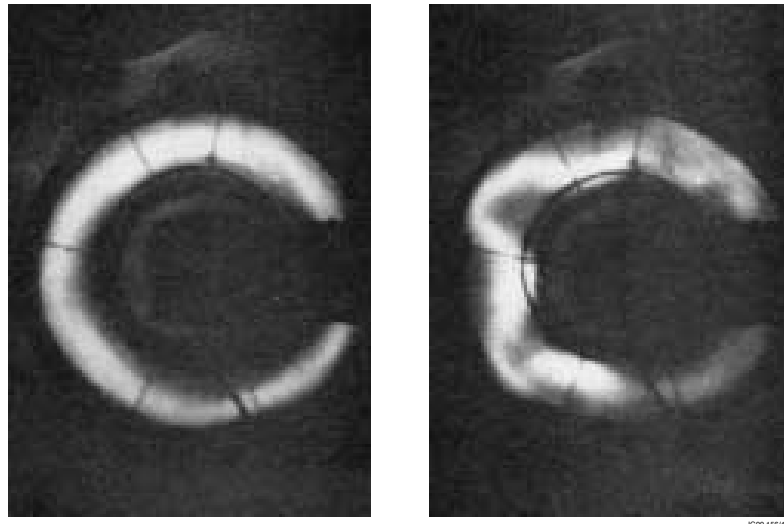


Figure 1.21 Image of a small pinch experiment early in its development, and then after a kink instability has grown up.

Macroscopic instability can be driven not only by poloidal magnetic energy density due to the plasma current, but also by plasma stored energy

density, or pressure. A key parameter that characterizes plasma stability as a function of pressure is β , the ratio of plasma pressure to magnetic pressure, discussed in Chapter 11.

$$\beta \equiv \frac{p}{B^2/2\mu_0} \quad (1.7)$$

(It can be confusing that the same variable, p , is used both for pressure and power density. We will mitigate this unavoidable problem by *always* providing a descriptive subscript for power density.)

Generally magnetic configurations are characterized by a β limit, above which the plasma pressure will distort the configuration and allow the confined plasma to escape rapidly. Most aspects of these limits are now well understood for tokamaks, both experimentally and theoretically. Conventional tokamaks, with $R_0/a \sim 3$ have achieved $\beta_t \sim 10\%$, while low aspect ratio tokamaks, or spherical tori, have achieved $\beta_t \sim 40\%$, where the t subscript indicates that only the toroidal field is included in the denominator of β . ITER is designed to achieve 500 MW(th) of fusion power at conservative values of $\beta \sim 2.5\%$. A cost-effective fusion power source with the size of ITER will need to make more fusion power than this however, and one option will be to operate at higher values of β , closer to the known limits. This will be studied in ITER and in other experimental devices around the world.

Interestingly, since fusion power density, p_{fus} , rises as the square of pressure, p^2 , at fixed T , and p rises as B^2 at fixed β , fusion power density rises as B^4 at fixed T and β . Thus another approach to achieving higher fusion power at fixed system size is to operate at higher magnetic field. The new high temperature superconductors, such as YBCO, when operated well below their maximum operating temperature, allow higher current densities than present low-temperature superconductors, such as NbSn. These may permit operation at higher magnetic fields and so higher power density without approaching β limits too closely, but more R&D is needed to determine how to take advantage of the properties of this material, and how much advantage can be gained. For example, the critical current density for losing superconductivity is highly sensitive to the orientation of the magnetic field at the conductor. Ultimately, of course, the maximum attainable field will be limited by the strength of the material used to construct the coil.

Question: ITER is planned to operate with a toroidal magnetic field of 5.3 T. If that field could be increased to 7 T, roughly how much fusion power could it make at the same value of β ?

Energy confinement

Referring back to figure 1.19, we can see that the maximum DT fusion power density as a function of temperature in a pure DT plasma with $T_i = T_e = T$, and a particle kinetic pressure of 1 MPa, is about 8 MW/m³. The ideal gas ratio of 3/2 between energy density and particle kinetic pressure is appropriate for magnetic fusion plasmas, because they have little energy stored in the electrostatic fields around the individual charged particles and in the electromagnetic radiation field within the plasma. Thus a magnetic fusion plasma with a kinetic particle pressure of 1 MPa has an energy density of 1.5 MJ/m³. In a practical situation with a finite-size plasma, energy density is continually leaking away, both by thermal transport carried by charged particles leaving the plasma and so draining heat from both the electrons and the ions, and also by radiative loss carried by photons leaving the plasma draining heat from the electrons, as we will discuss in more detail in Chapters 9, 13 and 14. Together these two losses constitute a loss power density, p_{loss} . Let us define a characteristic “energy confinement time,” τ_E , as the ratio of the stored energy density to the loss power density, a quantity which has units of time. Specifically, this is the time it would take for the loss power density to drain away all of the energy density, if the loss power density did not change as the plasma cooled and/or rarified.

$$\tau_E \equiv \frac{(3/2)(n_e + n_i)T}{p_{loss}} \quad (1.8)$$

Now we consider that in a useful, steady-state DT fusion plasma p_{loss} must be largely compensated by the alpha particle power density, p_α , produced by fusion, since we probably cannot afford to resupply all of the heat needed for steady-state power balance externally. Let us therefore equate the alpha heating power density with a fraction, f_α , of the power loss density from the plasma:

$$p_\alpha = f_\alpha p_{loss} \quad (1.9)$$

Substituting p_{loss} derived from equation 1.9 into equation 1.8 and recognizing that $n_e = n_i = n$ for a pure DT plasma, we have:

$$\tau_E = \frac{3nT}{p_\alpha/f_\alpha} = f_\alpha \frac{p_{fus}}{p_\alpha} \frac{3nT}{p_{fus}} = f_\alpha \frac{15nT}{p_{fus}} \quad (1.10)$$

where we have recognized that $p_{fus}/p_\alpha = 5$ holds for the DT reaction. Remembering that, with our definitions, $p = 2nT$, we can read from figure 1.19 that the minimum needed τ_E for full self-sustainment, $f_\alpha = 1$, of a pure DT plasma at a pressure of 1 MPa is a little under one second, at T

somewhat above 100M K:

$$\tau_E = f_\alpha \frac{15 \cdot p}{2 \cdot p_{fus}} \approx \frac{7.5 \cdot 10^6}{8 \cdot 10^6} \quad (1.11)$$

Next it is helpful to remember that p_{fus} and p_α scale as the square of the plasma pressure, p^2 , at fixed T . This gives us

$$\tau_E = f_\alpha \frac{15nT}{p_{fus}(1 \text{ MPa}, T)} \left(\frac{1 \text{ MPa}}{2nT} \right)^2 \quad (1.12)$$

as the condition for the minimum energy confinement time required for f_α fractional self-sustainment. This translates to a requirement on the “fusion triple product”, $nT\tau_E$:

$$nT\tau_E = f_\alpha \frac{(15/4)(1 \text{ MPa})^2}{p_{fus}(1 \text{ MPa}, T)} \quad (1.13)$$

For a given desired f_α there is a minimum requirement on $nT\tau_E$ as a function of temperature. This optimum occurs at the temperature where p_{fus} is maximum at fixed pressure. Thus this triple product is a measure of the approach to self-heating, assuming the optimum temperature can be achieved. Figure 1.22 shows progress over time on this parameter in tokamaks.

Figure 1.22 has some features that bear explanation. First, since it is not addressing local power balance, but attempting to characterize global fusion performance, it needs some simple way to characterize the $nT\tau_E$ of the particular plasmas measured. The parameters listed in the figure caption do a reasonable job of defining a global $nT\tau_E$ that is proportional to the global f_α . You will note, however, that the curves on the plot are labeled by the global fusion gain, Q , which is defined as $Q \equiv P_{fus}/P_{ext}$, where P_{ext} is the total externally applied heating power. The relationship between global f_α and global Q in a steady state DT plasma is simple:

$$f_\alpha = \frac{P_\alpha}{P_{loss}} = \frac{P_{fus}}{5P_{loss}} = \frac{P_{fus}}{5(P_{ext} + P_\alpha)} = \frac{P_{fus}}{5P_{ext} + P_{fus}} = \frac{Q}{Q + 5} \quad (1.14)$$

Thus $Q = 1$ corresponds to $f_\alpha = 1/6$, $Q = 10$ to $f_\alpha = 2/3$ and $Q = \infty$, or full ignition, to $f_\alpha = 1$.

The upper left region is “inaccessible” because of unavoidable radiation of photons from the electrons. When electrons encounter nuclei they are deflected, which amounts to a form of acceleration, and accelerating electrons radiate energy. This process is analogous to how an energetic electron beam stopping in a high-Z material makes X-rays, so it is called “bremsstrahlung”, German for “stopping radiation.” Magnetic fusion plasmas are transparent

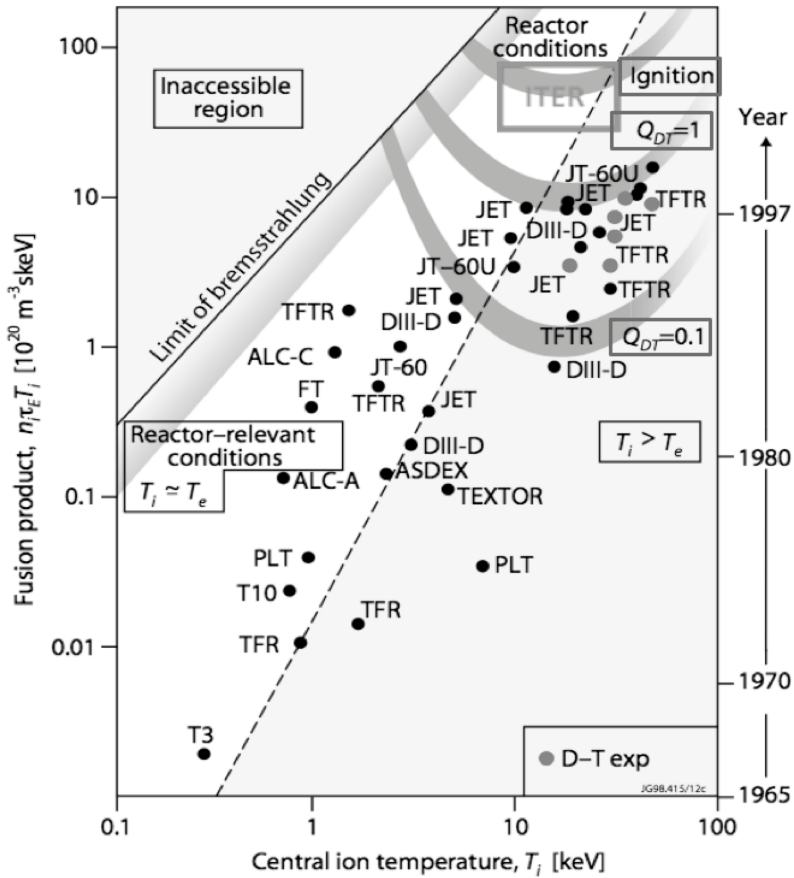


Figure 1.22 $nT\tau_E$ in tokamaks, where n_i here is the central hydrogenic ion density, $n_H + n_D + n_T$, T_i is the central ion temperature and τ_E is the energy confinement time defined over the full volume of the plasma. Data points are labeled by the experimental tokamak devices on which they were measured, and DT cases are indicated by gray dots. All other cases are DD.

to this radiation, so it is an unavoidable loss mechanism that limits $nT\tau_E$ as a function of T .

The lower right region is the region where the energy confinement time is less than the time it takes ions and electrons to equilibrate in temperature through collisions, so this is a region where, with dominant ion heating, $T_i > T_e$. It is not completely accurate to say that this region is not reactor-relevant, since you can see that the ignition region, $f_\alpha = 1$, straddles the boundary of this region. However, unless extraordinary measures are taken, the alpha particles from fusion mostly transfer their energy to the electrons

in the plasma, so in this region in a fusion power system we are likely to see, if anything, $T_e > T_i$. However many of the experimental data points to right on the plot have powerful ion heating, so $T_i > T_e$.

It is worth noting that only tokamaks are shown on this plot. Stellarators have achieved parameters towards the middle of the plot, as have very low aspect ratio ($R_0/a \leq 2$) tokamaks, sometimes called Spherical Tokamaks or Spherical Torii. Other devices, various kinds of mirrors and toroidal pinches with different amounts of toroidal field relative to poloidal field, have not yet achieved the $nT\tau_E$ measured in T-3 fifty years ago. On the other hand, they generally have less externally supplied magnetic energy than T-3, and they each offer potential advantages in their power-plant implementation relative to tokamaks.

Question: Some fusion researchers are interested in pursuing the reaction $p + {}^{11}\text{B} \rightarrow 3\alpha + 8.7\text{ MeV}$ because it does not produce neutrons nor does it require tritium breeding. We noted before that for fixed plasma pressure the power density from $p + {}^{11}\text{B}$ is ~ 2400 times lower than from D + T. How much higher is its required $nT\tau_E$? On the positive side, note that unlike the DT reaction, all of its fusion products are charged, and so can be counted as heating the plasma.

While figure 1.22 shows dramatic progress over time, it is important that this progress be consistent and predictable, something that you cannot tell from the figure. Empirical trends in the data already observable in the early 1980's accurately predicted the performance of the next generation of much larger devices that began to produce significant experimental results in the late 1980's and beyond. Now, taking all of the data together, a highly consistent database has been accumulated that predicts that ITER will have the desired performance, as shown in figure 1.23. Remarkably, and to the credit of the both the researchers operating these experiments and those making the measurements, the RMS error of this fit is only about 12%.

The experimental progress discussed so far required the construction of a series of experimental facilities of increasing size. Figure 1.24 shows the largest current tokamak, about twice the size of the devices studied in the 1970's, and half the size of ITER. In parallel with this, however, possibly even more impressive progress has been made in understanding the physics of the small-scale nonlinear turbulence that drives thermal transport in tokamaks. Now massively parallel computer simulations predict the thermal transport in the hot core of tokamak plasmas with good accuracy. In the 1980's the best calculations typically predicted an order of magnitude too much transport in the hot core of the plasma, and an order of magnitude too little transport at

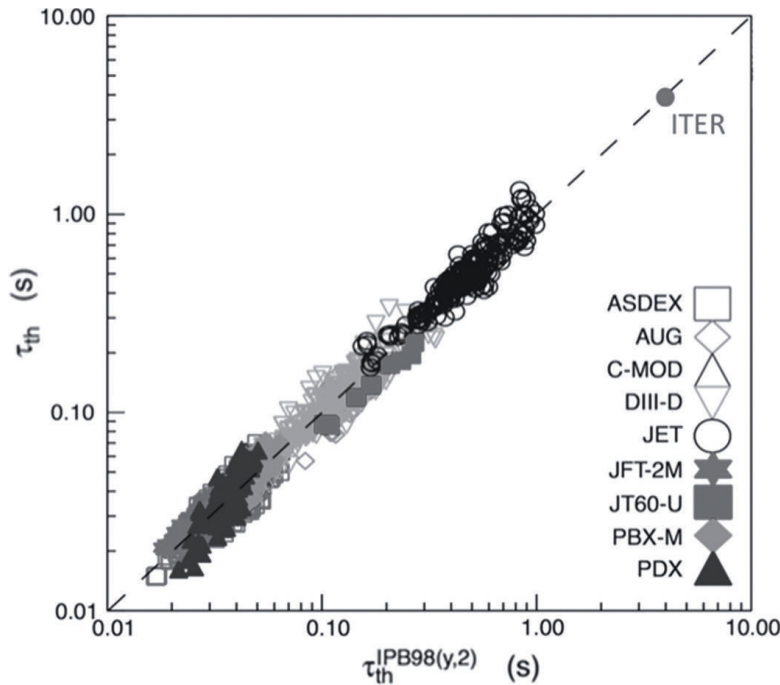


Figure 1.23 Measured energy confinement time, defined as thermal stored energy divided by heating power, on tokamaks world-wide, vs. regression fit.

the cooler edge. A combination of theoretical insight and massively parallel computing power has completely turned this situation around, as discussed in Chapter 14. The results from ITER will provide a very strong test of the empirical regression fits and especially of the theoretical projections. ITER should “nail down” experimentally the confinement in large-scale tokamaks in a manner that could not be done by any other means.

Power efflux

If a DT plasma is successfully heated to fusion temperature, and then it holds onto the power from the alpha particles produced by fusion well enough that a steady high-temperature burn is established, there will be a strong flow of power out of the plasma, equal to the total stored energy in the plasma divided by the global confinement time. This power flow needs to be handled on material surfaces without damage to plasma-facing components, or impurity influx to the fusion plasma that would deteriorate its performance. If a fusion power plant plasma produces 2500 MW of fusion power at $Q = 25$,

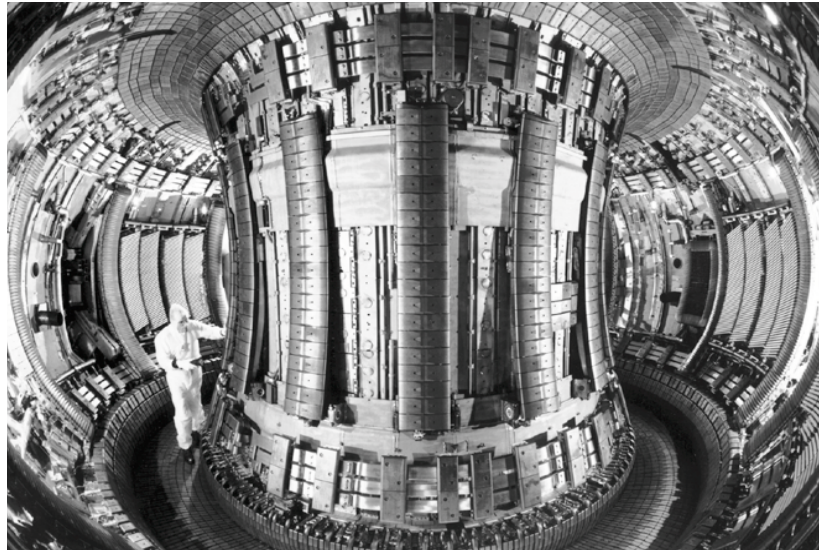


Figure 1.24 Joint European Torus. $R_0 = 3\text{m}$, $a = 1\text{m}$.

it necessarily produces 600 MW of loss power. (We leave the neutrons to the next section.) A favorable aspect of magnetic confinement is that magnetic fields are very effective at holding heat in the main plasma. Unfortunately this quality of magnetic confinement extends to the plasma on the field lines in the “scrape-off layer”, or SOL, just beyond the edge of the magnetically confined plasma.

As shown in figure 1.25, and discussed in Chapter 15, the magnetic field lines just outside the edge of the main plasma divert the SOL plasma away from the main plasma towards material surfaces in the “divertor” chamber, which is generally at some distance. A divertor chamber is visible at the bottom of figure 1.24. The plasma flows into the divertor chamber at a fraction of the ion thermal speed, and during the time it takes to get to the divertor target, where it first contacts a material surface, it spreads very little. Recent detailed experimental measurements and a relatively simple “heuristic” theory that matches the data well, indicate that the spreading may be as little as 1 – 2 mm in ITER. The thermal loss power in ITER with 500 MW of fusion power at $Q = 10$ is only 150 MW, and the duty factor (fraction of operational time) will be less than $\sim 5\%$. While challenging, it appears that at these parameters the heat flux can be handled by intercepting the field lines at a glancing angle, as planned. ITER’s plasma-facing components will also need to handle the transient power efflux from the plasma during disrupt-

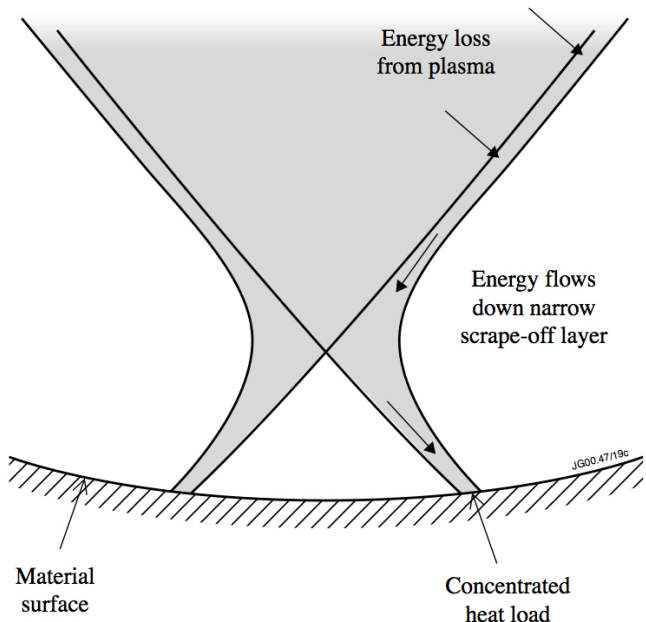


Figure 1.25 Plasma crosses edge of confined plasma into scrape off layer, and is directed to material surfaces.

tions and during bursts of loss from near the edge of the plasma, called Edge Localized Modes. Research is ongoing on means to suppress these transient heat fluxes and to spread the steady heat flux in a fusion power plant with four times higher thermal loss power and near-continuous service. These are problems that will need to be solved by research on ITER and in parallel with ITER operation.

Materials and blanket

As discussed in Chapter 16, the 14.1 MeV neutrons produced by DT fusion are much more energetic than the neutrons even in fast-spectrum reactors. For the most part, however, the damage to materials is similar, because the individual clusters of atomic displacements are very similar. A significant difference, however, is that 14.1 MeV neutrons cause many more (n,α) reactions, reactions in which a neutron is absorbed and a helium nucleus (or α particle) is emitted. The helium gas that accumulates as a result in steels and other materials to be used in a fusion power plant can cluster in bubbles along the boundaries between different crystal grains in the material, and cause the material to become very brittle. New steels, however,

are being developed with nano-inclusions dispersed within the crystal grains themselves. These inclusions, for example of yttrium oxide, make the steel tougher. Interestingly, they also scavenge helium atoms, and prevent them from accumulating at grain boundaries.

Europe and Japan are working together on the design and R&D for an International Fusion Materials Irradiation Facility, IFMIF, which should provide the neutron fluence needed to irradiate test samples to qualify materials for fusion applications.

In addition to materials that can stand up to the neutron flux, fusion systems will require “blanket” systems constructed of these materials that can absorb the heat from neutrons and transfer it to coolant systems, preferably at high temperature for high efficiency electricity production. These blankets must also multiply neutrons and breed tritium using lithium. ITER will have six test-blanket modules for testing different engineering approaches. ITER will not, however, provide a fluence (flux x time) of neutrons that approaches what a power plant will produce, so the next step facility in the development of fusion, perhaps an energy-producing pilot plant, will need to address this issue, using blankets constructed from materials qualified in an irradiation test facility such as IFMIF.

Magnets

The superconducting magnets for ITER are at the full scale that might be anticipated for a fusion power plant, and produce the magnetic field strength that is called for in some designs. One could say that the practical knowledge that the world is developing from construction of the ITER magnets will complete the magnet technology development needed for fusion. This may be so, but modern high-temperature superconducting magnets may be able to support higher current densities than the magnets now being wound for ITER. As noted before, if this can lead to higher fields, one may be able to make more compact and less expensive fusion systems, so R&D in this area for fusion could be very valuable.

Inertial confinement fusion

Very soon after the laser was invented in 1960, the idea was conceived that a small sphere of frozen DT could be compressed and heated to fusion temperature using this new technology, and so produce net energy. The research to test this new idea was pursued in the U.S. using a series of more and more powerful laser systems, with the primary policy motivation to study the closely related physics of nuclear weapons. The U.S. scientists, however, were also motivated by energy applications, as was a team in Japan.

Two barriers were found to producing significant amounts of fusion energy using high-power lasers. First, when the laser light traverses the plasma that is inevitably produced outside the frozen DT sphere, it can drive up waves in that plasma that deflect the incoming laser beams or even produce energetic electrons that prematurely heat the frozen DT gas. The former is obviously problematic, and the latter makes it more difficult to compress the fuel adequately, since it has too high a pressure to begin with, and pushes back. Second, the best kind of target for inertial confinement fusion is a thin, hollow sphere of fuel, and it is very hard to compress rapidly a very thin, hollow shell without breaking it up. If the originally spherical shell breaks into pieces, it does not fly inwards symmetrically and the kinetic energy per unit mass invested in the motion of the material won't show up as heat and pressure at the exact geometric center of the original sphere. This is what is needed to cause fusion in a small, central "hot spot" containing only a few % of the fuel, which is then to drive a propagating burn wave through the remaining fuel.

When more energetic lasers are used, it is possible to implode heavier shells, with less acceleration, and so suffer less from instability. Experiments with the current generation of lasers in the National Ignition Facility (NIF), capable of providing about 2 MJ of laser light in 20 nsec, continue to suffer from these two problems. The first round of experiments on NIF clearly pushed the shell far too hard, and achieved only about 2.5 kJ, $\sim 0.125\%$ of the stated goal of 2 MJ. This goal had been dubbed "ignition," in a very different sense from ignition in magnetic fusion. If the hot spot in the core of an inertial confinement pellet starts to burn, this is analogous to a match being lit under a pile of logs. If the match sets the fuel on fire, that could be called igniting the fire. When the analogous process occurs, the compressed but initially cold fuel begins to burn due to heating from the hot spot, that is what is called "ignition" in inertial confinement fusion, and the production of 2 MJ of fusion energy would be a good sign of this. Experimenters on NIF in late 2013 tried pre-heating the shell with an early laser pulse so it compressed more weakly, and achieved much more symmetric implosions and about 10x higher fusion output, but still only about 1.3% of the goal. It was a nice accomplishment, however, that the fusion energy produced was greater than the small fraction, less than 1%, of the laser energy that was originally deposited in the DT fuel. One could say that these experiments demonstrated that an inertial confinement fusion match has been lit in the laboratory, but this has not yet resulted in a burn wave in the accumulated fuel.

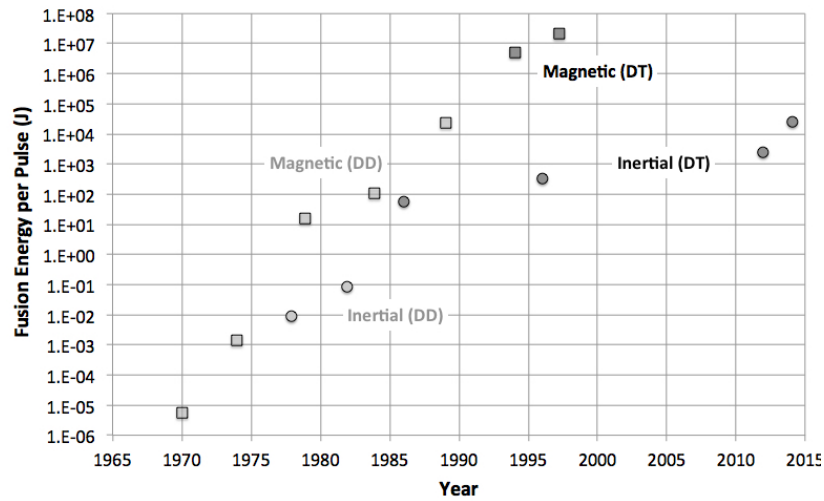


Figure 1.26 Fusion energy produced per pulse in magnetic and inertial fusion, both in deuterium-only (DD) plasmas and in DT plasmas. ITER is designed to produce $> 200,000$ MJ of fusion energy, while NIF is designed to produce > 2 MJ.

Measured fusion energy production per pulse from magnetic and inertial confinement fusion experiments are shown in figure 1.26.

1.2.4 Prospects

The ubiquitous joke about fusion energy is that it is always 20 years away. At the same time the facts show that rapid progress has been made in fusion R&D. Certainly the early pioneers underestimated the difficulty of mastering the science of plasma physics (vis., the “Perhapsatron”), and at later times fusion researchers made projections that depended on funding levels that did not materialize. Four of the ITER partners, China, Europe, Japan and South Korea have articulated specific plans for major next steps, in some cases even before DT results from ITER will be available. As we discuss in Chapter 18, R&D is needed in ITER and in parallel with ITER on the issues discussed above, in particular steady-state operation either by current drive in tokamaks or via stellarators, means to handle the very high heat fluxes that emerge from fusion plasmas, and validation of new materials for use in the high flux of energetic neutrons. But with success in these endeavors it should be possible for the next generation of major fusion devices to put net fusion electricity onto the grid.

Review**Resources**

- World Nuclear Association
Descriptive material on fission energy technologies.
<http://www.world-nuclear.org>
- International Institute for Applied Systems Analysis, Global Energy Assessment, Chapter 14: Nuclear Energy.
Critical evaluations of fission and fusion energy technologies.
<http://www.iiasa.ac.at/web/home/research/Flagship-Projects/Global-Energy-Assessment/Chapte14.en.html>
- IAEA Nuclear Technology Review 2015, Report by the Director General
Annual review of IAEA-related developments in nuclear technology.
https://www.iaea.org/About/Policy/GC/GC59/GC59InfDocuments/English/gc59inf-2_en.pdf
- OECD-NEA/IAEA Uranium 2014: Production, Resources and Demand
Generally semi-annual assessment of uranium production, resources and demand.
<https://www.oecd-nea.org/ndd/pubs/2014/7209-uranium-2014.pdf>
- Joint Comprehensive Plan of Action
Example of extreme constraints and safeguards applied to Iran.
<http://www.state.gov/e/eb/tfs/spi/iran/jcpoa/>
- Climate Change, Nuclear Power, and Nuclear Proliferation: Magnitude Matters
Assessment of proliferation risks associated with a large expansion of fission energy, possible role of fusion energy.
R.J. Goldston, Science and Global Security 19:130–165, 2011
DOI: 10.1080/08929882.2011.589223
- The World Scientific Handbook of Energy, G.M. Crawley, Editor, World Scientific, 2013, ISBN: 978-981-4343-51-0
Assessemnt of many energy sources, including fission and fusion
- FUSION: Science, Politics, and the Invention of a New Energy Source, J.L. Bromberg, MIT Press, 1982
History of the intertwined science and politics of fusion R&D through 1978
- A Piece of the Sun: The Quest for Fusion Energy, D. Clery, Overlook Duckworth, Peter Mayer Publishers, 2013, ISBN-13: 978-1468304930
More up-to-date history of fusion R&D, with less emphasis on the pioneers.

Exercises

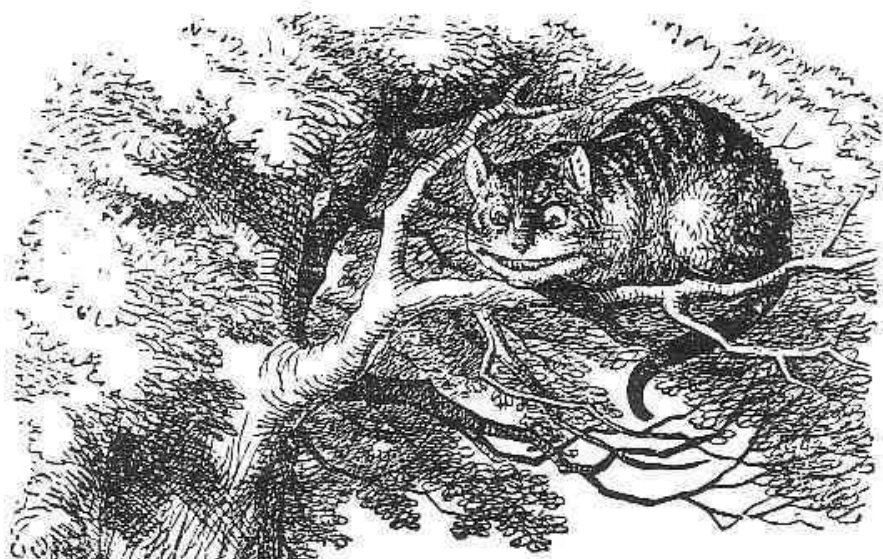
- 1.1 Sitting on the tree trunk with Lise Meitner
- 1.2 Chemical energies vs. nuclear energies
- 1.3 Thermal ion energies, in the frame of one of them
- 1.4 etc., etc.

PART ONE

FISSION

Chapter 2

Neutron Interactions with Matter



“All right,” said the cat; and this time it vanished quite slowly, beginning with the end of the tail, and ending with the grin, which remained some time after the rest of it had gone.

Lewis Carroll, Alice’s Adventures in Wonderland

In this chapter we will learn how neutrons interact with matter, such as hydrogen and uranium nuclei. For the most part we are interested in fission, absorption and scattering. But first we review the concepts of beam attenuation, mean free path and reaction rate in a hard-sphere classical context. Then we touch on some ways in which we can understand how the Alice-in-Wonderland effects of quantum mechanics play a role in nuclear physics, and finally we look at the specific processes of interest for producing nuclear energy from fission.

2.1 Cross-sections

Consider a collection of small, hard spheres, say BBs, flying through a randomly distributed field of larger stationary billiard balls, as illustrated in figure 2.1. Let's say the radius of the BBs is 2mm, and that of the billiard balls 30mm. The projection of the billiard balls, along any angle, is of course a circle of radius 30mm. However if the center of one the BB's is headed to within 32mm of the center of a billiard ball, if nothing else happens first, they will interact. Thus we define the effective cross-sectional area for this interaction, or effective cross-section, as $\pi \cdot 0.032^2 m^2$. The more general expression for hard spheres is $\sigma = \pi(r_b + r_t)^2$, where we consider the BBs to form a “beam” of moving hard spheres all going in the same direction, denoted by subscript b , and the billiard balls to form a “target” of stationary particles, denoted by subscript t . In nuclear reactor theory, this σ is called the “microscopic” cross-section.

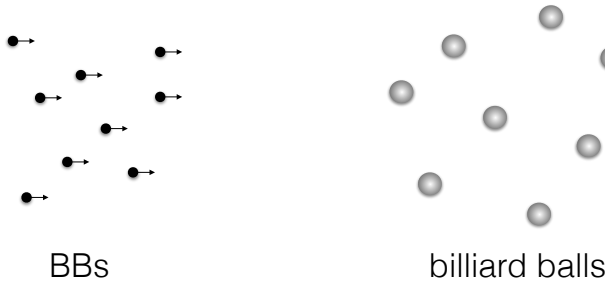


Figure 2.1 BBs flying into a field of billiard balls.

Now suppose that the density of billiard balls is N_t , with units m^{-3} . Consider that the billiard balls are very much further apart than their diameters, and they are randomly distributed in space. Furthermore, for mathematical simplicity, let us assume that the BBs are all flying along precisely in the x direction. Now consider some differentially small incremental distance along their flight path amongst the billiard balls, dx . The meaning of “differentially small” is that differential values are as small as necessary to make any terms that vary as $(dx)^2$ negligibly small compared with those that vary as dx . The expected number of billiard balls in the volume formed by a macroscopic area of A square meters, in the $y - z$ plane, and depth dx in the x direction, is just $N_t A dx$. The sum of all of the cross-sectional areas of each billiard ball is $N_t \sigma A dx$. If we can ignore the possibility that cross-sections overlap, the fraction of the beam that will collide, and so be taken out of the mono-directional beam of BBs, in length dx is $N_t \sigma A dx / A = N_t \sigma dx$. So

long as this value is sufficiently small, which can be achieved by making dx sufficiently small, i.e., differential, we can ignore overlaps. This is because an overlap requires, in effect, two collisions along a given straight-line trajectory, and so has probability $(N_t\sigma dx)^2$. In nuclear reactor theory, $N_t\sigma$ is called the “macroscopic” cross-section of the target, $\Sigma_t \equiv N_t\sigma_t$.

Question: What can happen if the billiard balls are arranged in an orderly, rather than random, fashion? Qualitatively, what happens if randomly distributed billiard balls are moving much faster than the BB’s?

2.2 Beam attenuation and mean free path

Now what happens to the density, which we denote n_b , of our beam of BBs as it travels through the field of billiard ball target particles? From the argument in the last section we can say that $\delta n_b/n_b = \Sigma_t \delta x$ or $\delta n_b/\delta x = \Sigma_t n_b$. If we are considering macroscopic distances, this process is well approximated by the common differential equation that describes attenuation in an absorbing medium:

$$\frac{dn_b}{dx} = -\Sigma_t n_b \quad (2.1)$$

The solution to this equation is well known:

$$n_b(x) = n_0 e^{-x\Sigma_t} \quad (2.2)$$

where n_0 is evidently the value of n_b at $x = 0$. If you are not familiar with this solution, you can check it simply by substituting it into equation 2.1.

We are going to find it useful to know the mean distance beam particles travel before they collide with a target particle. To find this we consider the average, over all the beam particles, of the distance they travel before they collide, which we will call the mean free path, λ_{mfp} . Consider that some differential chunk of beam density $dn_b = \Sigma_t n_b dx$ collides in each differential distance dx around location x . Multiply the differential chunk of beam density deposited near x by the local value of x . Integrating over all of these x -weighted differential chunks dn_b , and dividing by the integral of all of the chunks dn_b of beam density (without the factor of x) gives us the average distance to collision for all of the beam particles.

$$\frac{\int_0^{n_0} x dn_b}{\int_0^{n_0} dn_b} = \frac{\int_0^{\infty} x \Sigma_t n_b dx}{\int_0^{\infty} \Sigma_t n_b dx} = \frac{n_0 \int_0^{\infty} \Sigma_t x e^{-x\Sigma_t} dx}{n_0 \int_0^{\infty} \Sigma_t e^{-x\Sigma_t} dx} \quad (2.3)$$

To make progress we need to integrate the numerator of the last term by

parts, using

$$\int u dv = uv - \int v du; \quad u = \Sigma_t x; \quad dv = e^{-x\Sigma_t} dx; \quad v = -e^{-x\Sigma_t}/\Sigma_t; \quad du = \Sigma_t dx \quad (2.4)$$

giving us

$$\frac{\int_0^{n_0} x dn_b}{\int_0^{n_0} dn_b} = \frac{n_0 \left(-xe^{-x\Sigma_t} \Big|_0^\infty + \int_0^\infty e^{-x\Sigma_t} dx \right)}{-n_0 e^{-x\Sigma_t} \Big|_0^\infty} = \frac{n_0/\Sigma_t}{n_0} \quad (2.5)$$

Thus the “mean free path” is given by

$$\lambda_{mfp} = \frac{1}{\Sigma_t} \quad (2.6)$$

Incidentally, the calculation we did along the denominators has, reassuringly, shown us that the integral of all of the differential chunks of beam density dn_b from $x = 0$ out to infinity, where surely no beam density at all is left, equals the total beam density that entered the system at $x = 0$, n_0 .

2.3 Reaction rates

Sometimes we are interested in the rate at which collisions occur, rather than the distance over which they occur. A reaction with a given reaction rate coefficient is represented (not surprisingly) by a “rate” equation:

$$\frac{dn_b}{dt} = -\nu n_b \quad (2.7)$$

where ν is the reaction rate coefficient, in units of inverse seconds. We found dn_b/dx in equation 2.1, and we know that if we move along with the beam $dx/dt = v_b$, where v_b is the beam speed. Thus we can, if we like, consider beam attenuation in the framework of equation 2.7 by evaluating the total time derivative of the density, traveling with the beam. This will give us the rate at which the beam particles with which we are traveling are disappearing.

$$\nu = -\frac{1}{n_b} \frac{dn_b}{dt} = -\frac{1}{n_b} \frac{\partial n_b}{\partial x} \frac{\partial x}{\partial t} = \Sigma_t v_b \quad (2.8)$$

giving us an effective reaction rate coefficient $\nu = \Sigma_t v_b$. On the other hand, if the underlying physics is an interaction characterized by a rate coefficient ν , independent of the beam velocity, we can find an effective macroscopic cross-section for the interaction, Σ_t .

$$\Sigma_t = -\frac{1}{n_b} \frac{dn_b}{dx} = -\frac{1}{n_b} \frac{\partial n_b}{\partial t} \frac{\partial t}{\partial x} = \frac{\nu}{v_b} \quad (2.9)$$

The consequence of this is that if a particle interacts with a fixed reaction rate coefficient, independent of speed, the effective cross-section of the target particles gets larger as it goes slower, $\Sigma_t = \nu/v_b$. As we will see this $1/v$ dependence is common in low-energy nuclear reactions that involve the absorption of neutrons, because the absorption *rate coefficient* is generally independent of neutron energy at low energies.

Another quantity of interest is the “volumetric reaction rate,” the number of collisions per unit time, per unit volume. Appropriately, this has units, in SI, of #/(s m³). By the physical argument that loss in beam density is exactly reaction density, we have simply for the volumetric reaction rate:

$$-\frac{dn_b}{dt} = -\frac{\partial n_b}{\partial x} \frac{\partial x}{\partial t} = \Sigma_t n_b v_b = \Sigma_t \phi_b \quad (2.10)$$

where $\phi_b \equiv n_b v_b$ will turn out to be very useful in fission reactor analysis. Note that we didn’t use the fact that the beam was traveling in the x direction in this analysis, so it could have been going in any direction. Indeed ϕ_b could be composed of many beams traveling in all directions, each attenuating as it goes along. In particular \vec{v}_b could have been isotropically distributed. For all of these cases, the local volumetric reaction rate is just $\Sigma_t \phi_b$. When we have a range of neutron energies we will need to take into account the energy dependences of Σ_t and of ϕ_b . This, in essence, is the topic of the next chapter. But first let’s learn something about the Alice-in-Wonderland world of the quantum mechanics of atomic nuclei.

2.4 Elements of non-relativistic quantum mechanics

So far we have been working with BBs and billiard balls, at the familiar spatial scale of millimeters and centimeters. However, if we travel down to the quantum-mechanical world of nuclear physics, where cross-sections are measured in barns (10^{-28} m²), things are more Cheshire-Cat like. First of all, according to the rules of quantum mechanics, particles are best understood as wave packets, composed of quantum wave functions with mean wave number $k \equiv 2\pi/\lambda$ and angular frequency $\omega \equiv 2\pi f$ given by

$$k = p/\hbar \quad (2.11)$$

$$\omega = E/\hbar \quad (2.12)$$

where p is the particle momentum ($p = mv$ in the non-relativistic range of $v^2 \ll c^2$) and E is the total (kinetic + potential) energy of the particle. \hbar is Planck’s constant divided by 2π , $1.0546 \cdot 10^{-34}$ J·s. The quantum wavelength is called the “de Broglie” wavelength, after Louis de Broglie who

first proposed, in his 1924 Ph.D. thesis (!), that matter could have wave-like properties, just as light has particle-like properties.

In free space the wave function, ψ , is a complex quantity with spatio-temporal dependence

$$\psi(x, t) = \psi_0 e^{i(kx - \omega t)} \quad (2.13)$$

where ψ_0 is a complex constant. You might well ask, in the company of a number of very smart people including Albert Einstein, “What is ψ ?”. The name “wave function” conveys little. In quantum mechanics, we compute probabilities for what may happen, rather than make deterministic predictions. For example, if we want to know the probability that a particle will be found at a particular place x at time t , we use the quantum rule that $\psi^*(x, t)\psi(x, t)$ is the local probability density for finding the particle. (The “*” superscript indicates a complex conjugate.) Integrating $\psi^*\psi$ over a small distance in x , we arrive at the probability that we will find the particle in that range. Similarly, the quantum formula for x -directed momentum density is $-i\hbar\psi^*(x, t)\partial\psi(x, t)/\partial x$, and it can be used in the same way.

A wave packet localized in free space can be constructed by superposing free-space wave functions over a range in k . It is a well-known result from Fourier transforms that if we superpose a continuous Gaussian-shaped distribution of waves with mean wavenumber k_0 and root-mean-square deviation $\delta k \equiv \langle (k - k_0)^2 \rangle_{wp}^{1/2}$ (where $\langle \dots \rangle_{wp}$ indicates the average over the wave packet) we get a spatially localized wave packet with $\delta x_{wp} \equiv \langle (x - x_0)^2 \rangle_{wp}^{1/2} = 1/\langle (k - k_0)^2 \rangle_{wp}^{1/2}$, as shown in figure 2.2. Since the probability density and the momentum density are each proportional to the square of ψ they are each $\sqrt{2}$ narrower than ψ . Thus the widths of the physical probability densities for x and p_x define the limit of Heisenberg’s uncertainty principle.

$$\delta x \delta p_x \leq \frac{\hbar}{2} \quad (2.14)$$

Question: Check out the claim that the Fourier transform of a Gaussian is a Gaussian with $\delta x \delta k = 1$. If you want to do the integral yourself, the trick is to use the “completing the square” technique. While you are at it, confirm for yourself that the Gaussian width of $\psi^*\psi$ is $\sqrt{2}$ narrower than the Gaussian width of ψ .

Now if we sum wave functions over an isotropic distribution of \vec{k} , distributed in a Gaussian way around \vec{k}_0 , the spatial part of the wave-function dependence will form a nice spherical quantum fuzz-ball, as illustrated qualitatively in figure 2.3. This is the probability density of a particle produced

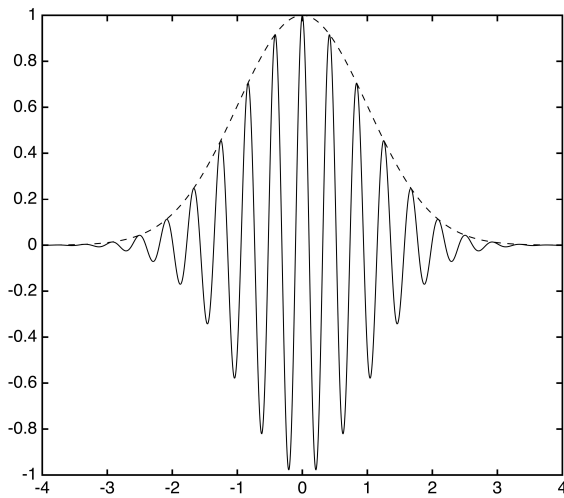


Figure 2.2 Wave packet. Solid line is $\text{Re}(\psi)$. Dotted line is $|\psi| = \sqrt{\psi^*\psi}$.

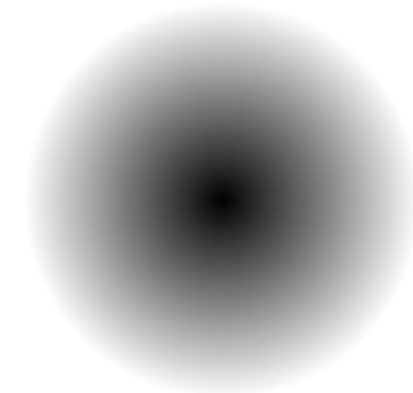


Figure 2.3 Representation of the quantum probability density of a particle.

or selected to be in a particular range of momentum: a mean value with equal uncertainty range in all directions.

2.5 Elements of nuclear physics

The first formulations of non-relativistic quantum mechanics were developed by Heisenberg and Schrödinger in 1925, and immediately applied to

Table 2.1 *de Broglie wavelengths and Neutron energies*

Comparison	Distance = λ_n (m)	Neutron Energy (eV)
Atomic lattice spacing, UO ₂	$3.44 \cdot 10^{-10}$	$6.90 \cdot 10^{-3}$
Molecular spacing, H ₂ O	$3.10 \cdot 10^{-10}$	$8.50 \cdot 10^{-3}$
Atomic lattice spacing, U metal	$2.75 \cdot 10^{-10}$	$1.09 \cdot 10^{-2}$
Thermal neutron (1/40 eV)	$1.81 \cdot 10^{-10}$	$2.5 \cdot 10^{-2}$
Fission neutron (2 MeV)	$2.02 \cdot 10^{-14}$	$2 \cdot 10^6$
Nuclear diameter, U	$1.67 \cdot 10^{-14}$	$2.92 \cdot 10^6$
Nuclear diameter, O	$6.80 \cdot 10^{-15}$	$1.77 \cdot 10^7$
Nuclear diameter, H	$1.75 \cdot 10^{-15}$	$2.67 \cdot 10^8$

understanding the physics of atoms. These ideas were already applied in the newly emerging field of nuclear physics in the 1930's. To orient ourselves in this world, let us evaluate the neutron energies whose quantum mechanical wavelengths in free space equal some relevant physical sizes, using $\lambda_n = 2\pi/k_n = h/p_n = h/\sqrt{2m_n E_n}$ and so $E_n = h^2/(2m_n \lambda_n^2)$, where h is Planck's constant and the "n" subscript stands for neutron. This equation is in SI units, so energy is in Joules. If we want E_n in electron volts, (eV), we divide Joules by $e = 1.602 \cdot 10^{-19}$. We are justified in using the non-relativistic formulation because the energies we will find are much less than the rest energy of the neutron, 940 MeV.

The first observation we can make using table 2.1 is that inter-atomic spacings are typically sub-nanometer ($1 \text{ nm} = 10^{-9} \text{ m}$) in scale, corresponding to number densities in the range of a few times $10^{28}/\text{m}^3$. This is somewhat below the De Broglie wavelength of thermal neutrons. A wavepacket with some definition in its momentum and so $\delta k/k$ well less than unity, will have spatial extent $\delta x = 1/\delta k > 1/k$, so a thermal neutron of defined momentum (and thus energy) will contain multiple wavefronts, as in figure 2.2, and so will likely overlap with at least a few atomic nuclei. On the other hand, a thermal neutron's wavelength and wave packet are vastly larger than nuclear diameters, which are measured in femtometers ($1 \text{ fm} = 10^{-15} \text{ m}$), which are also called "Fermis," in honor of Enrico Fermi. The wavelength of neutrons emitted by fission are in the range of nuclear diameters, since nuclear energies naturally correspond to neutron wavelengths that "fit" within a nuclear diameter, just as electron wavelengths "fit" within atoms.

Nuclei, however, are fundamentally different from atoms. They do not contain a concentrated central attractant, and the basic force holding nucleons (neutrons and protons) together, the strong force, is very short-range. Since the 1970's we have known that the strong force is a manifestation of the color force that acts between the three quarks in a nucleon and "leaks out" to interact with the quarks in other nucleons, but we don't need to go to that level of analysis here. We just need to know that all nucleons attract each other, very similarly, through the strong force. On the other hand, protons repel each other through their positive charges. Furthermore, protons and neutrons – separately – obey Pauli's exclusion principle. You cannot have two neutrons in the same state, so you can have only two, with opposite spin, in each orbital. The same holds true, separately, for protons. One more thing: nuclear spin has a much stronger effect in nuclear physics than in atomic physics. The energetic coupling between spin and orbital angular momentum is relatively weak in atomic physics, giving rise to what is called "fine structure," but this effect is much bigger in nuclear physics. Similarly, the interaction between two nucleons depends very strongly on their spin, with stronger attraction for the same spin direction.

The number of protons in a nucleus is its atomic number, denoted by " Z ", and the total number of nucleons is its atomic mass, denoted " A ". Two nuclei with the same Z but different A are called isotopes of one another.

The two most basic, but insight-providing, approaches to understanding the nucleus are to consider it either as a set of orbital shells, like the atom, or to consider it as a drop of a very special nuclear liquid. These are called the "shell" and "liquid drop" models. The shell model can allow us to understand some puzzling features of nuclei quite simply. For example, why are there more neutrons than protons as the atomic number, the number of protons in a nucleus, Z , increases? Because of Pauli's exclusion principle larger and larger radius orbitals become occupied with increasing Z . Meanwhile, however, the protons repel each other through the long-range electrostatic force, so the attractive short-range strong force between nearby nuclei begins to be weakened with increasing size. It is obviously energetically favorable to fill up the same volume with neutrons as the proton orbitals, to strengthen the strong attraction without adding electrostatic repulsion. However, since the neutrons do not repel each other, they experience a deeper potential energy well at a given radius. As a consequence their wavelengths are shorter and their orbital shells are smaller. Thus more neutrons than protons can be packed into the same space. This effect grows as the long-range electrostatic repulsion competes more and more effectively with the short-range strong force, as the number of protons grows.

Another curious feature of nuclear physics that can be explained using the shell model is that nuclei with even numbers of protons and even numbers of neutrons are energetically favored compared with those with odd numbers of either. The most stable nuclei have even numbers of both. This is because of the strong spin-spin and spin-orbit couplings that favor even numbers, for example two spin up neutrons with equal but opposite orbital angular momenta. When you have an even number of nucleons, the next odd one must occupy a significantly higher energy state, in an unfavorable spin-orbit configuration.

A powerful result of the alternative *liquid-drop* model is its explanation of the curve of binding energy, seen in figure 1.1. The total negative potential energy in a nucleus can be seen as being dominantly composed of the strong attractive nuclear potential acting between neighbors, minus the long-range electrostatic repulsion between the protons. The strong-force attraction is linear in the total number of nucleons, so long as all nucleons are fully surrounded by neighbors. This approximation breaks down of course for very small numbers of nucleons (as does the liquid drop model in general), but it also needs to be corrected for all of the nucleons near the surface of a large nucleus that have fewer neighbors, and so are less deeply bound. This corresponds to a form of nuclear surface tension just like for a macroscopic drop of fluid; it takes more energy to have more surface, so the nucleus is forced to a near-spherical shape. The electrostatic repulsion goes as the atomic number, Z , squared, divided by its radius, since the electrostatic potential goes as $1/r$. Together these do a good job of explaining why the binding energy per nucleon grows at first, due to the falling fraction of nucleons near the surface, and then falls, due to the growing effect of electrostatic repulsion.

The most famous result of the liquid-drop model is that it shows how if you add enough vibrational energy to a nucleus, you can cause it to break apart, or fission, in analogy to the way that a drop of liquid can break up when its vibrational energy overcomes its surface tension. It is remarkable that this picture, which presupposes in its most primitive form a kind of localization of nucleons, like water molecules, works so well. The empirical result that the radius of the charge density of a nucleus, r_{cd} , scales as the cube root of its nucleon number, A , is consistent with this liquid-like picture as well. It amounts to assuming a constant mass density, such as would be expected in an incompressible fluid like water. The strong nuclear force becomes repulsive at short enough distances, and together with the Pauli exclusion principle, sets this up.

$$r_{cd} \approx 1.35 \text{ fm} \cdot A^{1/3} \quad (2.15)$$

The energy states of neutrons in nuclei shown in figure 2.4 bear some resemblance to electronic states in atoms, but because the potential well, $V(r)$ is closer to a square well than a $1/r$ shape, and because of the strong effect of spin, there are some important differences. For example, unlike atomic states, the bound states of neutrons do not become arbitrarily densely packed near the transition to free states. Also the wave function of a free neutron is partially reflected by the presence of the steep wall of the nuclear potential, and can, in effect, bounce back-and-forth at the location of the nucleus. If the neutron wavelength is just right, this can form a positive interference and so a “resonance” that can very strongly enhance the neutron probability density, $\psi^* \psi$, in the vicinity of the nucleus, even though the neutron is not energetically confined by the potential well of the nucleus. Another interesting difference between atomic and nuclear physics is that the stable atomic numbers are different. The most stable atoms are the noble gases, helium, neon, argon, krypton, xenon and radon having $Z = 2, 10, 18, 36, 54$ and 86 . However the most stable numbers of protons (Z) and, separately, of neutrons ($N = A - Z$, where N is the number of neutrons) are the so-called “magic numbers”, $2, 8, 20, 28, 50, 82$ and 126 . This difference between atomic and nuclear physics arises from the strong spin-orbit and spin-spin energy coupling of the strong force, that changes the locations of the big energy gaps between states. At magic numbers of neutrons taking away a neutron costs a lot of energy, and adding a neutron gains little. The same holds for magic numbers of protons. As Z and A increase, both the bound and resonant states become more closely spaced, narrower in energy, and take on more collective characteristics.

Here is a question you may not have thought about: why does the deuteron ($Z = 1, A = 2$) exist, but not the a di-neutron ($Z = 0, A = 2$)? The proton and neutron in a stable deuteron have the same spin, and so stronger mutual attraction than the two neutrons in a putative di-neutron, which must have opposite spins due to the Pauli exclusion principle. The attractive well is shallow enough that not even one bound state can fit into it!

There are two fundamental categories of ways in which free neutrons can interact with nuclei, as shown in figure 2.5. In the first category, they interact internally with the nucleus. In this case they are *absorbed* and form an excited “compound nucleus,” which can then decay to its ground state by γ emission, and/or emit α or β particles, or emit one or more neutrons. (γ 's are simply photons with MeV-range energy, α 's are helium nuclei, two pro-

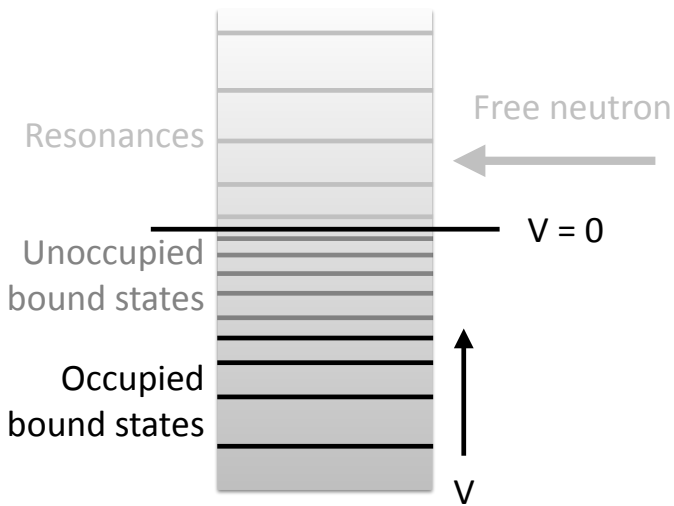


Figure 2.4 Energy states in the vicinity of a nuclear potential field, V .

tons and two neutrons, and β 's are electrons. Positrons or anti-electrons, β^+ , can also be emitted.) Of greatest interest to us in the absorption category are fission and radiative capture of a neutron, in which the excess energy is radiated away in one or more γ rays. In the second category of interactions, the neutron's wave function can be *scattered* externally, not interacting directly with the nucleus, which sends it off in a different direction without changing the internal state of the nucleus. Since no energy is transferred between kinetic and potential, this constitutes elastic scattering. Nonetheless, since some kinetic energy is transferred to the originally stationary nucleus, the neutron does lose kinetic energy. *Inelastic scattering* is strictly speaking absorption of the incoming neutron and emission of a neutron (n') at a lower energy, along with a γ , but it is categorized in nuclear reactor physics as scattering, so this is how it is shown here. The standard nuclear physics notation for the main interactions of interest to us are also shown in figure 2.5. The form is (incoming particle, outgoing particle or particles). Fission is an exception, simply denoted with an "f". The γ emitted in an inelastic collision is sometime omitted, as here.

Neutron absorption and scattering can be modeled using what is called the “cloudy crystal ball” model of the nucleus. The idea is that a neutron’s wave function is diffracted as it enters the potential field around a nucleus just as light is diffracted as it passes from free space into a crystal with a non-unity index of refraction. Just as with light, matching conditions are required at the surface, including the neutron wave-function entering the ball and exiting

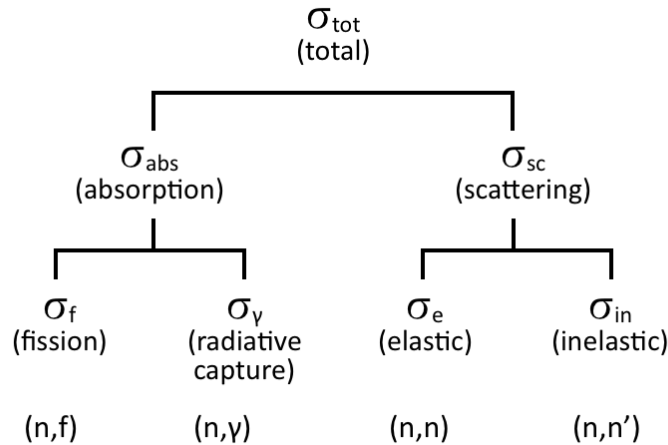


Figure 2.5 Primary neutron-nucleus interactions of interest

the ball. The “cloudy” feature, which corresponds to absorption, is modeled by including an absorption rate that acts to draw down the probability density within the nucleus. In this picture resonances naturally enhance both absorption and scattering, by greatly enhancing the probability density of the incoming neutron within, and in the vicinity of, the nucleus.

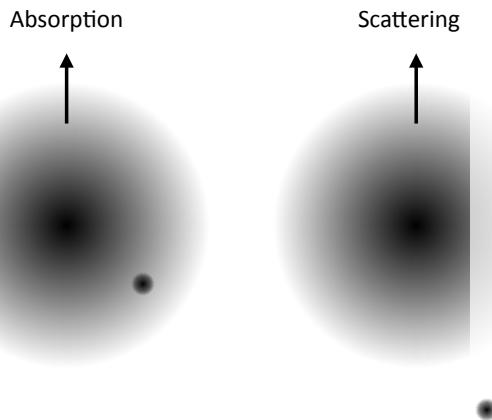


Figure 2.6 Mechanisms of absorption and scattering

The physics of neutron absorption is not well described by the classical cross-section picture discussed in section 2.1; it is much more closely related to the discussion of reaction rate coefficients and resulting effective cross-sections in section 2.3. The wave packet of a free neutron with thermal

energy, or even keV energies, is much, much wider than the diameter of a nucleus, as shown schematically on the left-hand side of figure 2.6. During some or all of the time this wave packet passes through an absorbing medium, its probability density bathes one or more nuclei. So long as the neutron's energy is far from any resonance, or it is on a very broad resonance, the absorption rate is largely independent of the incident neutron velocity. A low-velocity incoming neutron's wavelength within the nuclear potential well is determined dominantly by its new-found momentum, corresponding to the MeV-range nuclear potential, not by its much lower free-space momentum. The reaction rate coefficient (equation 2.10) depends on the basic physics of the nucleus, the number density of nuclei, and the probability density of a neutron inside the nuclei, but not on the free neutron velocity. As we saw in section 2.9 a reaction rate coefficient that is independent of velocity implies an effective cross-section that varies as $1/v$. For higher energy neutrons, or in the case of narrow low-energy resonances, this $1/v$ dependence is not seen, but it is a remarkably common feature. At resonances, whether at low energies or higher ones, we see the strong effect of the high neutron probability density inside the nucleus.

Enrico Fermi won the 1938 Nobel Prize in physics for his discovery of new radioactive elements produced by neutron radiation, and for his discovery that low-energy neutrons activate nuclei much more efficiently than high-energy ones - to everyone's surprise at the time. One day he took his neutron activation apparatus off of its customary marble table (it was Rome after all) and placed it on a wooden mantle piece. Suddenly the device made much more activation. This was due to collisions between neutrons and hydrogen nuclei in the wood, which slow the neutrons effectively through elastic collisions as we will discuss in the next chapter. When Fermi went to accept his Nobel Prize in Sweden in 1938, he took his family with him including his Jewish wife, Laura, and traveled on to the U.S., escaping Fascist Italy and Mussolini's new racial laws. He was a key player in the Manhattan Project to build the atomic bomb, but he fought against the decision to build the much more powerful hydrogen bomb (see Chapter 7). Otto Frisch made important contributions at Los Alamos as well.

Question: After Meitner escaped from Germany, she found a scientific job in neutral Sweden, working for 1924 Nobel Laureate Manne Siegbahn. However he was not interested in her work and provided her little support. She was offered a well-paying senior position at Los Alamos, with her own research group and unlimited funds. And of course real security from the war. Despite the fact that most of her relatives were killed by the Nazis, and she had been

forced to live as a refugee, she refused. She said that nuclear physics was too beautiful to be used for making weapons. Would you have made the same decision? Even if you would not have, can you understand her decision?

Neutron scattering is more like classical scattering in its final result, but still has much of the Cheshire Cat about it. Now, again, the neutron wave packet is much larger than the nucleus, at least at sub-MeV neutron energies. The nucleus can only scatter away the fraction of the probability density contained in the wave packet that passes closest to it, typically at a distance from the center of the nucleus somewhat greater than r_{cd} . The efficiency of this scattering interaction is proportional to the volume of the cylinder it scatters from the wave packet, as shown on the right side of figure 2.6. This volume is given by the effective area of the neutron wave function scattered by the nucleus perpendicular to its direction of motion, πa_{sc}^2 , times its average height, which is the ratio of the volume of the neutron wave packet to its own cross-sectional area: $(4/3)a_{wp}$. The fraction of the wave packet scattered away, which functions as a reduction factor for the geometrical cross-section of the wave packet being scattered, is then given by:

$$f = \frac{(4/3)a_{wp}\pi a_{sc}^2}{(4/3)\pi a_{wp}^2} = \frac{a_{sc}^2}{a_{wp}^2} \quad (2.16)$$

so the *effective* cross-section is just $f\pi a_{wp}^2 = \pi a_{sc}^2$, exactly what we would get in the extreme opposite classical case of infinitesimal BBs and finite billiard balls. In the sub-MeV energy range, far from resonances or on a broad resonance, scattering cross-sections tend to be independent of energy. Perhaps this is why the Cheshire Cat is grinning as it vanishes. Just as with absorption, resonances can greatly increase the scattering cross-section. For example the proton + neutron (= deuteron) system has a resonance very near $E = 0$, so hydrogen has a very large scattering cross-section at sub-MeV energies. As we will see this helps to make water a very important component of most modern fission reactors. In general, resonant scattering has a different structure from resonant absorption. The outgoing scattered wave depends on the structure of the oscillating wave function. In general, scattering is depressed just below the resonance, and enhanced just above.

2.6 Fission

Let's return to the snowy woods in Sweden, in early 1939, with Lise Meitner and her nephew Otto Frisch. Fermi, in Rome, had been using neutrons to bombard his way up the periodic table, making both new stable and new

radioactive nuclei, and had indeed struck uranium. But his nuclear chemistry was not good enough, and he had not recognized the fission fragments that emerged. As she was preparing to escape from Germany, Meitner had encouraged Otto Hahn to repeat the uranium experiments, and to look more closely. He found unmistakable traces of barium. The nucleus had not been chipped, but split! And yet this was completely contrary to all previous experience. (The female German chemist, Ida Noddack, however, had suggested the possibility of fragmentation to explain Fermi's experiments.) Sitting on a tree trunk in the snow, Meitner realized that while nuclear surface tension and electrostatic repulsion both reduce the strength of binding, the first resists deformation of the shape of the nucleus, since the surface area must grow with deformation, but the other favors such deformation, since like charges are given the opportunity to separate. It is as if the surface tension were decreased by the electric charge. She estimated that at $Z \approx 100$ these effects would balance, causing large nuclei to be deformable and subject to shape oscillation!

But if a uranium nucleus could be excited into oscillation with a modest amount of energy, could it be split into two parts? She reasoned that if a uranium nucleus could break into two approximately equal parts, there would have to be, at some point along the way, two approximately half-mass and half-charge fragments separated approximately by twice their nuclear radius, as shown in figure 2.7. The electrostatic potential energy associated with this configuration would be

$$U = \frac{e^2 Z^2}{4\pi\epsilon_0(2r_{cd})} \quad (2.17)$$

You can understand this by imagining holding one fission fragment at $x = -r_{cd}$ and moving the other in from $x = \infty$ to $x = r_{cd}$. There would be no work done on the stationary fragment, since for it $e\vec{E} \cdot \vec{v} = 0$, while equation 2.17 corresponds to the work required to bring the second one into place. When they fly apart, work is done by the electrostatic field on both.

Question: Calculate the electrostatic energy contained in the system shown in figure 2.7. Assume $Z = 46$ and $A = 117$ for each nucleus. Use equation 2.15 for the radii of the nuclei and the SI value $\epsilon_0 = 8.854 \cdot 10^{-12}$. Convert from the SI unit of Joules to electron Volts (eV) by dividing by the electron charge, $e = 1.602 \cdot 10^{-19}$. Your answer should be about 230 MeV.

So, asked Meitner and Frisch (brushing snow off their clothing), where could this energy come from? Meitner knew that the binding energy per nucleon falls at the rate of about 1 MeV per nucleon in this range of atomic

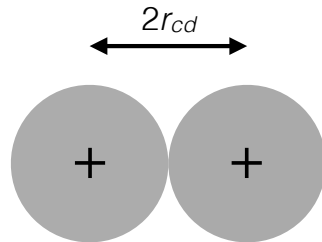


Figure 2.7 Cartoon of two fission-product nuclei “touching”.

numbers (see figure 1.1). So just about the right amount of internal energy, 200 MeV or so, would be released by the formation of two half- Z nuclei from a uranium nucleus. This internal energy could be transformed into external electrostatic energy as the nucleus oscillated. Talk about an “aha” moment!

Frisch rushed back to the lab and within a few weeks found the \sim 100 MeV fission fragments, clearly confirming their theory, about the same time as others around the world did this experiment. Soon it was also found that 2 to 3 neutrons “evaporate” out of the system during fission events, and it became clear to many physicists that a “chain reaction” might be possible, explosively releasing immense amounts of energy. As WWII began, nuclear physicists in America and Britain suddenly stopped publishing about fission. As Fermi put it, “Contrary to their traditions, they set up a voluntary censorship and treated the matter as confidential long before its importance was recognized by the government, and secrecy became mandatory.” Fermi, himself, was a leader of this effort. The unofficial silence about nuclear fission was noted by the Soviets, along with direct reports from British spies about efforts to look into atomic weapons, before secrecy was officially imposed.

Figure 1.2 shows the probability distribution of the neutrons that are produced by fission of uranium. Their average energy is 2 MeV, while their most probable energy is 0.72 MeV. Table 2.2 shows their average number per fission, $\bar{\nu}$, when fission is induced by thermal neutrons and also directly by fission neutrons themselves, for uranium and plutonium. An important feature of the overall fission process is that a very small fraction, less than 1%, of the nuclei that result from fission (“fission products”) produce neutrons that are delayed by \sim 10 seconds after the fission event itself. This delay, due to the chain of radioactive decays of the fission products, is very important for the controllability of fission reactors.

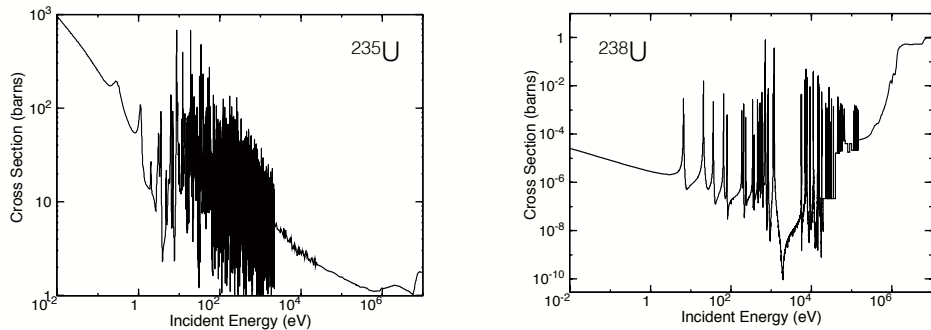
Many years later, when Fermi was shown a sketch for the bas-relief to be placed over the entrance to the future Institute for Nuclear Studies at the

Table 2.2 *Neutrons produced per fission*

Neutron Speed	Nucleus	$\bar{\nu}$
Thermal	^{235}U	2.44
Thermal	^{239}Pu	2.88
Fast	^{235}U	2.6
Fast	^{238}U	2.6
Fast	^{239}Pu	3.09

University of Chicago, he wryly guessed that it was of a scientist who had missed the discovery of fission. Hahn won the 1944 Nobel Prize in Chemistry for the discovery of fission. Many think that, as Bohr recommended, Meitner should have won the Nobel Prize in Physics.

Now we are ready to look at fission cross-sections for the nuclei of greatest interest to us, ^{235}U and ^{238}U , shown in figure 2.8. The x -axis represents neutron energy in eV. The y -axis represents cross-section area, in barns. 1 barn is 10^{-28} m^2 . This is convenient, since number densities tend to be in the range of a few times $10^{28}/\text{m}^3$. A cross section of a few barns, roughly characteristic of nuclear interactions in the MeV energy range, and a number density of a few times $10^{28}/\text{m}^3$ gives $\Sigma \approx 10/\text{m}$, so the mean free path is about 0.1m, or 10cm.

Figure 2.8 Fission cross-sections vs. energy for ^{235}U and ^{238}U .

There are a lot of interesting features in these graphs that we can now understand. First of all, at low energies we see approximately a $1/v$ dependence in both graphs, as is expected because fission starts with absorption of a neutron. On log-log graphs of σ vs. E_n , such as these, a $1/v$ variation

shows up as a fall in σ by one order of magnitude for two orders of magnitude increase in E_n , since a factor of 10 increase in v , and so decrease in $1/v$, is a factor of 100 increase in E_n . Next up in energy we can see many narrow spikes, which are due to the resonances we have discussed, which concentrate neutron probability density at the location of the nucleus, through positive interference. (As you can see, there is also negative interference, where the neutron probability density is actually depleted.) Perhaps most interesting, the fission cross-sections for ^{235}U and ^{238}U are similar above 1 MeV, but the cross-section for ^{238}U is dramatically lower at low energies. This is because ^{235}U has an *odd* number of neutrons, 143, while ^{238}U has an *even* number, 146. When a low-energy neutron is absorbed into a ^{235}U nucleus, the resulting ^{236}U nucleus has an even number of neutrons. Conversely, when a ^{238}U nucleus absorbs a low-energy neutron it has an odd number. A “new” neutron that can pair with an existing neutron goes into a lower energy state, and releases about 1 MeV more energy that can be invested into the deformation and ultimately fission of the nucleus. The ^{238}U nucleus needs that extra MeV to arrive in the form of neutron kinetic energy in order to have a high probability of fission.

^{235}U is called “fissile,” because it has a significant probability of fission by thermal neutrons. ^{238}U is called “fissionable,” because, while it does not have a significant probability of fission by thermal neutrons, it can be fissioned by MeV-energy neutrons. ^{239}Pu is also fissile, and ^{240}Pu is fissionable, due to the same underlying physics as the uranium isotopes. Nuclei that produce fissile isotopes when they capture neutrons are called “fertile”. The most important for nuclear energy (and nuclear weapons) applications are ^{238}U , which produces ^{239}Pu , and ^{232}Th , which produces ^{233}U .

Question: Neptunium has $Z = 93$, and its most stable isotopes are ^{236}Np and ^{237}Np . Which do you think is fissile, and which fissionable?

When uranium fission occurs, about 211 MeV of energy, in all forms, is released. 9 MeV is in the form of anti-neutrinos, which are not stopped in the reactor. The remaining energy is almost all captured within the reactor core. 169 MeV is in the form of fission products (the nuclei that emerge from the fission process), which are stopped within the fuel pin where they are created. The neutrons that emerge from fission carry about 5 MeV of energy, and are mostly stopped within the reactor, while γ 's emitted during fission, almost all stopped within the reactor, carry about 7 MeV. Neutrons that are absorbed in the fuel and structure, without producing further fission, result in about 9 MeV of energy release, mostly in “capture γ 's” (see next section). Many of the fission products are unstable, and emit about 13 MeV

of β s and γ s during their decay after the fission process. This is the “decay heat,” or “after-heat” that presents safety challenges.

To put this in macroscopic terms, fission of 1t of uranium or plutonium produces about 960 GWth-days of heat. Since a light-water fission reactor might be 35% efficient, and might run on average, counting refueling and maintenance periods, at 90% of its “nameplate” power (= 90% “capacity factor”), such a reactor fissions about 1t of “heavy metal” (uranium or plutonium) per year. On the other hand, fission of 1 kg of heavy metal produces the same amount of energy as 17.8 kt of TNT, roughly equal to the yields of the weapons that destroyed Hiroshima and Nagasaki in WWII. The US-Russia “Megatons to Megawatts” program, that lasted from 1993 to 2013, involved down-blending 500t of Russian weapons-grade uranium, $\approx 90\%$ ^{235}U , to reactor-grade, $\approx 4\%$ ^{235}U , thus using the explosive material for about 18,000 nuclear weapons to produce fuel for about 450 reactor-years of power, roughly a quarter of US nuclear power production during that period.

There is one last interesting piece of the nuclear physics of fission that we should cover here. When ^{235}U or ^{239}Pu fissions due to capture of a thermal neutron, it does not produce many fission products with mass number in the range of 1/2 of the initial mass number, say 118. As shown in figure 2.9 the production is split between higher and lower masses. This is because of the particularly stable nuclei near the magic numbers 50 for protons and 82 for neutrons and, to a lesser degree, 50 for protons and 50 for neutrons. At higher incoming neutron energies the valley in figure 2.9 begins to fill in, since the energetic value of magic numbers becomes less important.

2.7 Radiative Absorption

The type of radiative absorption of most interest to us is rather simple. A nucleus absorbs a neutron and becomes a new nucleus in an excited state, with atomic mass increased by unity, but retains its original atomic number. This nucleus then relaxes to its ground state by emitting one or more γ photons in the MeV energy range.

Radiative absorption is important for us in two neutron energy ranges. First, as neutrons slow down from their MeV birth energy range, they encounter sharp resonances in ^{238}U , that lead to large spikes in the cross-section for absorption, as shown on the left-hand panel of figure 2.10. The databases that are used to make these plots only track individual resonances up to a certain energy, above which the cross-section is averaged over resonances. As you can see, the absorption resonances between about 5 and

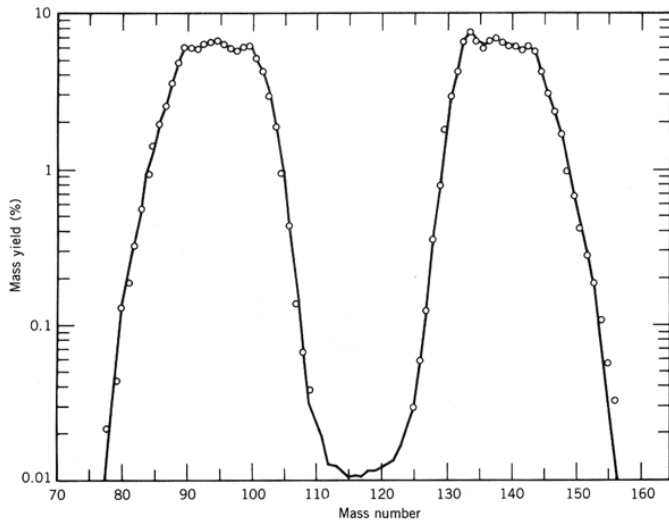


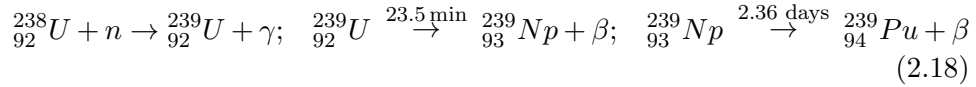
Figure 2.9 Probability of production of masses of fission products from thermal fission of ^{235}U . The sum of probabilities is 200%, since two fission products are produced per event.

500 eV dominate over the ^{235}U fission cross-section in the same range, as shown in figure 2.8. This dominance is amplified by the fact that the ^{235}U enrichment in a fission power reactor is typically only in the range of 4%, meaning that there is 24 times more ^{238}U than ^{235}U nuclei. Secondly, radiative absorption by ^{238}U and, to a lesser degree ^{235}U , competes at low energy with fission. The $1/v$ region ^{238}U absorption cross-sections is much smaller than that for fission of ^{235}U , but again we must remember that there is much more ^{238}U than 235 around.

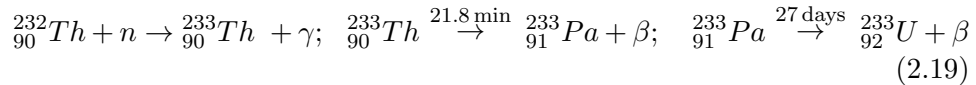
Radiative absorption by ^{238}U plays a key role in the neutron economy of uranium-based fission reactors, as it removes neutrons from the steady chain reaction necessary to sustain power production. We will discuss this in some detail in chapter 3. On the other hand, radiative absorption also results in build-up of ^{239}Pu in a uranium-fueled reactor, which is fissile, and functions as additional fuel. Thus while it hurts the short-term neutron economy of the chain reaction, it helps the long-term fuel economy of the reactor. Depending on parameters, about 1/3 of the energy produced in a LWR may come from the built-up ^{239}Pu , about making up for the fact that about 1/3 of the initially supplied ^{235}U does not undergo fission.

In uranium/plutonium “fast breeder” reactors, in which the neutrons are not slowed down to thermal energies, but remain “fast”, the goal is to make more fissile material than is burned, by transmuting ^{238}U to ^{239}Pu using

neutrons predominantly in the range of a few 100 keV. It is also possible to breed ^{233}U from ^{232}Th , potentially creating a thorium-based fuel cycle. This is in principle achievable even with thermal neutrons. The reaction chains for these two processes (neglecting anti-neutrino production) are



and



Resonant radiative absorption is also important for the stability of fission reactors. As we will discuss in Chapter 3, there is a Doppler broadening effect that increases radiative absorption as fission fuel heats up. This contributes self-regulation to a fission reactor.

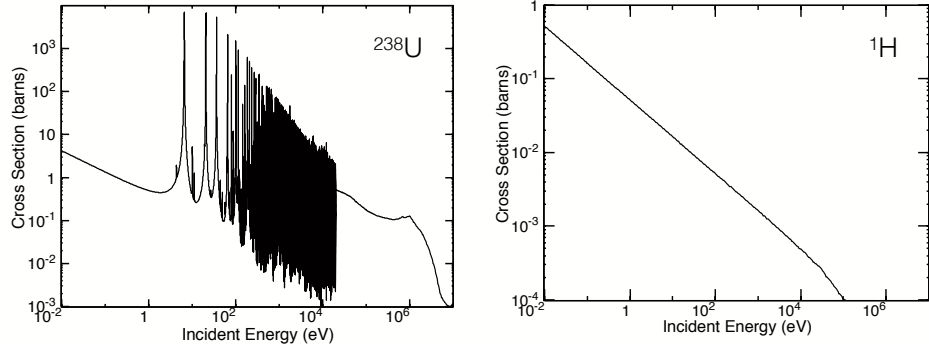


Figure 2.10 Cross-sections for radiative absorption of neutrons by ^{238}U and by protons, ^1H .

When neutrons slow down to thermal energies, $1/v$ radiative absorption becomes important in ^{238}U as discussed above, and to a lesser degree in ^{235}U . It also becomes important in the elements composing the moderator (the material that slowed the neutrons down in the first place) and in the structural materials that make up the reactor. For a light-water reactor, the dominant absorption is by the hydrogen in the moderating water, whose cross-section is shown on the right-hand panel of figure 2.10. This absorption is greatly enhanced by the broad resonance of the D-H system (the deuteron) near zero binding energy. Deuterium, oxygen and carbon have $1/v$ neutron scattering cross-sections that are 100 to 1000 times smaller than hydrogen's. This is why heavy water (D_2O) and graphite can be used as moderators for natural uranium, but light water requires enriched uranium.

Finally, neutrons also interact with Pu and fission products as they build up in the reactor core during operation. Pu can undergo fission, and both Pu and fission products are targets for radiative absorption. Pu has the interesting property that as it absorbs neutrons and climbs up from ^{239}Pu to ^{240}Pu to ^{241}Pu to ^{242}Pu , it goes back and forth from fissile to fissionable. The ^{135}Xe fission product has an immense radiative absorption cross-section of two million barns at thermal energy, so it has a significant effect on reactor operation. As we will see, it has to be managed carefully. Mismanagement of ^{135}Xe contributed to the Chernobyl accident.

2.8 Elastic and Inelastic Scattering

Neutrons can also scatter in angle when they encounter target nuclei. While the internal state of the target nucleus and of the neutron do not change, in the lab frame the target nucleus does gain kinetic energy when it recoils in an elastic collision, so the neutron loses kinetic energy.

Elastic scattering involves reflection of some of the neutron wave-function off of the nuclear potential, as shown schematically on the right-hand side of figure 2.6, and discussed there. In general, elastic scattering cross-sections on light nuclei are independent of the incoming neutron energy over a wide range. This is because the kinetic energy of the neutron within the nuclear potential is far dominated by the depth of the potential well of the nucleus, and the resonances of light nuclei are both broad and spaced well apart. Due to a broad resonance of the deuteron, just above zero energy, hydrogen has a very large scattering cross-section, indeed much greater than that of oxygen, as shown in figure 2.11. Since r_{cd} of the oxygen nucleus is much greater than that of the proton, this illustrates again the power of a resonance. This is such a powerful effect that the mean free path of sub-MeV energy neutrons in light water is in the range of 1cm, rather than the 10 cm for neutrons in most materials.

Notice that over much of the slowing-down range of neutrons, from birth at ~ 2 Mev to thermal energy, the scattering cross-sections for hydrogen and oxygen are roughly independent of energy. Again this is because the process is not one of *absorption*, which is characterized by a rate coefficient associated with simply being in the presence of absorbing nuclei and does not depend on the neutron velocity. Instead this is *scattering* (albeit quantum-mechanical), that depends on passing target nuclei, and scattering away probability density at each such encounter. In this case the number of encounters per unit distance is what matters, just as in classical scattering, so the effective cross-section tends to be independent of energy. Both

reactions, of course, depend linearly on the target density. At the highest energies shown the nuclear structures come into play. The broad resonance of the deuteron system tails off, and the resonance structure of the oxygen nucleus becomes visible. The cross-sections increase at the lowest energies also. There are effects associated with the fact that the nuclei are bound in molecules, and with scattering off of more than one nucleus at a time. However the cross-section variation shown in these data libraries arises from the fact that at low enough neutron energies the rate of encounter between neutrons and nuclei depends only on the motion of the target nuclei, and is independent of the neutron motion — giving the same $1/v$ variation as typically characterizes absorption. Indeed if you were to expand these plots to even lower energies you would see a clear $1/v$ variation at very low energies. In these plots the thermal target motion is assumed to correspond to 293° K.

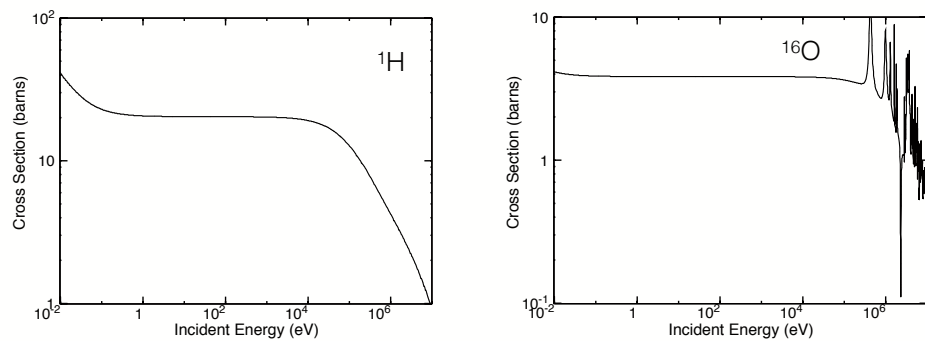


Figure 2.11 Cross-sections for elastic scattering of neutrons by protons, ^1H , and oxygen nuclei, ^{16}O .

For heavy nuclei, resonances are closely spaced and narrow, and play a role in elastic scattering, as can be seen in figure 2.12, because the neutron wave function is amplified in the region of the nuclear potential. Generally scattering is maximum close to an absorption resonance peak, and – interestingly – is reduced below the peak. This is because the wavefunction within the nucleus at these energies has a low value near its edge, and so little of the neutron probability density is radiated way. If you smooth the elastic scattering cross-section shown in figure 2.12 over the resonances it is $\sim 15\text{b}$ from 1 keV to where it begins to fall off in the high-energy range.

Inelastic scattering is really a form of absorption of an energetic neutron, formation of an excited state of the target nucleus, followed by emission of a γ and a neutron of lower energy. In the energy range of interest to us,

inelastic scattering is only available for mid-range to heavy nuclei. Inelastic scattering on U reduces the neutron energy to a mean value of (very roughly) $\sim (E_{\text{MeV}}/12)^{0.5}$ MeV, for the majority of fission-energy neutrons. It has a threshold around 45 keV, as shown in figure 2.12. In the energy range below 500 keV, the main excited state that is produced is the lowest, at 45 keV, so the energy loss can be neglected for our purposes.

Inelastic scattering is not available in the case of the proton and deuteron, since neither has any bound, excited states. Thus the neutron and γ cannot escape from a bound, excited state.

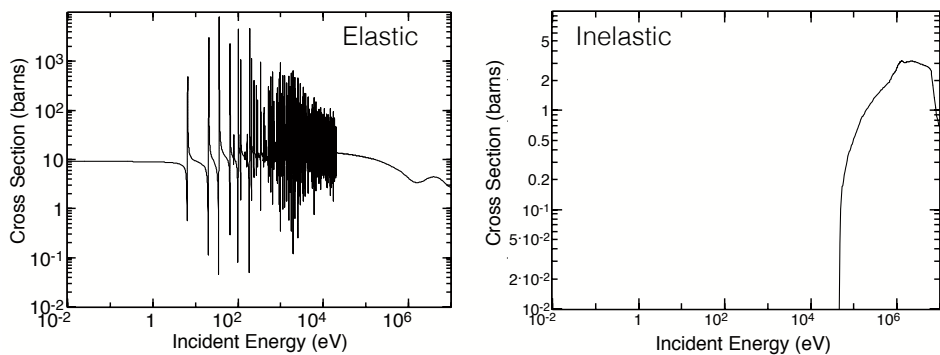


Figure 2.12 Cross-sections for elastic and inelastic scattering of neutrons by ^{238}U .

2.9 Try This at Home

There are many places to access nuclear data on line. Each has different advantages and disadvantages. But in all cases it is interesting to use these tools to get a feel for what is going on. Here is a bit of a curated list. All of these let you download the data from which plots are made, if you want to plot or manipulate the data yourself.

- <https://www-nds.iaea.org/exfor/endf.htm>
A bit of a bare-bones interface, but it does let you download figures. You have some control over the formatting; not all of the controls work. This is what I used to make the plots in this chapter.
- <http://www.nndc.bnl.gov/sigma/index.jsp?as=10&lib=endfb7.1&nsub=10>
A simpler interface, but it doesn't let you (on a Mac) download plots except as screen shots. It lets you overlay different cross-sections and it lets you do numerical manipulations on the "Plot Cart" data. This is my "go-to" website.

- <http://www.oecd-nea.org/janis/>
A nice interface, and very nice plots. The JAVA version lets you download nice plots. The “books” that are available here are for comparison with experimental data.
- <http://atom.kaeri.re.kr/nuchart/>
A nicer-yet interface, but doesn’t let you download plots except as screen shots. A unique feature of this interface is that it assumes zero thermal motion of the target nuclei.

You might as well use the latest US library, ENDF/B-VII.1 as of this writing. The ENDF library, and the different interfaces to it have a special language. For the IAEA interface, you need to know that the target nucleus is specified, for example, as U-235. You also need to know that for the cross-sections listed below you use SIG for “Quantity.” For average neutron production per fission event you leave “Quantity” blank.

In the ENDF formatting the neutron-nucleus reactions are classed as Incident-Neutron Data, with specific reactions:

- Fission: N,F (#18)
- Radiative absorption: N,G (#102)
- Elastic scattering: N,EL (#3)
- Inelastic scattering: N,INL (#4)
- Average total, prompt plus delayed, number of neutrons released per fission event: N,nu_tot (#452)
- Average number of delayed neutrons released per fission event: N,nu_d (#452)

Note that N,NON (#3), “Nonelastic neutron cross-section” is just the total cross-section, including all interactions, minus the elastic scattering cross-section. You can show this by summing N,NON + N,EL to get N,TOT.

Review

Resources

- “Lise Meitner, a Life in Physics,” Ruth Lewin Sime, University of California Press, Berkeley and Los Angeles, London, 1996
- “Enrico Fermi, Physicist,” Emilio Segrè, University of Chicago Press, Chicago and London, 1970
- “Introductory Nuclear Physics,” Kenneth S. Crane, John Wiley and Sons, Hoboken NJ, 1988

- “The Elements of Neutron Interaction Theory,” Anthony Foderaro, MIT Press, Cambridge MA and London, 1971

Exercises

- 2.1 Los Alamos, New Mexico was selected for the design and construction of nuclear weapons during WWII because General Groves, who managed the whole Manhattan Project, wanted an out-of-the-way location. J. Robert Oppenheimer, who was the Scientific Director of Los Alamos during the war, had attended a private high school there and loved the region. The local residents were ranchers; it is too dry for farming. Presumably this is why the physicists who gathered there chose to measure cross-sections in “barns,” as in the expression, “You could not hit the broad side of a ...” Less well known is their unit of time, the “shake”, 10^{-8} s, or 10 ns, presumably honoring the local lamb population. This is roughly how long it takes a 1 MeV neutron to drive fission in uranium metal. Least well known is the fact that the scientists developed a short-hand code for referring to the fissile and fissionable nuclei of most interest to them, as shown in Table 2.3.

Table 2.3 *Los Alamos Code*

Type	Code Name	Nucleus
Fissile	25	^{235}U
Fissile	49	^{239}Pu
Fissionable	28	^{238}U
Fissionable	40	^{240}Pu

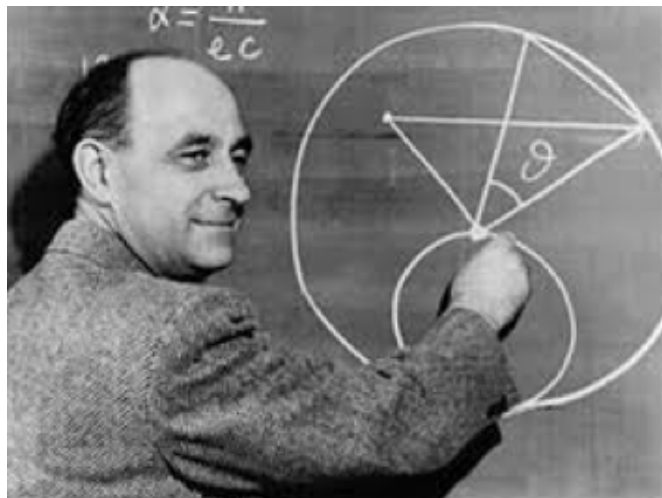
Explain the code and give the code name for ^{239}Np . Is it fissile or fissionable? Why?

- 2.2 Show how the two fission products that Lise Meitner visualized as touching each other turn their electrostatic potential energy into kinetic energy. Imagine that the right-hand fission product starts at location $x = x_1 > 0$ at time $t = t_0$, and the left-hand product starts at $x = x_2 < 0$ at the same time. Evaluate their acceleration as a function of $x_1 - x_2$. Now multiply the acceleration of the right-hand product by $m_1 v_1$ and the acceleration of the left-hand by $m_2 v_2$. Summing these together you have the time derivative of the total kinetic energy. Show

- that integrating this from t_0 to ∞ gives a kinetic energy equal to the original electrostatic potential energy.
- 2.3 Reproduce the hydrogen scattering cross-section shown in figure 2.11 using the IAEA and KAERI interfaces to the ENDF/B-VII.1 library. They are very different at extremely low energies. Why?
 - 2.4 Use the IAEA and KAERI interfaces to the ENDF/B-VII.1 data library to examine a resonance of your choosing from the left-hand side of figure 2.10. Show that the two interfaces give quite different results. Estimate the thermal velocity of a ^{238}U nucleus at 293° K. How much does this change the neutron energy, in the frame of reference of the nucleus? Does this, roughly, explain the difference?

Chapter 3

Neutron Energy Distribution



Indeed the neutrons produced by a primary fission must be used very sparingly in order to keep a positive surplus in spite of the loss due to the large parasitic absorption of U-238. Great care must be exerted in order to make the balance between useful and parasitic absorption of the neutrons as favorable as possible. Since the ratio of the two absorptions depends on the energy of the neutrons and, aside from details, is greater for neutrons of low energy, one of the steps consists in slowing down the neutrons from their initial high energy, which is of the order of 1 MeV, to an energy as low as that of thermal agitation. A simple process to achieve this end has been known for some time. It is based on the fact that when a fast neutron collides against an atom some of its energy is lost as recoil energy of the atom. The effect is greatest for light atoms which recoil more easily and is maximum for hydrogen but quite appreciable for all light elements.

Enrico Fermi, Proceedings of the American Philosophical Society,
Read November, 1945

In this chapter we will learn how the MeV neutrons produced in fission lose energy by colliding with light nuclei in a reactor, and eventually at low energies themselves drive fission through the strong $1/v$ variation of the fis-

sion cross-section. They transfer from the Fast energy region, above about 500 keV, through an Intermediate energy region, down to about 0.5 eV, and finally to the Thermal region where the neutrons have energies characteristic of their thermal environment. This history governs the neutron “lifecycle,” which of course requires each fission neutron to reproduce, on average, exactly one new fission neutron during its lifetime, in order to sustain the reaction at a constant level. We will also look briefly at so-called “fast” reactors, in which the neutrons only slow down to the energy range of some hundreds of KeV, dominantly due to inelastic collisions.

3.1 Energy change in elastic scattering

Let us start by examining how neutrons lose energy in elastic collisions, due to the kinetic energy invested in the recoil of target nuclei. As we will see, this process is dominated by collisions with light nuclei. The cross-sections for such collisions (see figure 2.11) can be approximated as independent of energy over a fairly wide range of interest for fission neutrons slowing down to thermal energies.

Consider figure 3.1 showing a neutron-nucleus collision in the lab frame. If we are taking a macroscopic perspective like this, we can consider the neutron and target nucleus as point particles. We assume that before the collision we have a neutron moving with speed v_0 and a stationary target nucleus. After the collision the neutron scatters off at some angle ψ from its original trajectory, with speed v_1 . The nucleus, of course, recoils, but we will not need to calculate its recoil speed.

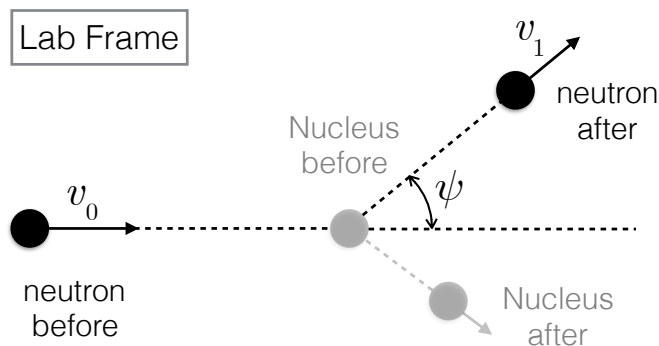


Figure 3.1 Diagram of a neutron-nucleus collision in the lab frame.

In all of our calculations we will assume that the mass of the neutron

can be adequately approximated as a single atomic mass unit, 1u, while the mass of the nucleus can be taken as Au. Since $1\text{u} = 1.66 \cdot 10^{-17} \text{ kg} = 931 \text{ MeV}/c^2$, we can ignore relativistic effects for our neutrons with at most a few MeV of kinetic energy. In general, the accuracy of the approximations we will be making does not justify greater precision than this. The center of mass of the neutron-nucleus system is located at

$$\vec{x}_{CoM} = \frac{A\vec{x}_N + \vec{x}_n}{A + 1} \quad (3.1)$$

where the subscript “N” denotes the target nucleus and “n” denotes the neutron.

The time-derivative of the position of the center of mass (its velocity) follows from the velocity of its components:

$$\vec{v}_{CoM} \equiv \dot{\vec{x}}_{CoM} = \frac{A\dot{\vec{x}}_N + \dot{\vec{x}}_n}{A + 1} = \frac{\vec{v}_0}{A + 1} \quad (3.2)$$

By conservation of momentum, proportional to $A\dot{\vec{x}}_N + \dot{\vec{x}}_n$, we can see that the center-of-mass velocity must be conserved, and in particular must be equal before and after a collision.

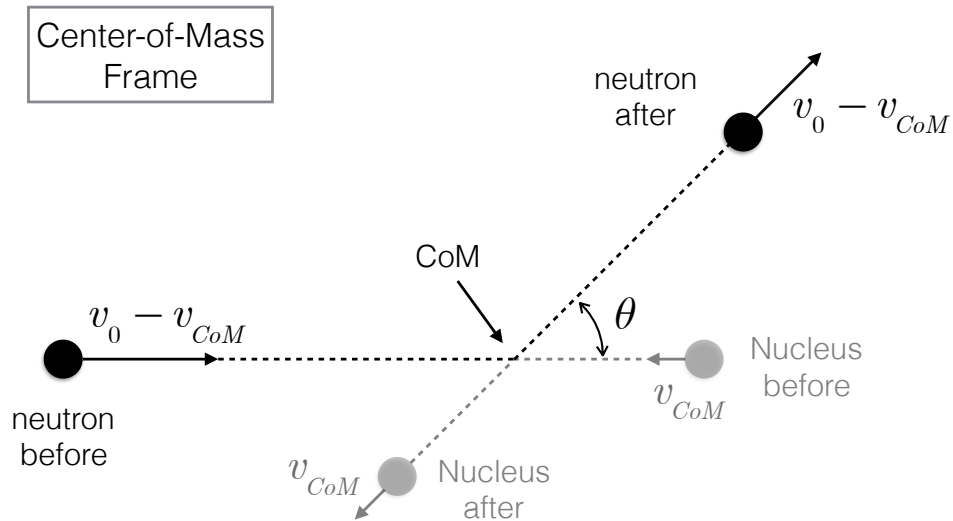


Figure 3.2 Diagram of a neutron-nucleus collision in the center-of-mass frame.

Conservation of v_{CoM} suggests that it may be convenient to transfer to the center-of-mass frame. In our non-relativistic conditions, to determine velocities in the center-of-mass frame given velocities in the lab frame, we

simply subtract the velocity of the center of mass, \vec{v}_{CoM} , equation 3.4. Thus the incoming velocity of the neutron in the CoM frame is given by

$$\vec{v}_0 - \vec{v}_{CoM} = \frac{\vec{v}_0(A+1)}{A+1} - \frac{\vec{v}_0}{A+1} = \frac{A\vec{v}_0}{A+1} \quad (3.3)$$

The target nucleus is stationary in the lab frame, so its incoming velocity in the center-of-mass frame is simply given by

$$-\vec{v}_{CoM} = \frac{-\vec{v}_0}{A+1} \quad (3.4)$$

Combining this with the previous equation, we see that the total momentum in the center-of-mass frame is zero.

Since we are considering elastic collisions only, with no changes in potential energy, total kinetic energy must be conserved in this system, while the total momentum is maintained at zero. From this we can deduce that the outgoing speeds of the neutron and the nucleus must equal their incoming speeds, as indicated in figure 3.2. Of course their vector velocities change.

Question: Explain, in words if you can, why the outgoing speeds of the neutron and nucleus equal their incoming speeds.

With just these very simple results, we now transfer back to the lab frame. To determine velocities in the lab frame given velocities in the center-of-mass frame, we obviously add the velocity of the center of mass, \vec{v}_{CoM} , equation 3.4. For the square of the outgoing neutron speed we can write down, using the law of cosines,

$$v_1^2 = (v_0 - v_{CoM})^2 + v_{CoM}^2 + 2(v_0 - v_{CoM})v_{CoM} \cos \theta = \\ \frac{A^2 v_0^2}{(A+1)^2} + \frac{v_0^2}{(A+1)^2} + \frac{2Av_0^2 \cos \theta}{(A+1)^2} = v_0^2 \frac{A^2 + 2A \cos \theta + 1}{(A+1)^2} \quad (3.5)$$

This gives us a simple expression for the outgoing neutron energy in the lab frame, in terms of the incoming lab frame energy. Let us define E_0 as the incoming kinetic energy, and E_1 as the outgoing. Then we have

$$\frac{E_1}{E_0} = \frac{v_1^2}{v_0^2} = \frac{A^2 + 2A \cos \theta + 1}{(A+1)^2} \quad (3.6)$$

The maximum possible lab-frame outgoing energy is for zero-angle scattering – effectively no interaction at all:

$$E_{1, max} = E_0 \frac{A^2 + 2A \cos(\theta = 0) + 1}{(A+1)^2} = E_0 \frac{A^2 + 2A + 1}{(A+1)^2} = E_0 \quad (3.7)$$

while the minimum possible lab-frame outgoing energy is for perfect backscattering:

$$E_{1, \min} = E_0 \frac{A^2 + 2A \cos(\theta = \pi) + 1}{(A + 1)^2} = E_0 \frac{A^2 - 2A + 1}{(A + 1)^2} = E_0 \frac{(A - 1)^2}{(A + 1)^2} \quad (3.8)$$

Let us define a parameter α

$$\alpha \equiv \frac{(A - 1)^2}{(A + 1)^2} \quad (3.9)$$

This allows us to bound the range of outcome energies, E_1 , both from above and from below

$$\alpha E_0 < E_1 < E_0 \quad (3.10)$$

so we can define a range of energy decrements

$$\Delta E = E_0 - E_1 < E_0 - \alpha E_0 \quad (3.11)$$

$$\frac{\Delta E}{E_0} < 1 - \alpha = \frac{4A}{(A + 1)^2} \quad (3.12)$$

We now have the range of possible energy loss, but we need to know the relative probability of any given energy loss to fully understand the slowing-down process. Thus we need to know the relative probability of any given center-of-mass scattering angle, θ . Since the de Broglie wavelength of the neutrons of interest is generally much greater than the effective scattering radius of the target nuclei (see table 2.1), a target nucleus “experiences” a nearly isotropic oscillation of the neutron wave function with time, with relatively little difference across the nucleus. This results in an outgoing wave with a probability density that is essentially isotropic. Thus a scattered neutron has equal probability of leaving the target nucleus in any increment of solid angle, $d\Omega$, over the full 4π available. This isotropy holds in the center-of-mass frame because it is in this frame that the neutron + nucleus system is at rest when the outgoing wave is launched.

We know that a range of solid angle $d\Omega$ can be expressed as

$$d\Omega = \sin\theta d\theta d\phi = -d\cos\theta d\phi \quad (3.13)$$

Since all ranges of $d\phi$ are equally probable by the symmetry of the problem, and all ranges of $d\Omega$ are equally probable as just derived, we can deduce that all ranges of $-d\cos\theta$ must be equally probable, from $\cos\theta = 1$ to -1 . (Note that the sign of $d\cos\theta$ plays no physical role here; it just happens to be

counting downwards in this case.) Starting from equation 3.6 we can deduce

$$dE_1 = E_0 \left[\frac{2A(d\cos\theta)}{(A+1)^2} \right] \quad (3.14)$$

so all outcoming lab-frame differential energy increments, dE_1 , in the range from αE_0 to E_0 are equally probable.

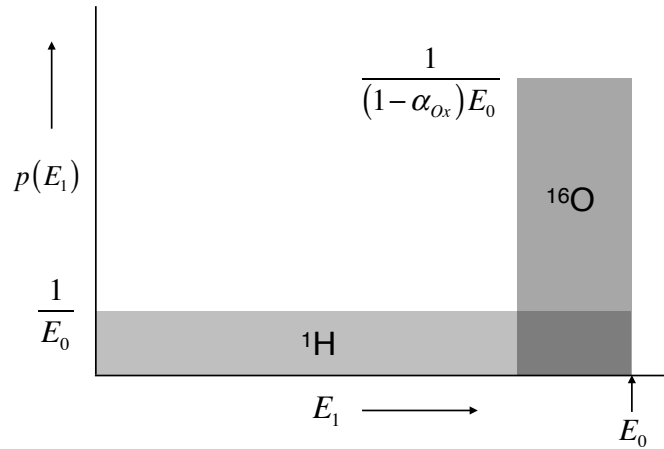


Figure 3.3 Probability of outcoming energy for neutron collision with protons and ${}^{16}\text{O}$ nuclei.

Question: Explain, perhaps literally by waving your hands around, why it would not be physical to have an even distribution in θ as opposed to $\cos\theta$.

The probability of E_1 landing in a differential energy increment dE is given by $p(E_1)dE$. Since it must land somewhere, we require

$$\int_0^\infty p(E_1) dE_1 = \int_{\alpha E_0}^{E_0} p(E_1) dE_1 = 1 \quad (3.15)$$

from which we derive

$$p(E_1) = \frac{1}{\Delta E_{max}} = \frac{1}{(1-\alpha)E_0} \quad (3.16)$$

over the range of possible values of E_1 (equation 3.10). Elsewhere $p(E_1) = 0$. Figure 3.3 illustrates this for ${}^1\text{H}$ and ${}^{16}\text{O}$, with $\alpha = 0$ and 0.78 respectively.

3.2 Logarithmic energy decrement

Fermi noted that the range of possible energy loss at a collision is proportional to the incoming energy, and this loss happens over and over again as a neutron slows down. Thus neutron slowing down can be seen as a process similar to exponential decay of the neutron energy, but with finite-size steps.

Exponential decay is characterized by an equation of the form

$$E_{N_c} = E_0 \exp(-N_c \xi) \quad (3.17)$$

where N_c is a continuous variable such as distance or time. Following Fermi, however, we will be taking N_c as an integer, representing the *number of collisions* undergone. We can then write finite-step exponential decay as

$$N_c \xi = \ln(E_0/E_{N_c}) = \ln[(E_0/E_1)^{N_c}] = N_c \ln(E_0/E_1) \quad (3.18)$$

so this finite-step model assumes energy drops in equal “logarithmic energy decrements,” ξ , with each collision, similar to what we expect. We have previously, in effect, derived a range for the logarithmic energy decrement, which is independent of neutron energy, but we cannot predict the specific value at each collision.

$$\ln(\alpha) < \ln(E_1/E_0) < 0 \quad (3.19)$$

It is particularly daring for the case of hydrogen, but let us press ahead and approximate the energy loss process with a mean logarithmic energy decrement per collision, where the average is taken over all possible energy decrements.

$$\xi \approx \langle \ln(E_0/E_1) \rangle \quad (3.20)$$

This approach gives us the appropriate average for determining the mean number of collisions required to get down to a specified final energy.

$$\langle N_c \rangle = \frac{\ln(E_0/E_{N_c})}{\xi} \quad (3.21)$$

In particular for the energy to drop by one factor of e , on average $1/\xi$ collisions are required, or more generally $1/\xi$ collisions are required per downwards e -fold in energy. $\ln(10)/\xi \approx 2.303/\xi$ collisions are required on average for a 10-fold, or order-of-magnitude drop.

Now we can evaluate

$$\xi \equiv \left\langle \ln \left(\frac{E_0}{E_1} \right) \right\rangle \equiv \int_{\alpha E_0}^{E_0} \ln \left(\frac{E_0}{E_1} \right) p(E_1) dE_1 = \frac{1}{(1-\alpha) E_0} \int_{\alpha E_0}^{E_0} \ln \left(\frac{E_0}{E_1} \right) dE_1 \quad (3.22)$$

The derivation simplifies greatly if we define $\tilde{E} \equiv E_1/E_0$ before we proceed.

$$\xi = \frac{-1}{1-\alpha} \int_{\alpha}^1 \ln(\tilde{E}) d\tilde{E} \quad (3.23)$$

Now we use $\int \ln x dx = x \ln(x) - x + C$ (which you can check by taking the derivative of both sides) to arrive at

$$\xi = \frac{-1}{1-\alpha} [-1 - \alpha \ln(\alpha) + \alpha] = 1 + \frac{\alpha}{1-\alpha} \ln(\alpha) \quad (3.24)$$

This result is shown in figure 3.4. As noted above, ξ is the inverse of the

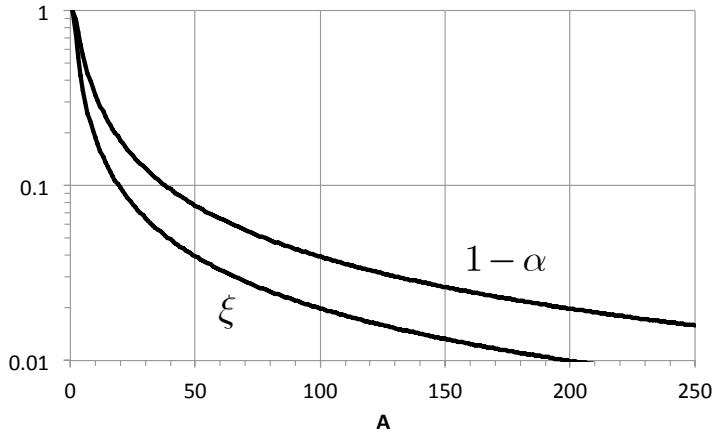


Figure 3.4 $1 - \alpha$ and ξ vs. atomic mass.

number of collisions required, in Fermi's model, to reduce the energy of a neutron by a factor of e . For example for $A = 200$ it takes about $N_c = 100$ collisions. On the other hand it takes only a single collision with a proton, for which $\alpha = 0$. Mathematically this is because $\ln(\alpha)$ diverges as α goes to zero more weakly than $1/\alpha$. As a result $\alpha \ln(\alpha)$ goes to zero as α goes to zero. For ^{16}O it takes 8.3 collisions to drop the neutron energy by a factor of e .

$1 - \alpha$ is the maximum fractional energy loss. It is never in fact very far from ξ , since ξ is a logarithmically weighted average fractional energy loss. $1 - \alpha$ is unity for protons, as is ξ . It is higher than ξ for greater values of A , with an asymptotic ratio of two.

To evaluate the power of neutron slowing down we are not only interested in ξ but also the mean free path between collisions. Since there are two protons for each oxygen nucleus in light water, and the proton elastic scattering

cross-section is about five times higher than that of the oxygen nucleus, it is evident that the oxygen in light water plays an even more modest role in neutron thermalization than indicated by ξ . To quantify this we first define a total macroscopic elastic scattering cross-section, summed over all species of nuclei (elements and isotopes) present.

$$\overline{\Sigma_e} \equiv \sum_{nuclei} \Sigma_e \quad (3.25)$$

Because Σ is already used for the macroscopic cross-section (section 2.1), we use the overbar to indicate the sum over all elements and isotopes. It is natural to sum macroscopic cross-sections in this way, since they each represent the differential probability of scattering out of a beam, $-dn/n$, per differential path length, dx , along the neutron's path, for a particular type of nucleus (section 2.2). Now if we are interested in the total differential logarithmic energy decrement per differential path length, we can sum the contributions from each as well, to get the “slowing down power” of a medium.

$$\overline{\xi \Sigma_e} \equiv \sum_{nuclei} \xi \Sigma_e \quad (3.26)$$

Table 3.1 shows the total macroscopic elastic scattering cross-section, slowing down power, radiative absorption cross section, radiative absorption rate coefficient, and slowing-down time (see section 3.3) for the neutron moderators used in nuclear reactors. The elastic scattering cross-sections for hydrogen, deuterium, carbon and oxygen, used as moderators, or components of moderators, in thermal-spectrum reactors, are evaluated at a representative value of 1 keV, midway logarithmically between the MeV and the eV energy range. The radiative absorption rate coefficients, $\nu_\gamma = \overline{\Sigma_\gamma v}$ are calculated by choosing any point in the $1/v$ absorption range, and evaluating $n\sigma_\gamma v$. In both cases, the sum is then taken over the species of nuclei present. (Oxygen and carbon are nearly mono-nuclidic.) Sodium and lead are used as coolants in fast reactors, in which moderation is undesirable, but of course they still provide some moderation and absorption. Their cross-sections are averaged over the range of 100 to 500 keV, meant to be representative of the neutron spectra found in fast-spectrum reactors. Sodium is mono-nuclidic, but there are four naturally-occurring isotopes of lead, which are averaged appropriately, as indicated.

Question: $(\overline{\Sigma_e})^{-1}$ is the mean free path to an elastic scattering event. What is $(\overline{\xi \Sigma_e})^{-1}$?

As can be seen light water is much more effective than other moderators

Table 3.1 *Total macroscopic elastic scattering cross-section, slowing down power, radiative absorption rate coefficient, and slowing-down time for neutron moderators.*
(See text for energies of evaluation.)

	N	$\overline{\Sigma_e}$	$\overline{\xi \Sigma_e}$	$\overline{\Sigma_\gamma}$	$\nu_\gamma = \overline{\Sigma_\gamma v}$	τ_s
Light water	$3.33 \cdot 10^{28}$	132	121	2.22	4890	$1.69 \cdot 10^{-6}$
Heavy water	$3.33 \cdot 10^{28}$	35	18	$4.01 \cdot 10^{-3}$	8.82	$1.13 \cdot 10^{-5}$
Graphite	$1.14 \cdot 10^{29}$	51	8	$4.40 \cdot 10^{-2}$	96.8	$2.55 \cdot 10^{-5}$
Sodium	$2.43 \cdot 10^{28}$	8.91	0.753	$1.69 \cdot 10^{-3}$		
Lead	$3.10 \cdot 10^{28}$	25.1	0.242	$1.17 \cdot 10^{-2}$		

at slowing down neutrons. Its weakness is that the (n,γ) radiative capture reaction on protons — once the neutrons have slowed down — competes strongly with the ^{238}U fission reaction. As a result, light water can only be used as a moderator with enriched uranium. On the other hand, heavy water and graphite moderators are used with natural or near-natural uranium. This is possible because these moderators do not contain protons that scavenge thermal neutrons, which compensates for the high ratio of ^{238}U to ^{235}U . However, as a result of this high ratio radiative capture on ^{238}U is greatly enhanced relative to fission, so heavy-water and graphite moderated reactors are prodigious producers of Pu, per unit fission power. This makes them attractive for the production of plutonium for weapons.

3.3 Slowing Down Time

We are now in a position to use Fermi's continuous slowing-down model to calculate the time required for a neutron to slow down from the MeV energy range to the eV energy range. Working from equations 3.21 and 3.26, we can write

$$\frac{1}{E} \frac{dE}{dt} = \frac{d \ln(E)}{dt} = \frac{dx}{dt} \sum_{\text{nuclei}} \left[\frac{d \ln(E)}{dN_c} \frac{dN_c}{dx} \right] = -v \overline{\xi \Sigma_e} \quad (3.27)$$

which gives us a pretty and simple result:

$$\frac{dE}{dt} \approx -v \overline{\xi \Sigma_e} E \quad (3.28)$$

This equation can be solved straightforwardly for the slowing-down time:

$$\tau_{slow} \approx \int_{E_{min}}^{E_{max}} \left(\frac{dE}{dt} \right)^{-1} dE = \frac{1}{\xi \Sigma_e} \int_{E_{min}}^{E_{max}} \frac{dE}{v(E) E} \quad (3.29)$$

$$= \frac{1}{\xi \Sigma_e} \int_{v_{min}}^{v_{max}} \frac{2vdv}{v^3} = \frac{2}{\xi \Sigma_e} \left(\frac{1}{v_{min}} - \frac{1}{v_{max}} \right) \quad (3.30)$$

For MeV neutrons slowing down to the energy where the spectrum of thermalized neutrons is conventionally taken to dominate, ~ 0.5 eV, we can neglect the $1/v_{max}$ term. The neutron velocity at 0.5 eV is $9.8 \cdot 10^3$ m/s, giving a slowing-down time in light water of $1.69 \mu\text{sec}$. It is interesting to multiply this slowing-down time by the absorption rate coefficient, $\nu_\gamma = \overline{\Sigma_\gamma v}$, shown in table 3.1. We can see that there is less than 1% absorption during the slowing down process in light water, which we will neglect, and truly tiny absorption in heavy water or graphite. As we will see, however, there is significant resonant absorption on ^{238}U during slowing down, and there is significant absorption by protons after the neutrons thermalize. In a light-water reactor, perhaps 50% of the active volume of the reactor is filled with light water, the rest being structure and fuel. Since neither of these contribute significantly to the slowing-down process, the effective slowing-down time is in practice perhaps twice longer than in pure light water. On the other hand, the effective absorption rate in the moderator is reduced by the same factor, so $\nu_{abs}\tau_s$ is unchanged.

3.4 Neutron flux vs. energy, $\phi(E)$, and vs. lethargy, $\phi(u)$

In section 2.3 we defined $\phi \equiv nv$, in the context of a collection of particles of given density and speed. Now we are interested in working with neutrons that have a wide distribution of speeds and so energies. To define $\phi(E)$, neutron flux as a function of energy, let us start by positing that ϕ is the integral over energy of $\phi(E)$:

$$\int_0^\infty \phi(E)dE \equiv \phi \quad (3.31)$$

Now we can say that an element of $d\phi$ is given by

$$d\phi = \phi(E)dE \quad (3.32)$$

allowing us to define

$$\phi(E) \equiv \frac{d\phi}{dE} \quad (3.33)$$

We can use the same analysis to define neutron density as a function of energy.

$$\int_0^\infty n(E)dE \equiv n \quad (3.34)$$

$$n(E) \equiv \frac{dn}{dE} \quad (3.35)$$

It is intuitive to assume $\phi(E) = n(E)v(E)$. We can show this formally by considering the case of a narrow energy distribution of neutrons, with width δE around energy E and corresponding neutron speed $v(E)$. This is exactly the case in which we earlier defined $\phi \equiv nv$. We can use this case to relate $\phi(E)$ to $n(E)$ by noting that

$$\phi = \phi(E)\delta E = nv = n(E)\delta E \cdot v(E) \quad (3.36)$$

$$\phi(E) = n(E)v(E) \quad (3.37)$$

This type of analysis is helpful as a model for the case of a different independent variable. It is not uncommon in nuclear reactor physics to define a quantity called “lethargy” for neutrons, denoted u , and defined as

$$u \equiv \ln\left(\frac{E_0}{E}\right) \quad (3.38)$$

where E_0 is generally taken to be 10 MeV, to encompass all of the neutrons of interest in a fission system. The idea here is that neutrons become more “lethargic” as they slow down, so lethargy increases with decreasing energy. On the basis of Fermi’s analysis of slowing-down, neutrons make approximately equal steps up in lethargy (down in $\ln(E)$) with each collision. By analogy with the discussion of $\phi(E)$ we can write down for a given differential increment of ϕ

$$d\phi = \phi(E)dE = -\phi(u)du \quad (3.39)$$

where the minus sign arises from the fact that u varies in the opposite direction from E . This gives us

$$\phi(E) = -\phi(u)\frac{du}{dE} = \frac{\phi(u)}{E} \quad (3.40)$$

$$\phi(u) = E\phi(E) \quad (3.41)$$

where $u = \ln(E_0/E)$. Note that $E\phi(E)$ has the same units as ϕ , $\text{m}^{-3}\text{s}^{-1}$.

Often $E\phi(E)$ is plotted, rather than $\phi(E)$. We will see in section 3.6 why this is convenient. Understandably, however, even in this case the x axis is almost always chosen to be E rather than u .

3.5 Fast energy region $\phi_F(E)$

Now we will look into the neutron flux as a function of energy, $\phi(E)$, in three different energy ranges: the Fast energy range, where the direct source of fast neutrons from fission is very important in setting $\phi_F(E)$, the Intermediate energy range, where $\phi_I(E)$ is set mostly by the slowing down process (although resonant absorption is important towards the lower end), and the Thermal energy range, where neutrons are largely in thermal equilibrium with their environment, although $\phi_T(E)$ is fed by neutrons slowing down into this range, and neutrons are finally either radiatively absorbed or drive fission. Then, of course, the process starts over again at the top.

This analysis is appropriate for thermal reactors, which take advantage of the favorable $1/v$ range of the fission cross-section. Later in this chapter we will discuss fast reactors, which are designed to minimize neutron moderation and utilize neutrons with energies of about 100 keV and above. In the next chapter we will discuss the spatial diffusion of neutrons during their lifetime. However in the present chapter we will treat the problem as if the reactor were infinite in spatial extent, with no spatial gradients.

In the Fast energy range, typically taken to include all neutrons above about 500 keV, the dominant source of neutrons is directly due to fission rather than due to slowing-down from higher energies. Empirically it was found that this source of neutrons can be well approximated by the Watt probability distribution, for ^{235}U fission driven by both thermal and MeV-range neutrons. B.E. Watt of Los Alamos first published data supporting a distribution of this form in 1952.

$$\chi(E_{\text{MeV}}) = 0.484 \sinh(\sqrt{2E_{\text{MeV}}}) e^{-E_{\text{MeV}}} \quad (3.42)$$

$\chi(E)$, as shown in figure 1.2, is normalized such that $\int_0^\infty \chi(E_{\text{MeV}}) dE_{\text{MeV}} = 1$.

Let us define S as the total volumetric neutron source rate due to fission, with units $\text{s}^{-1}\text{m}^{-3}$. Then the neutron source rate per unit energy is given by $s(E) = S\chi(E)$. Note that we will work with $\chi(E)$ in SI units of $\text{s}^{-1}\text{m}^{-3}\text{J}^{-1}$. Typical values for S in commercial light-water reactors are in the range of $10^{19} \text{ s}^{-1}\text{m}^{-3}$.

Question: Estimate the volume of a reactor with volume average $S = 10^{19} \text{ s}^{-1}\text{m}^{-3}$. Assume 3 GW(th) of power production. Take the energy production to be 202 MeV per fission event, and $\bar{\nu} = 2.44$ neutrons, on average, per fission. If you further assume a cylindrical reactor fuel volume of typical height 4m, what is its radius?

Neutron source rates and power densities are higher in fast-spectrum reactors, and lower in graphite or heavy-water moderated reactors. The fuel

rods are more closely packed in liquid-metal-cooled fast-spectrum reactors, in order to minimize moderation, while the fuel is much more widely spaced in graphite or heavy-water moderated reactors, because, as shown in table 3.1, these moderators slow down neutrons less rapidly. As we will see in section 3.6.1 in thermal-spectrum reactors we need to slow down neutrons past the radiative absorption resonances with minimum absorption, in order to maximize their chance of thermalizing and driving fission. If the neutrons drift slowly down in energy, then the ratio of moderator volume to fuel volume needs to be large in order to reduce the chance that a neutron will find the fuel as it passes through the resonant energies of ^{238}U .

Equation 2.10 describes the depletion, or loss, of a mono-energetic beam of particles due to collisions with target particles. We can apply the same formalism to a small energy range, dE , of fast neutrons with average energy E . We can also include, for the case at hand, the source rate of fission neutrons. This gives us:

$$\frac{dn_F}{dt}dE = s(E)dE - \Sigma_{loss}(E)\phi_F(E)dE \quad (3.43)$$

Solving this with the assumption of steady state operation we have:

$$\phi_F(E) = s(E)/\Sigma_{loss}(E) \quad (3.44)$$

Now we need to ask ourselves what we mean by $\Sigma_{loss}(E)$ in this case. Elastic collisions of fast neutrons with heavy nuclei such as uranium or plutonium, with $\xi \sim 0.008$, barely change neutron energies, so we can neglect the effect of these collisions on the neutron spectrum. Elastic collisions with protons, with $\xi = 1$, cause substantial energy loss, so they can be considered to take neutrons out of the “Fast” energy spectrum altogether. One can make a similar argument for deuterons, with $\xi = 0.725$. Elastic collisions with carbon and oxygen are intermediate cases, with $\xi = 0.158$ and 0.120 , respectively. For present purposes, we will neglect these, although we will see later that their resonances leave some detailed signatures on the shape of the spectrum. Their contribution to slowing down is also reduced because, at fission energies, their center-of-mass scattering is becoming forward-directed, rather than isotropic. This is because the neutron de Broglie wavelength begins to approach the nuclear diameter. Interestingly, at these same energies scattering on protons remains quite isotropic, in the center-of-mass frame, because the proton nuclear diameter is so small, table 2.1.

Inelastic collisions and radiative absorption should both “count” since they take neutrons out of the Fast spectral region. Hydrogen and deuterium cannot support inelastic scattering, since they do not have bound excited

states. The thresholds for inelastic scattering on carbon and oxygen are at 5 MeV and 6 MeV, respectively, where the Watt spectrum has fallen to low values, so we can neglect inelastic scattering on them. However inelastic collisions on zirconium in LWR fuel rod cladding can have some effect, since the threshold is quite a bit lower. We will neglect here other such “parasitic” absorption mechanisms. Fission events extract neutrons, but also inject them, so we can include fission events as absorptions, but we must also count them within $s(E)$ defined to include contributions from fission driven both by thermal neutrons and by fast ones, $s(E) = s_T(E) + s_F(E)$. The energy spectrum of neutrons from fission due to neutrons in the “Fast” energy region is not significantly different from that due to thermal neutrons.

Fast neutrons have mean free paths of about 4 cm or more in most materials, including both water and uranium dioxide fuel. Fuel pins are about 1 cm in diameter, and they are spaced apart by of order 1 cm. Thus we can assume, rather roughly, that $\phi_F(E)$ is equal in the fuel, the cladding, and the moderator, in a light-water reactor. Thus the fuel, cladding and moderator contribute to the overall loss in proportion to their own volume and macroscopic cross-section, giving

$$\begin{aligned} V^{tot}\Sigma_{loss}(E)\phi_F(E) &= V^{mod}\overline{\Sigma_e^{mod}}(E)\phi_F(E) + V^{clad}\overline{\Sigma_{in}^{clad}}(E)\phi_F(E) \\ &+ V^{fuel}\left[\overline{\Sigma_f^{fuel}}(E) + \overline{\Sigma_\gamma^{fuel}}(E) + \overline{\Sigma_{in}^{fuel}}(E)\right]\phi_F(E) \end{aligned} \quad (3.45)$$

This is equivalent to “homogenizing” the materials, but it is physically based on the (imperfect) assumption that $\phi_F(E)$ is homogeneous. Not surprisingly, this is called the “homogeneous approximation.” In practice, fast neutrons are slightly denser in the fuel, where they are produced, than in the moderator. This is taken into account using a “fast advantage factor,” but we will neglect it here.

Dividing by $V^{tot}\phi_F(E)$ we have

$$\begin{aligned} \Sigma_{loss}(E) &= \frac{V^{mod}}{V^{tot}}\overline{\Sigma_e^{mod}}(E) + \frac{V^{clad}}{V^{tot}}\overline{\Sigma_{in}^{clad}}(E) \\ &+ \frac{V^{fuel}}{V^{tot}}\left[\overline{\Sigma_f^{fuel}}(E) + \overline{\Sigma_\gamma^{fuel}}(E) + \overline{\Sigma_{in}^{fuel}}(E)\right] \end{aligned} \quad (3.46)$$

where the superscripts on the $\bar{\Sigma}$'s indicate the volumes over which the constituent Σ 's are summed, and the subscripts indicate elastic scattering (only on hydrogen or deuterium), inelastic scattering on cladding and fuel nuclei, and absorption on fuel nuclei, including both fission and a small amount of radiative absorption. Radiative absorption on moderator and cladding nuclei is negligible in the fast energy region, and fission is of course impossible.

V with superscripts indicates the volume of moderator, cladding, and fuel, as well as the total volume.

We are now in a position to evaluate the neutron multiplication in the fast energy region, conventionally denoted ϵ , which is defined by $\epsilon \equiv S/S_T = (S_T + S_F)/S_T$. First we write down our equation for ϕ_F including fission induced both by thermal and fast neutrons:

$$\phi_F(E) = \frac{s_T(E) + s_F(E)}{\Sigma_{loss}(E)} = (S_T + S_F) \frac{\chi(E)}{\Sigma_{loss}(E)} \quad (3.47)$$

as well as the equation for the production rate of neutrons by this spectrum,

$$S_F = \frac{V^{fuel}}{V^{tot}} \int_0^{\infty} \phi_F(E) \overline{\nu_F \Sigma_f^{fuel}}(E) dE \quad (3.48)$$

where the integral corresponds to summing the neutron production from each differential range, dE , of energy. $\overline{\nu_F}$ represents the mean neutron production per fission event, due to fast neutrons, for each type of nucleus.

Substituting equation 3.47 into equation 3.48 we have:

$$S_F = (S_T + S_F) \frac{V^{fuel}}{V^{tot}} \int_0^{\infty} \frac{\overline{\nu_F \Sigma_f^{fuel}}(E)}{\Sigma_{loss}(E)} \chi(E) dE \quad (3.49)$$

Now we note that the complicated factor on the right is just the number of neutrons produced per neutron lost from a Watt spectrum of neutrons. Thus if we start with a generation of Watt-spectrum fast neutrons, this tells us how many fast neutrons are produced in the next generation as the present generation is lost. This generation over generation gain is called k . Since we are talking only about gain in the Fast spectrum, due to Fast-spectrum neutrons, and we are considering an infinite homogeneous medium we assert:

$$k_{F,\infty} = \frac{V^{fuel}}{V^{tot}} \int_0^{\infty} \frac{\overline{\nu_F \Sigma_f^{fuel}}(E)}{\Sigma_{loss}(E)} \chi(E) dE \quad (3.50)$$

Now equation 3.49 is simpler to work with:

$$S_F = (S_T + S_F) k_{F,\infty} \quad (3.51)$$

from which we can derive simply

$$S_F (1 - k_{F,\infty}) = S_T k_{F,\infty} \quad (3.52)$$

Thus we have

$$\epsilon = \frac{(S_T + S_F)}{S_T} = \frac{(S_T + S_F) k_{F,\infty}}{S_T k_{F,\infty}} = \frac{S_F}{S_F (1 - k_{F,\infty})} = \frac{1}{1 - k_{F,\infty}} \quad (3.53)$$

This makes perfect sense, as we expect

$$\epsilon = 1 + k_{F,\infty} + k_{F,\infty}^2 + k_{F,\infty}^3 \dots = \frac{1}{1 - k_{F,\infty}} \quad (3.54)$$

Substituting back in our definition of $k_{F,\infty}$, we have

$$\epsilon = \frac{S_T + S_F}{S_T} = \left[1 - \frac{V^{fuel}}{V^{tot}} \int_0^\infty \frac{\overline{\nu_F \Sigma_f^{fuel}}(E)}{\Sigma_{loss}(E)} \chi(E) dE \right]^{-1} \quad (3.55)$$

Since we have already made a number of approximations to this point, it is conventional to eliminate the integral by using fission-spectrum weighted values for $\Sigma_{loss}(E)$ and $\Sigma_f(E)$ of the form

$$\begin{aligned} \Sigma_{F,loss} &\equiv \int_0^\infty \chi(E) \Sigma_{loss}(E) dE \\ \Sigma_{F,f} &\equiv \int_0^\infty \chi(E) \Sigma_f(E) dE \end{aligned} \quad (3.56)$$

where we have taken advantage of the normalization of $\chi(E)$ arranged to make its integral dE from 0 to ∞ equal to unity. This gives us a simplified result:

$$\epsilon \approx \left[1 - \frac{V^{fuel}}{V^{tot}} \frac{\overline{\nu_F \Sigma_{F,f}^{fuel}}}{\Sigma_{F,loss}} \right]^{-1} \quad (3.57)$$

Table 3.2 provides relevant fission-spectrum weighted “Fast” microscopic cross-sections, and Table 3.3 relevant number densities, for evaluating equation 3.88. Sodium and lead are included, anticipating that we will want to calculate ϵ for liquid-metal-cooled fast-spectrum reactors.

Since the fuel volume is generally quite a bit less than the total volume, and the fission cross-section is quite a bit less than the sum of all the cross-sections that extract neutrons from the fast spectrum, this “fast fission factor” is generally only about $5 \pm 2\%$ above unity in light-water reactors. The higher values occur when the fuel corresponds to a larger fraction of the total volume, and the lower values when this fraction is smaller. Let’s compute an example. A typical fuel pin diameter in an LWR is 1 cm, within which the zircaloy cladding might be 0.5 mm thick. The spacing between fuel rod centers (the so-called “lattice pitch”) might be 1.3 cm. This gives $V^{fuel}/V^{tot} = 0.376$, $V^{clad}/V^{tot} = 0.088$, and $V^{mod}/V^{tot} = 0.535$. Let us assume fresh 4% enriched uranium fuel.

Table 3.2 *Watt-spectrum weighted (Fast) microscopic cross-sections (barns = $10^{-28} m^2$) and $\bar{\nu}$*

Atom	At. Mass	$\sigma_{F,f}$	$\sigma_{F,\gamma}$	$\sigma_{F,e}$	$\sigma_{F,in}$	$\bar{\nu}$
Hydrogen	1	—	$5.02 \cdot 10^{-5}$	4.01	—	—
Deuterium	2	—	$7.12 \cdot 10^{-6}$	2.54	—	—
Carbon	12	—	$2.51 \cdot 10^{-5}$	2.33	$1.01 \cdot 10^{-2}$	—
Oxygen	16	—	$1.20 \cdot 10^{-4}$	2.74	$2.46 \cdot 10^{-3}$	—
Sodium	23	—	$2.66 \cdot 10^{-4}$	2.72	0.513	—
Magnesium	Natural	—	$3.74 \cdot 10^{-4}$	3.14	0.327	—
Iron	Natural	—	$3.06 \cdot 10^{-3}$	2.60	0.644	—
Zirconium	Natural	—	$9.70 \cdot 10^{-3}$	5.07	0.687	—
Lead	Natural	—	$2.88 \cdot 10^{-3}$	5.72	0.704	—
Uranium	235	1.23	$9.52 \cdot 10^{-2}$	4.35	1.98	2.6
Uranium	238	0.303	$7.11 \cdot 10^{-2}$	4.87	2.59	2.6
Uranium	Natural	0.309	$7.13 \cdot 10^{-2}$	4.87	2.59	2.6
Uranium	4% enriched	0.340	$7.21 \cdot 10^{-2}$	4.85	2.57	2.6
Uranium	20% enriched	0.488	$7.59 \cdot 10^{-2}$	4.77	2.47	2.6
Plutonium	239	1.85	$4.10 \cdot 10^{-2}$	4.38	1.59	3.18
Plutonium	240	1.39	$8.31 \cdot 10^{-2}$	4.57	1.78	3.11
Plutonium	241	1.62	$9.39 \cdot 10^{-2}$	4.27	1.79	2.93
Plutonium	242	1.15	$8.09 \cdot 10^{-2}$	4.79	2.01	3.05

We can derive the macroscopic cross-sections from tables 3.2 and 3.3. For $\Sigma_{F,loss}$ we start from the Watt-spectrum averaged version of equation 3.46. It is convenient that 1 barn = $10^{-28} m^2$, and typical densities are in the $10^{28} m^{-3}$ range. Thus one doesn't need to carry along these two large factors in evaluating macroscopic cross-sections, since they cancel.

$$\begin{aligned} \Sigma_{F,loss} &= 0.535 \cdot 6.69 \cdot 4.01 + 0.088 \cdot 4.31 \cdot 0.687 \\ &\quad + 0.376 \cdot 2.34 \cdot [0.34 + 0.0721 + 2.57] = 17.2 \text{ m}^{-1} \end{aligned} \quad (3.58)$$

which is dominated by elastic scattering on hydrogen, but with a significant

Table 3.3 Molecular weights, mass densities and number densities

Material	Atoms	Molecular Weight g/mole	Mass Density kgm^{-3}	Number Density m^{-3}
Graphite	C	12.011	2267	$1.14 \cdot 10^{29}$
Water	O	18.016	1000	$3.35 \cdot 10^{28}$
	H			$6.69 \cdot 10^{28}$
	D			$6.69 \cdot 10^{28}$
Sodium	Na	22.99	997	$2.43 \cdot 10^{28}$
Iron	Fe	55.84	7874	$8.49 \cdot 10^{28}$
Zirconium	Zr	91.22	8520	$4.31 \cdot 10^{28}$
Lead	Pb	207.2	10660	$3.10 \cdot 10^{28}$
Uranium metal	U	238.03	19100	$4.83 \cdot 10^{28}$
UO_2	U	270.3	10500	$2.34 \cdot 10^{28}$
	O			$4.68 \cdot 10^{28}$

Table 3.4 Example Light Water Reactor Lattice Cell

Parameter	Value
Fuel pin diameter	0.01 m
Zirc cladding	0.0005 m
Lattice pitch	0.013 m
V^{fuel}/V^{tot}	0.376
V^{clad}/V^{tot}	0.088
V^{mod}/V^{tot}	0.535

contribution from inelastic scattering on ^{238}U . We can also calculate

$$\overline{\nu_F \Sigma_{F,f}^{fuel}} = 2.6 \cdot 2.34 \cdot 0.34 = 2.07 \text{ m}^{-1} \quad (3.59)$$

which is dominated by collisions with ^{238}U . From these two, and $V^{fuel}/V^{tot} = 0.376$ found in table 3.4 we find

$$\epsilon = (1 - 0.376 \cdot 2.07/17.1)^{-1} = 1.05 \quad (3.60)$$

Question: Qualitatively, do you expect ϵ to decline rapidly with fuel burn-up? You can ignore fast neutron absorption or scattering on built-up fission products.

Radiative absorption is the only mechanism that on net extracts fast neutrons from the slowing down process (fission recycles them and multiplies them), and its cross-section in this energy range is very small. One could in principle count it as a small deduction from ϵ but this effect is of order 0.4% and is generally neglected at this level of analysis. It is assumed that all of the neutrons produced by fission in the “Fast” energy region are slowed down by elastic and inelastic scattering to the Intermediate energy region. Thus the number of neutrons per second per m³ provided to the Intermediate energy region equals ϵS_T .

3.6 Intermediate energy region $\phi_I(E)$

Now we are interested in the Intermediate energy region, between about 500 keV and about 0.5 eV. Evidently this region covers a broad range, some six orders of magnitude in energy. We will use our results on slowing down by elastic collisions to calculate the neutron flux spectrum in this region. The key findings we will use are

- An elastic collision causes a neutron of energy E_0 to fall to an energy between αE_0 and E_0
- For isotropic center-of-mass scattering, the neutron falls with equal probability to any energy within this range.

Once we have derived the resulting “slowing down” spectrum, we will discuss the effects of the key neutron loss mechanism near the lower end of this energy range, resonant radiative absorption. Because of this process, the Intermediate energy range is also called the “resonance region.” We can neglect fission due to neutrons in the Intermediate energy range, since it is much weaker than absorption – in part because thermal-spectrum reactors generally have uranium enriched to at most 5% ²³⁵U, and this energy range is below the threshold for fission of ²³⁸U. Finally we will calculate the “resonance escape probability,” p , the probability that a neutron entering the Intermediate energy range will escape being captured by the resonances, and will be delivered to the next energy range down, the Thermal energy range.

To make progress we need to define a new quantity, $q(E)$, which represents the flux of neutrons downwards in energy across energy E . The units of $q(E)$

are the same as those of the source rate of neutrons into the Intermediate energy range, ϵS_T , $\text{m}^{-3}\text{s}^{-1}$. Indeed everywhere above the range of significant resonant radiative absorption $q(E)$ must equal ϵS_T , if neutrons are not going to pile up above E with time.

In some differentially short interval of time, dt , the only neutrons that can cross energy E are those with initial energy E' in the range $E/\alpha > E' > E$. This is because their final energies must be at least α times their initial energies and must be below their initial energies. We can ignore the case of more than a single collision in this calculation, because we are considering a differentially short period of time and the probability of two collisions is differentially small compared with the probability of one. The energy range available to the neutron after the collision is from E' down to $\alpha E'$. These initial and final ranges are shown in figure 3.5.

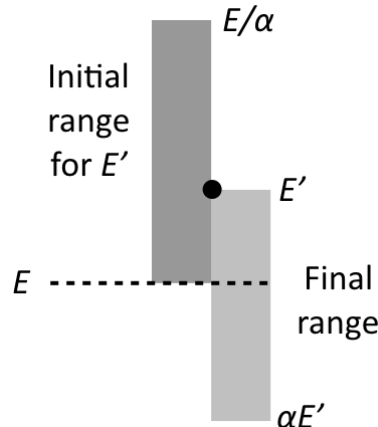


Figure 3.5 Initial and final energy ranges for a neutron crossing energy E .

Assuming isotropic center-of-mass scattering, the probability that a collision will cause a neutron of energy E' to cross energy E is proportional to the fraction of its final energy range below E , $(E - \alpha E')/(E' - \alpha E')$. Thus, assuming that Σ_e is independent of energy, the rate of neutrons crossing energy E in the absence of losses is given by

$$q(E) = \epsilon S_T = \Sigma_e \int_E^{E/\alpha} \phi_I(E') \left(\frac{E - \alpha E'}{E' - \alpha E'} \right) dE' \quad (3.61)$$

where the integral corresponds to a sum over dE' of the rate of neutrons crossing E , including the probability that such a crossing happens at a collision.

If we define $\tilde{E}' \equiv E'/E$ and change the integration variable from E' to \tilde{E}' (E is fixed since we are evaluating q of a given E) this becomes

$$q(E) = \epsilon S_T = \Sigma_e E \int_1^{1/\alpha} \phi_I(E\tilde{E}') \left(\frac{1/\tilde{E}' - \alpha}{1 - \alpha} \right) d\tilde{E}' \quad (3.62)$$

The term in parentheses, which weights the integral over $\phi(E\tilde{E}')$, has no explicit energy dependence. This implies that the only way for $q(E)$ to be independent of energy, as required in the absence of losses, is for $\phi_I(x)$ to be proportional to $1/x$, making $\phi_I(E\tilde{E}') = \psi/(E\tilde{E}')$ where ψ is a constant. Uniquely in this case will the E dependence of q drop out.

We should really be considering a mix of target nuclei. This would add terms of the same form on the right hand side of equation 3.62. These new terms would have different values of Σ_e and α , but would each still require the variation of $\phi_I(E) \propto 1/E$ in order to maintain q constant vs. energy.

We now proceed to evaluate the integral in equation 3.62, using our result that $\phi(E) = \psi/E$ where ψ is a constant.

$$\begin{aligned} q(E) &= \epsilon S_T = \frac{\psi \Sigma_e}{1 - \alpha} \int_1^{1/\alpha} \left(\frac{1/\tilde{E}' - \alpha}{\tilde{E}'} \right) d\tilde{E}' = \frac{\psi \Sigma_e}{1 - \alpha} \left[-\frac{1}{\tilde{E}'} - \alpha \ln(\tilde{E}') \right]_1^{1/\alpha} \\ &= \frac{\psi \Sigma_e}{1 - \alpha} [-\alpha + 1 + \alpha \ln(\alpha)] = \psi \Sigma_e \left(1 + \frac{\alpha \ln \alpha}{1 - \alpha} \right) = \psi \xi \Sigma_e \end{aligned} \quad (3.63)$$

giving the simple result

$$\phi_I(E) = \frac{\psi}{E} = \frac{\epsilon S_T}{E \xi \Sigma_e} \quad (3.64)$$

Question: Outline how to take into account multiple types of scatterers and arrive at the more general result:

$$\phi_I(E) = \frac{\psi}{E} = \frac{\epsilon S_T}{E \xi \Sigma_e} \quad (3.65)$$

3.6.1 Resonant absorption

While the neutrons are slowing down due to elastic scattering, they can undergo other collisions. Inelastic scattering is largely cut off except at the very highest energy end of the intermediate energy region. Fission and resonant

absorption on ^{235}U are generally neglected and fission on ^{238}U is almost non-existent. However resonant absorption on ^{238}U does play a significant role in the energy range below about 500 eV, the logarithmic mid-point of the Intermediate energy range. As is characteristic of quantum-mechanical calculations, the energy dependence of the absorption cross-section for stationary nuclei, the so-called “natural” line shape, is given by a Lorentzian profile, in this case multiplying the background $1/v$ variation of absorption.

$$\sigma_\gamma(E) = \left(\frac{E_r}{E}\right)^{1/2} \frac{\sigma_0}{1 + 4(E - E_r)^2/\Gamma^2} \quad (3.66)$$

The peak value of this function is σ_0 and its width at half-maximum is $\pm\Gamma/2$. By the uncertainty principle relating uncertainty in energy to uncertainty in time, $\Gamma = \hbar/\tau$ where τ is the lifetime of the excited state of the nucleus after it absorbs the neutron.

These absorption lines in uranium are generally quite narrow. Figure 3.6 shows the “natural” line width of the ^{238}U resonance near 102.6 eV. It has a width of only about ± 0.075 eV at half-height. The same figure also shows the effect on the line profile of thermal motion of the uranium nuclei at 300° K, resulting in a line width of about ± 0.2 eV at half height.

Let us assume that the thermal motion of the nuclei corresponds to that of the atoms in an ideal gas, which is a decent first-order approximation at the neutron energies and material temperatures of interest here. Thus the energy of motion in each degree of freedom should be $\approx T/2$, with T expressed in energy units. At 300° K the average total energy of thermal motion corresponds to about $(3/2) \cdot 0.026\text{eV}$. Because of the much greater mass of uranium nuclei compared with neutrons, the speed of the nuclei corresponds to that of a neutron with energy reduced from this by a factor of 238. The energy of a neutron with this speed would be just $1.6 \cdot 10^{-4}$ eV.

How can this tiny effective neutron energy cause a significant spreading of the line profile? The answer is that the energy of an incoming neutron in the frame of a moving nucleus is found by first adding the two velocities as a vector sum. The energy of a neutron in the frame of a moving nucleus is then given by

$$E = \frac{1}{2}m_n v^2 = \frac{1}{2}m_n(v_n^2 - 2v_n v_N \cos\theta + v_N^2) \quad (3.67)$$

where m_n is the neutron mass, v_n is the incoming neutron speed in the lab frame, v_N is the speed of the incoming nucleus in the lab frame and θ is the angle between their lab-frame velocities. The third term is negligible, $1.6 \cdot 10^{-4}$ eV as calculated above. But the spreading due to the second

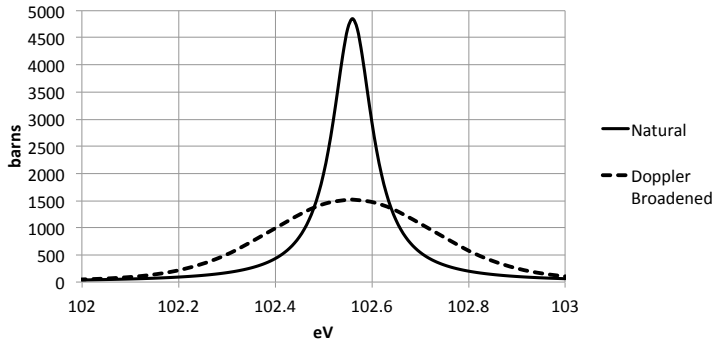


Figure 3.6 Natural and Doppler broadened resonant absorption line in ^{238}U . $T = 300^\circ \text{ K}$.

term is of order $\sqrt{E_n E_N / A} = \sqrt{102.6 \text{ eV} \cdot 1.6 \cdot 10^{-4} \text{ eV}} = 0.128 \text{ eV}$. Thus a nucleus undergoing thermal motion will have a chance to absorb neutrons over a considerably wider range of incoming energies than indicated by the natural absorption line width – higher neutron energies if the nucleus is moving away from the incoming neutron, and lower energies if the nucleus is moving towards it. Concomitantly, neutrons right on the resonance peak in the lab frame will have a lower chance of being absorbed, since many nuclei are moving fast enough that the neutron, in the frame of the nucleus, is well off the resonance peak.

Neutrons that slow down into an absorption resonance, and enter a fuel rod before slowing down further, have a substantial probability of being absorbed. Fuel rods are typically about 1 cm in diameter, and the number density of uranium in uranium dioxide fuel is $2.4 \cdot 10^{28} \text{ m}^{-3}$. Thus an absorption cross-section of 1000 b gives a mean free path of less than 1/2 mm, and neutrons striking the fuel will be absorbed even fairly far from the resonance. Thus as the resonance broadens due to heating of the fuel, absorption will be increased. The absorption cross-section on peak is very much overkill, so the broadening of the wings increases the ability of the fuel to scavenge neutrons, without sacrificing any significant probability of absorption at the peak.

The depletion of the neutron slowing down flux, $q(E)$, across the absorption band of resonance i is given by

$$\begin{aligned} \Delta q(E) &= \phi(E) \Delta E_{eff,i} N_{^{238}\text{U}} \sigma_{\gamma,eff,i} V^{fuel} / V^{tot} \\ &= q(E) \frac{\Delta E_{eff,i} N_{^{238}\text{U}} \sigma_{\gamma,eff,i} V^{fuel}}{E_i \xi^{mod} \Sigma_e^{mod} V^{mod}} \end{aligned} \quad (3.68)$$

Note that both sides of this equation characterize neutrons in units of $\text{m}^{-3}\text{s}^{-1}$. Thus the absorption process depletes the downward flow in energy of the neutrons. ΔE_{eff} is an “effective” energy width of the resonance and $\sigma_{\gamma,eff}$ takes into account the fact that much of the uranium near the center in energy of the resonance and near the geometrical center of the fuel rod sees very little neutron flux, so the “effective” cross-section is reduced. In fact, of course, the nuclear cross-section is unchanged, but the neutron flux is depleted, especially in the core of the fuel, at energies near resonance. We have used $q(E)$, rather than S , in the definition of $\phi(E)$, to take into account the depletion of the flux of neutrons downward in energy, at energy E , by resonances at energies greater than E . For small drops in $q(E)$, we can express the probability of a neutron traversing from above to below the resonance as

$$p_i = \exp \left(-\frac{\Delta E_{eff,i} N_{238U} \sigma_{\gamma,eff,i} V^{fuel}}{E_i \xi^{mod} \Sigma_e^{mod} V^{mod}} \right) \quad (3.69)$$

If we want to know the probability of slowing down through all of the resonances without absorption, we can multiply these probabilities for each resonance to find the overall “resonance escape probability”, p .

$$p = \exp \left(-\frac{N_{238U} I V^{fuel}}{\xi^{mod} \Sigma_e^{mod} V^{mod}} \right) \quad (3.70)$$

where

$$I = \sum_i \frac{\Delta E_{eff,i} \sigma_{\gamma,eff,i}}{E_i} \quad (3.71)$$

Now we have hidden the complex calculation of the effective line widths and absorption cross-sections in I , which has units of barns. Fortunately there are reasonable approximations for this sum in cases of interest. For the case where we can ignore the fact that a fuel rod partially shields its neighbors at near-resonance energies, we can approximate, for uranium dioxide fuel rods of diameter $2 \text{ mm} < D < 3.5 \text{ cm}$,

$$I \approx [4.45 + 16.7 D_{cm}^{-1/2}] [1 + 6 \cdot 10^{-3} (T_K^{1/2} - 300^{1/2})] \quad (3.72)$$

where D is measured in centimeters, and T in Kelvins. For fuel rods that partially shield one another, I is somewhat reduced.

An interesting feature of equation 3.70 is that it is very sensitive to the slowing down power of the moderator, $\xi^{mod} \Sigma_e^{mod}$. This suggests a significant problem for heavy-water or graphite moderators, whose slowing down power is much less than that of light water, as shown in table 3.1. As we discussed

when we looked at power densities in different types of reactors, this problem is compensated by increasing V^{mod}/V^{fuel} . This has the result that reactor cores based on heavy-water or graphite moderators are much larger, for a given power output, than those based on light-water moderators. This is, of course, a major economic attraction for LWRs, and largely why they have dominated the market. As we will see later, however, heavy-water and graphite-moderated reactors are very attractive for would-be proliferators.

A typical temperature operating point for the fuel in an LWR might be about $1000^\circ \text{ K} = 727^\circ \text{ K}$, considerably above the temperature of the coolant/moderator. The fission heat is largely deposited in the fuel in the form of fission fragments, and must diffuse down a strong temperature gradient to the coolant. This provides a very favorable negative feedback characteristic of nuclear reactors that depend on thermal neutron fission; it means that the reaction rate will be slowed as the fuel heats and the slowing-down neutrons are increasingly absorbed. If the reaction rate and so power production begin to increase, say because a neutron absorbing control rod is partially withdrawn from the reactor, the fuel temperature will of necessity also begin to rise. Now, however, so long as the control rod was not withdrawn too far, the reaction rate will be held from increasing indefinitely, because the radiative neutron absorption will increase at higher temperature and the reactor power will come to a new equilibrium.

The resonances for ^{235}U and ^{239}Pu are similar in magnitude to those for ^{238}U , and they are divided in the outcome of neutron capture between fission and radiative absorption. Since the density of fissile material in a thermal reactor is always much less than the density of ^{238}U , the net effect of all of the resonances is absorption, but there is an order 1% effect on neutron generation during slowing down in the resonance region, which we have neglected for our purposes here.

Let us evaluate p for the light-water reactor we considered at the end of section 3.5, described in table 3.4. The fuel diameter is $D = 0.9 \text{ cm}$, and let us take $T = 1000^\circ \text{ K}$. This gives $I = 23.9 \text{ b}$. Using table 3.3 multiplied by 0.96 for the number density of ^{238}U in the enriched uranium dioxide fuel and table 3.1 for the stopping power of light water, we arrive at $p = 0.73$. Note that we have divided the numerator and denominator of the fraction within the argument of the exponential by V^{tot} .

$$p = \exp\left(-\frac{0.96 \cdot 2.34 \cdot 23.9 \cdot 0.376}{121 \cdot 0.535}\right) = 0.732 \quad (3.73)$$

In sum, we note that p is an important and sensitive factor in the neutron lifecycle. It typically takes on values in the range of 0.6 – 0.85. The number

of neutrons per second per m² slowing down into the Thermal energy region equals $\epsilon p S_T$.

3.7 Thermal energy region $\phi_T(E)$

After neutrons slow down from the Fast energy region through the Intermediate energy region, it is clear that eventually they must stop, on average, losing energy. What happens is that they begin to gain energy from collisions predominantly with the nuclei of the moderator, due to the thermal motion of these nuclei, and eventually come into near thermal equilibrium with them. This is called the Thermal energy region. The neutrons in this region are close to thermal in their energy distribution, but never quite in equilibrium with their surroundings, however, because they are “fed” energetic neutrons from the intermediate energy region, and lose neutrons by radiative absorption and driving fission, whose rate coefficients are independent of energy in the low-energy “1/v” region. As a result the spectrum is somewhat harder, with a greater high-energy tail, than a corresponding bell-shaped Maxwellian distribution. The expression for a Maxwellian distribution, as a function of energy, is given by

$$n_M(E) = \frac{dn_M}{dE} = n_M \sqrt{\frac{4E}{\pi T^3}} e^{-E/T} \quad (3.74)$$

where T is expressed in the same energy units as E , for our purposes Joules. $T = k_B T_K$, where k_B is Boltzmann’s constant and T_K is temperature in Kelvins.

Question: Why do neutrons come into thermal equilibrium more closely with the moderator than with the (hotter) fuel? (How easily do white tennis balls come into thermal equilibrium with dump trucks? With yellow tennis balls?)

We can estimate the density of neutrons in the thermal energy region, under steady conditions, by equating the source rate of neutrons with their loss rate

$$q(0.5\text{eV}) = \epsilon p S_T = n_T \nu_{T,abs} = n_T \overline{\Sigma_{T,abs}} v \quad (3.75)$$

where $q(0.5\text{eV})$ is the flux of neutrons downwards in energy into the Thermal energy range. The subscript “ T ” indicates that we are considering the thermal energy range. In this energy range we assume that $\Sigma_{T,abs}$ varies dominantly as $1/v$, so we can take $\nu_{T,abs}$ to be independent of energy. Conventionally we evaluate all thermal cross-sections, Σ_T , at $E = 0.0253$ eV,

where the neutron velocity, v , is 2200 m/s. This also allows to calculate the mean lifetime of a thermalized neutron:

$$l = (\nu_{T,abs})^{-1} = (\overline{\Sigma_{T,abs}} v)^{-1} \quad (3.76)$$

$\Sigma_{abs} \propto 1/v$ is a good assumption for uranium fuel, but weaker when the fuel contains significant amounts of plutonium. ^{239}Pu has a strong resonance in the vicinity 0.3 eV, right near the conventional boundary between the Intermediate and Thermal energy regions of 0.5 eV. This resonance produces about 60% fission, 40% radiative absorption. Furthermore, this reaction has $\bar{\nu}$ of about 2.9, so it is clearly a net contributor of neutrons. ^{241}Pu has a resonance in the vicinity 0.26 eV that produces about 70% fission, 30% radiative absorption, so is also a net contributor. On the other hand ^{240}Pu has a very strong radiative absorption resonance just above 1 eV. A mitigating factor is that all of these resonances are strong enough that they are very much self-shielding, in part due to the fact that their width is reduced as a result of the low incoming neutron energy. In this work we will retain $\Sigma_{abs} \propto 1/v$ even for Pu, but we should keep this caveat in mind. In particular, the large low-energy resonances of fissile Pu can compete with (but not reverse) the stabilizing influence of the radiative absorption resonances of the much larger fraction of ^{238}U . They also can take quite a bite out of the thermal neutron spectrum, reacting as they do with the neutrons before they fully thermalize.

Remembering that fission is a form of absorption (in this case, obviously, in the evaluation of the distribution of thermal neutrons), we can write

$$\overline{\Sigma_{T,abs}} = \frac{V^{fuel}}{V^{tot}} \left(\overline{\Sigma_{T,f}^{fuel}} + \overline{\Sigma_{T,\gamma}^{fuel}} \right) + \frac{V^{mod}}{V^{tot}} \overline{\Sigma_{T,\gamma}^{mod}} + \frac{V^{clad}}{V^{tot}} \overline{\Sigma_{T,\gamma}^{clad}} \quad (3.77)$$

At thermal energies the strong absorption cross-sections can result in a fairly short mean free path for neutrons within the fuel rods, resulting in some depletion of ϕ_T in the fuel rod compared to its value in the moderator, thus reducing the absorption by the fuel. This is taken into account sometimes by a “thermal disadvantage factor,” which we neglect here, as we neglected the “fast advantage factor” in the Fast energy region.

With the above caveats we can evaluate equation 3.76 for the thermal neutron lifetime, l , in our example light-water reactor. Using table 3.4 for the volume ratios, table 3.3 for the number densities of the different elements, and table 3.5 for the microscopic thermal cross-sections, neglecting the tiny absorption on oxygen, and recognizing that the velocity at which these are

all evaluated is 2200 m/s, we get

$$l = \{[0.376 \cdot (23.4 + 6.52) \cdot 2.34 + 0.088 \cdot 0.191 \cdot 4.31 + 0.535 \cdot 0.322 \cdot 6.69] \cdot 2200\}^{-1} = 16.5 \mu s \quad (3.78)$$

This result is significantly longer than the slowing down time of $3.2 \mu s$ estimated from table 3.1, by dividing the neutron slowing down time in light water by the fraction of the moderator volume over the total volume. For a graphite or heavy-water moderated reactor the slowing down time is much longer, but the fraction of the moderator volume is greater and the absorption is slower (in part because these reactors operate with natural or low-enriched uranium), so again the slowing down time is less than the lifetime against absorption.

Real reactors are significantly more complex than our “example” light-water reactor loaded with fresh 4% enriched fuel. There are sources of parasitic absorption, occurring neither in the uranium fuel, nor in the cladding or pure moderator. These include

- Fuel assembly and reactor structures
- “Burnable poison,” e.g., gadolinium included in fresh fuel
- “Chemical shim,” e.g., boron added to moderator in form of boric acid
- Control rods and associated structure

Furthermore, the composition of the fuel itself evolves over time, affecting the the absorption of thermal neutrons:

- Build-up of fission products, especially ^{135}Xe and ^{149}Sm
- Depletion of ^{235}U due to fission and (n, γ) reactions
- Build-up and evolution of Pu isotopes, fissile and fertile
- Build-up of ^{236}U from (n, γ) reactions with ^{235}U

Fuel is designed to produce excess neutron multiplication when it is fresh, because it inevitably produces lower multiplication as it burns. So absorbing elements are used to increase radiative absorption when there is more fresh fuel present, and reduce this absorption when there is less. Burnable poisons deplete as the fuel itself becomes less reactive, and the level of boric acid in the moderator can be reduced as well to compensate. Control rods are movable absorbers used to adjust the power output.

In this context it is worth taking a bit of a tour through table 3.5, which displays relevant cross-sections in the Thermal energy region. These have each been evaluated at the $v = 2200$ m/s, or $E = 0.0253$ eV. Surveying this table we can find some interesting physics. The large, broad resonance of the proton + neutron (= deuteron) system near zero energy shows up

Table 3.5 *Thermal microscopic cross-sections evaluated at $v = 2200 \text{ m/s}$ (barns = 10^{-28} m^2) and $\bar{\nu}$*

Atom	At. Mass	$\sigma_{T,f}$	$\sigma_{T,\gamma}$	$\sigma_{T,e}$	$\sigma_{T,\alpha}$	$\bar{\nu}$
Hydrogen	1	—	0.322	30.1	—	—
Deuterium	2	—	$5.05 \cdot 10^{-4}$	4.25	—	—
Boron	Natural	—	0.104	4.51	764	—
Carbon	12	—	$3.86 \cdot 10^{-3}$	2.74	—	—
Oxygen	16	—	$9.56 \cdot 10^{-3}$	2.74	—	—
Magnesium	Natural	—	$6.27 \cdot 10^{-2}$	3.60	—	—
Iron	Natural	—	2.56	11.29	—	—
Zirconium	Natural	—	0.191	6.83	—	—
Cadmium	Natural	—	$2.45 \cdot 10^3$	7.58	—	—
Xenon	135	—	$2.66 \cdot 10^6$	$2.99 \cdot 10^5$	—	—
Samarium	149	—	$4.05 \cdot 10^4$	185	—	—
Gadolinium	Natural	—	$4.86 \cdot 10^4$	171	—	—
Uranium	235	585	98.5	15.1	—	2.44
Uranium	236	0.0473	5.16	8.84	—	2.37
Uranium	238	$1.68 \cdot 10^{-5}$	2.69	9.25	—	—
Uranium	Natural	4.21	3.38	9.29	—	2.44
Uranium	2% enriched	11.7	4.61	9.37	—	2.44
Uranium	4% enriched	23.4	6.52	9.48	—	2.44
Uranium	20% enriched	117	21.9	10.4	—	2.44
Plutonium	239	751	274	7.99	—	2.88
Plutonium	240	$6.43 \cdot 10^{-2}$	291	0.958	—	—
Plutonium	241	1013	363.3	4.27	—	2.94
Plutonium	242	$1.04 \cdot 10^{-3}$	19.27	7.75	—	—

as a large elastic scattering cross-section for hydrogen. This is enhanced by the thermal motion of the hydrogen itself. Next we can see the very small radiative absorption cross-section for deuterium, which is why heavy water is

an effective moderator even for natural uranium fuel. Boron is unremarkable, except for the very strong reaction $^{10}\text{B} + \text{n} \rightarrow ^7\text{Li} + ^4\text{He} + 2.31 \text{ MeV}$. This is called an (n,α) reaction, specifically $^{10}\text{B}(\text{n},\alpha)^7\text{Li}$. It is not included in the schema shown in figure 2.5; this is the main place that reactions like this are seen in nuclear reactor physics. In reactors, boric acid is dissolved in the water coolant, and – evidently – a rather small fraction can strongly increase its neutron absorption. Boric acid can also, however, lead to corrosion of low-alloy and carbon steels, as was discovered most dramatically in 2002 at the Davis-Besse nuclear power plant, in Ohio on Lake Erie. A football-sized cavity had been eaten out of the reactor pressure vessel.

We see that carbon and oxygen have very low radiative absorption cross-sections. Magnesium has an attractively low radiative absorption cross-section, so was used in the British Magnox graphite-moderated reactors, that both produced power and plutonium for weapons. It is also used in the North Korean plutonium production reactors for fueling nuclear weapons. It is not compatible with water over long periods of time, however, which makes it difficult to work with. Iron has rather a high radiative absorption cross-section at thermal energies, and a high number density (see table 3.3), which makes it unattractive for thermal-spectrum reactors. Zirconium is much better for fuel cladding.

^{113}Cd , ^{135}Xe , ^{149}Sm , ^{155}Gd and ^{157}Gd are all powerful neutron absorbers. They each have substantial low-energy resonances, so their cross-sections do not vary as $1/v$ over the full Thermal energy region. Cadmium is often present in control rods that are used to adjust a reactor's neutron multiplication. Xenon and Samarium are the main fission products that reduce neutron multiplication. Xenon also contributes multi-hour dynamics to reactor behavior, that notoriously contributed to the Chernobyl disaster. We will discuss the effects of these fission products in sections 5.4 and 5.5. Gadolinium is sometimes mixed into reactor fuel. It is so reactive that it is consumed during operation, so as it burns up its loss partially compensates for the reduction in neutron production due to the depletion of ^{235}U . Of course the production of ^{239}Pu also partially compensates for this loss.

The uranium and plutonium sections of the table illustrate the very high effective fission cross-sections that are found at thermal energies. However, you should note that the radiative absorption cross-sections also rise in the Thermal energy region, so the competition between fission and radiative absorption remains important. The table shows that the ratio of the two is strongly modified by enrichment level. In both the U and Pu sections you can see that nuclei with odd numbers of neutrons have much greater thermal fission cross-sections than those with even numbers. One interesting feature

is the very low thermal scattering cross-section of ^{240}Pu . This is because of a resonance at 1.06 eV, which suppresses scattering on its low-energy wing.

Since we are interested in following neutrons right to the point where they drive fission, we next calculate the “fuel utilization factor,” f , the fraction of the thermal neutrons that are absorbed in the fuel, divided by the total absorbed. Here we again neglect the “thermal disadvantage factor” that takes into account reduction of ϕ_T within the fuel, and assume fresh 4% enriched fuel, with no poisons.

$$f = \frac{V^{fuel} (\overline{\Sigma}_{T,f}^{fuel} + \overline{\Sigma}_{T,\gamma}^{fuel})}{V^{fuel} (\overline{\Sigma}_{T,f}^{fuel} + \overline{\Sigma}_{T,\gamma}^{fuel}) + V^{mod} \overline{\Sigma}_{T,\gamma}^{mod} + V^{clad} \overline{\Sigma}_{T,\gamma}^{clad}} \quad (3.79)$$

To evaluate this expression for our “example” LWR, we again use table 3.4 for the volume ratios (dividing top and bottom by V^{tot}), table 3.3 for the number densities of the different elements, and table 3.5 for the microscopic thermal cross-sections, neglecting the tiny absorption on oxygen. We get

$$\begin{aligned} f &= \frac{0.376 \cdot (23.4 + 6.52) \cdot 2.34}{0.376 \cdot (23.4 + 6.52) \cdot 2.34 + 0.088 \cdot 0.191 \cdot 4.31 + 0.535 \cdot 0.322 \cdot 6.69} \\ &= 0.955 \end{aligned} \quad (3.80)$$

This is a very high value, because we are starting with fresh fuel and no poisons. As we will see, this leads to a high multiplication value. In a realistic situation, either with poisons at startup or with much less fissile material after considerable burnup, this value is more typically in the range of 0.65 to 0.85.

The final step is to determine the efficiency of thermal neutrons captured in the fuel to produce fast neutrons through fission. This is called the “thermal efficiency” factor, η_T , but can be seen simply as the neutron multiplication in the fuel. As such, it is given by:

$$\eta_T = \frac{\overline{\nu \Sigma}_{T,f}^{fuel}}{\Sigma_{T,f}^{fuel} + \Sigma_{T,\gamma}^{fuel}} = \frac{\overline{\nu \sigma}_{T,f}^{fuel}}{\sigma_{T,f}^{fuel} + \sigma_{T,\gamma}^{fuel}} \quad (3.81)$$

where the second equality comes from the fact the fuel density cancels out. This is evaluated, as a function of neutron energy, in figure 1.3.

Again assuming 4% enrichment in our “example” reactor we can use table 3.5 to arrive at

$$\eta_T = \frac{2.44 \cdot 23.4}{23.4 + 6.52} = 1.91 \quad (3.82)$$

As shown on the left-hand side of figure 1.3, η_T depends strongly on the level of enrichment of the fuel. Thus this factor also drops with the burnup of ^{235}U .

The number of neutrons per second per m^2 that are produced from fission driven by thermal neutrons, S_T , equals $f\eta_T$ times the influx of neutrons per second per m^2 from the Intermediate energy region. At the end of section 3.6.1 we saw that this influx was $\epsilon p S_T$. If we multiply these together we have

$$S_T = \epsilon p f \eta_T S_T \quad (3.83)$$

For this equation to be satisfied we require

$$\epsilon p f \eta_T = 1 \quad (3.84)$$

This is known as Fermi's Four Factor Formula. If it is not satisfied, the neutron production, and so power production (in our infinite system) is either falling (\downarrow) or rising (\uparrow) in time. We will examine the so-called "kinetics" of the time-dependent process in Chapter 5.

In our case we found relatively high values for f and η_T , since we did not include the full panoply of poisons and parasitic absorbers and we did not consider any burn-up of the fuel. As a result our nominal LWR has $\epsilon p f \eta_T = 1.05 \cdot 0.732 \cdot 0.955 \cdot 1.91 = 1.40$. Note that just as this calculation is not completely realistic for a the neutron multiplication, the absorption time would be less with more poisons present at the start of operations, and actually greater at later times as fuel is burned up and poisons are removed.

3.8 Visualizing the four-factor formula

Fermi's four-factor formula for the neutron economy of an infinite thermal fission reactor, is generally presented in terms of the life cycle of a single neutron. In essence, steady operation of such a reactor requires that the life cycle of a neutron close precisely, with one parent neutron ultimately producing exactly one child.

$$k_\infty \equiv \epsilon p f \eta_T = 1 \quad (3.85)$$

where the ∞ subscript again reminds us that we are considering an infinite system, with no spatial losses. Every fast neutron produced from thermal fission results in ϵ neutrons delivered to the intermediate energy range. ϵp neutrons escape the resonances as they slow down and are then delivered to the thermal energy range. $\epsilon p f$ thermal neutrons are captured in the fuel, and this then produces $\epsilon p f \eta_T$ neutrons from thermal fission. For the reactor to operate at a steady rate of fission, every neutron produced by thermal

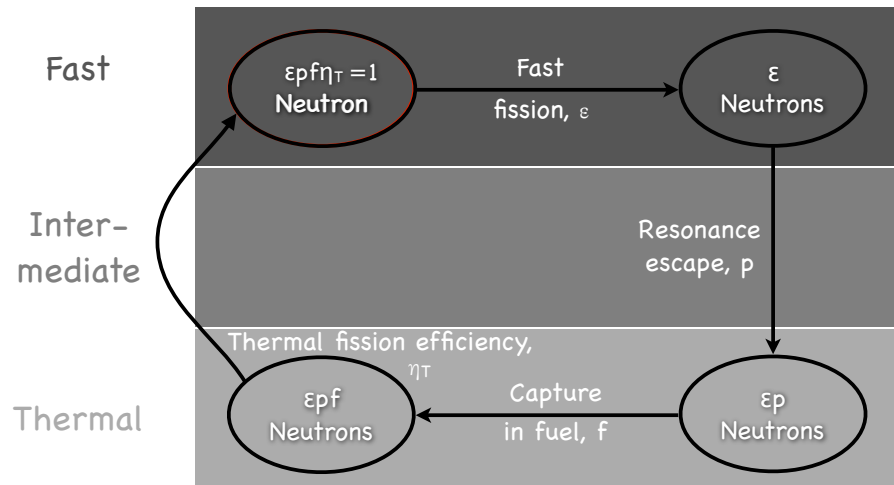


Figure 3.7 Neutron life cycle

fission must ultimately replace itself with exactly one neutron from thermal fission, as expressed in Fermi's formula. This is shown diagrammatically in figure 3.7.

Question: If Fermi's four-factor formula is satisfied, does it guarantee that a neutron leaving the intermediate energy region will precisely reproduce itself with a neutron entering the intermediate energy region? (This is a little tricky. Don't jump to the "obvious" conclusion.)

3.9 Fast reactors

Fast-neutron-spectrum reactors, sometimes called "fast reactors," operate quite differently from the thermal-neutron-spectrum reactors we have discussed so far in this chapter. Sustainment of the chain reaction in the case of fast reactors involves closing the neutron life cycle at energies above about 100 keV. This requires enrichment in the range of 20% to achieve η acceptably above unity, as can be seen in figure 1.3. If neutrons could be held at

1-2 MeV one could operate at lower enrichment in this energy range, since ^{238}U fissions at such high energies, but inelastic scattering rapidly degrades such neutrons to the range of a few hundred keV, making this impossible.

A signature feature of fast reactors is that the coolant, which extracts power from the fuel rods, must not contain low-Z materials, such as hydrogen, deuterium or carbon – used for slowing down neutrons in thermal-spectrum reactors. The most commonly used coolant is liquid sodium, but lead and lead-bismuth have been used, and high-temperature helium gas is proposed. Helium would be a moderator at liquid density, but as a gas, which is its only practically accessible form, it is essentially transparent to neutrons. A problem with gaseous He coolant is that it has very low volumetric heat capacity. This has the two consequences: it must be flowed through the reactor very quickly and it provides very little thermal “ballast” against temperature excursions.

Let us start to analyze fast reactors using the same approach for the “Fast” energy region, above about 500 keV, as we did for the “Fast” energy region of thermal spectrum reactors. One important difference is that there is no significant low-Z moderator present to extract neutrons from this energy region. You might think that sodium with $\xi = 0.0845$ is not so different from carbon with $\xi = 0.158$, but a graphite-moderated reactor has a very large ratio of moderator to fuel volume, while the coolant volume is generally less than the fuel volume in a fast reactor. Sodium also has a much lower number density than graphite.

We start by essentially copying equation 3.44:

$$\phi_F(E) = \frac{S\chi(E)}{\Sigma_{loss}(E)} = \frac{s(E)}{\Sigma_{loss}(E)} \quad (3.86)$$

As can be seen from Table 3.2 the dominant neutron interaction with both the moderator, which we will take to be sodium, and with the cladding and other structure, which we will take for simplicity to be iron, is inelastic scattering. Radiative capture on sodium and iron can be neglected. Special stainless steels, which are iron alloys, are best suited to the neutron environment of a fast reactor.

We can speed along the derivation by taking the Watt-spectrum average of 3.46, modified to recognize that the coolant affects the spectrum by inelastic, rather than elastic, scattering:

$$\Sigma_{F,loss} = \frac{V^{cool}}{V^{tot}} \overline{\Sigma_{F,in}^{cool}} + \frac{V^{clad}}{V^{tot}} \overline{\Sigma_{F,in}^{clad}} + \frac{V^{fuel}}{V^{tot}} \left[\overline{\Sigma_{F,f}^{fuel}} + \overline{\Sigma_{F,\gamma}^{fuel}} + \overline{\Sigma_{F,in}^{fuel}} \right] \quad (3.87)$$

and arrive at

$$\epsilon \equiv \frac{S_{FR} + S_F}{S_{FR}} \approx \left[1 - \frac{V^{fuel}}{V^{tot}} \frac{\overline{\nu_F \Sigma}_{F,f}^{fuel}}{\Sigma_{F,loss}} \right]^{-1} \quad (3.88)$$

where S_{FR} represents the source of neutrons from the fast reactor spectrum below 500 keV.

Most thermal reactors use a square grid of fuel rods, but fast reactors generally use a hexagonal grid, to allow a larger fraction of fuel volume. For our nominal fast reactor, let us assume 50% fuel, 30% coolant and 20% cladding and structure. We can carry along the result for the fast-region spectrum, above 500 keV, equation 3.47, taking into account both the neutrons due to the FR spectrum, and the multiplication in the “Fast” spectrum above 500 keV.

ϵ is generally a much more significant factor in fast reactors than in thermal reactors, since the large loss of fast neutrons by collisions with hydrogen is not present. Let us again work an example, using tables 3.2 and 3.3 to compute the desired macroscopic cross-sections. For our nominal case, assuming uranium oxide fuel enriched to 20% ^{235}U , we have

$$\begin{aligned} \Sigma_{F,loss} &= 0.3 \cdot 2.43 \cdot 0.513 + 0.2 \cdot 8.49 \cdot 0.644 \\ &\quad + 0.5 \cdot 2.34 \cdot [0.488 + 0.0759 + 2.47] = 5.02 \text{ m}^{-1} \end{aligned} \quad (3.89)$$

which is dominated by inelastic scattering on uranium, but with a significant contribution from inelastic scattering on the coolant and cladding + structure. We can also calculate

$$\overline{\nu_F \Sigma}_{F,f}^{fuel} = 2.6 \cdot 2.34 \cdot 0.488 = 2.97 \text{ m}^{-1} \quad (3.90)$$

which is mainly due to collisions with ^{238}U , but with significant enhancement to the 20% enrichment level. From these two we can find $\epsilon = 1.42$. Once again, by inspection we can see that the downscattering in energy, now due to inelastic scattering, is much greater than radiative absorption, so we can neglect the latter.

It is difficult to calculate the neutron spectrum of fast reactors below 500 keV. The spectrum is “fed” from above by inelastic scattering from the primary fission neutrons, and is depleted dominantly by fission, radiative absorption, and removal to lower energies due to slowing down on the coolant. Spectra vary from one design to another, but $E\phi(E)$ tends to peak at about 300 keV, consistent with the approximation for inelastic scattering on fuel as transferring neutrons down to mean energy $E_{MeV,sc} \approx (E_{MeV,0}/12)^{1/2}$,

where they suffer some modest further slowing down due to elastic and inelastic scattering. For simplicity, we will approximate “*FR*” cross-sections as those averaged from 100 keV to 500 keV. We will denote these as, for example for fission, $\sigma_{FR,f}$, $\Sigma_{FR,f}$ and $\bar{\nu}_{FR,f}$. Comparing the ^{238}U and ^{235}U fission cross-sections averaged from 100 - 500 keV (table 3.6) to the Watt-spectrum averaged cross-sections (table 3.2), we see that the ^{238}U fission really drops out of the picture at the lower energies.

Question: Remind yourself of the definitions of each of these kinds of cross-sections.

Table 3.6 *Fast-Reactor (“FR”) microscopic cross-sections (b) and $\bar{\nu}$, averaged from 100 keV to 500 keV.*

Atom	At. Mass	$\sigma_{FR,f}$	$\sigma_{FR,\gamma}$	$\sigma_{FR,e}$	$\sigma_{FR,in}$	$\bar{\nu}$
Oxygen	16	—	—	—	—	—
Sodium	23	—	$6.90 \cdot 10^{-4}$	3.67	—	—
Iron	Natural	—	$6.04 \cdot 10^{-3}$	3.69	—	—
Lead	Natural	—	$3.78 \cdot 10^{-3}$	10.18	—	—
Uranium	235	1.27	0.248	7.17	1.04	2.47
Uranium	238	$1.63 \cdot 10^{-4}$	0.121	8.42	1.34	—
Uranium	4% enriched	$5.10 \cdot 10^{-2}$	0.126	8.37	1.33	2.47
Uranium	20% enriched	0.254	0.146	8.17	1.28	2.47
Plutonium	239	0.452	0.232	7.8	1.31	2.88
Plutonium	240	0.151	0.205	8.35	1.23	2.9
Plutonium	241	1.74	0.191	6.1	1.51	2.92
Plutonium	242	$8.92 \cdot 10^{-2}$	0.146	9.07	1.2	2.92

There is no analog to the resonance escape probability, p , in the case of a fast reactor, since neutrons are not slowed down past resonances. But we can estimate f and η_{FR} , with the goal of ending up with a three-factor formula, $\epsilon f \eta_{FR}$. f will be defined by the absorption in the fuel divided by all forms of absorption. We have not yet defined, however, how to include slowing down on the coolant (and any structures) in this calculation.

It is conventional to estimate a removal rate of neutrons from the *FR* spectrum as the inverse of the slowing down time from the median energy

to the bottom end of the spectrum, as evaluated in equation 3.30. It is also conventional, in this analysis, to take the bottom end as 40 keV, where resonance absorption takes over, due to the very low slowing down power in fast reactors.

$$\tau_{slow} = \frac{2}{\xi \bar{\Sigma}_e} \left(\frac{1}{v_{40keV}} - \frac{1}{v_{300keV}} \right) = \frac{5.3}{\xi \bar{\Sigma}_e v_{300keV}} \quad (3.91)$$

Since for any reaction $\Sigma v = \nu = 1/\tau$, this allows us to define an “effective” macroscopic removal cross-section by slowing down, in a convenient form for addition to the macroscopic cross-sections for neutron loss by absorption.

$$\overline{\Sigma}_{FR,rem} = \frac{1}{v_{300keV} \tau_{slow}} = \frac{\overline{\xi \bar{\Sigma}_e}}{5.3} \quad (3.92)$$

where we should evaluate the elastic scattering cross-sections by averaging from 100 to 500 keV, as in table 3.1. This is a modest effect in sodium-cooled fast reactors, approaching negligible in lead-cooled reactors.

Now we are in a position to evaluate f , the fuel utilization factor, in analogy to how we evaluated it in the thermal case:

$$f = \frac{V^{fuel} \left(\overline{\Sigma}_{FR,f}^{fuel} + \overline{\Sigma}_{FR,\gamma}^{fuel} \right)}{V^{fuel} \left(\overline{\Sigma}_{FR,f}^{fuel} + \overline{\Sigma}_{FR,\gamma}^{fuel} \right) + V^{cool} \overline{\Sigma}_{FR,rem}^{cool} + V^{tot} \overline{\Sigma}_{FR,\gamma}^{par}} \quad (3.93)$$

where again, all of the cross-sections are averaged from 100 to 500 keV. Note that we are not including inelastic scattering in determining loss from the *FR* spectrum, since such scattering moves neutrons downwards in energy, but generally within the *FR* energy region. In effect, we have included this in the assumed limits of the *FR* spectrum we originally selected.

For our nominal fast reactor case, neglecting parasitic absorption, we can evaluate f ,

$$f = \frac{0.5 \cdot 2.34 \cdot (0.254 + 0.146)}{0.5 \cdot 2.34 \cdot (0.254 + 0.146) + 0.3 \cdot 0.753/5.3} \approx 0.92 \quad (3.94)$$

The final step is to evaluate η_{FR} the ratio of neutrons captured in the fuel, in the *FR* region of the energy spectrum to neutrons produced. By analogy with the thermal calculation we have:

$$\eta_{FR} = \frac{\overline{\nu \sigma}_{FR,f}^{fuel}}{\overline{\sigma}_{FR,f}^{fuel} + \overline{\sigma}_{FR,\gamma}^{fuel}} \quad (3.95)$$

For our nominal fast reactor this evaluates to

$$\eta_{FR} \approx \frac{2.47 \cdot 0.254}{0.254 + 0.146} = 1.57 \quad (3.96)$$

Summarizing the neutron life-cycle for our nominal fast reactor, we have

$$\epsilon f \eta_{FR} \approx 1.42 \cdot 0.92 \cdot 1.57 = 2.05 \quad (3.97)$$

Thus we see that fast reactors, running with 20% enriched uranium fuel, can have a great deal more multiplication than required to close the neutron life-cycle. Indeed, for the nominal case discussed here, there is one full extra neutron. If the fast-reactor core that we have been discussing is small enough in size, this neutron might be lost from the system. And if the core is surrounded by a “blanket” of ^{238}U then there is a high probability that the lost neutron will undergo radiative absorption, and a ^{239}Pu nucleus will be produced. This is in addition to the $0.146/.254 = 0.574$ radiative absorptions that are produced per FR fission, or $0.574/1.42 = 0.405$ per total fission. As a result of this, a fast reactor can, in principle, produce as much as about 1.5x as much fissile material as it consumes. Alternatively, it can in principle burn significantly less reactive fuel, consuming the plutonium and other transuranics that are produced in thermal reactors. These in-principle capabilities have proven difficult to achieve practically, but they continue to attract reactor designers.

Review

Resources

Exercises

- 3.1 Derive the asymptotic ratio of $1 - \alpha$ to ξ for high values of A . To do this, define $\epsilon \equiv 1 - \alpha$ and include terms as small as quadratic in ϵ . Explain this result based on the physics. Use it to estimate the number of collisions required for an e -fold downwards of neutron energy for target nuclei of $A = 200$ and $A = 238$.
- 3.2 Formulate equation 3.61 for the case where multiple species of nuclei contribute to $q(E)$ and then solve it as in equation 3.62. Compare with Fermi’s result.
- 3.3 Derive $\phi_I(E)$ in Fermi’s continuous slowing down approximation. First draw a diagram, analogous to figure 3.5, that depicts the differential energy range of neutrons that will cross energy E in differential time dt , given dE/dt . Using equation 3.35, determine the density of neutrons contained in this energy range and so the downward flux of neutrons crossing E , in units of $\text{m}^{-3}\text{s}^{-1}$. You should have:

$$q(E) = S = -\frac{dn}{dE} \frac{dE}{dt} = -n(E) \frac{dE}{dt} \quad (3.98)$$

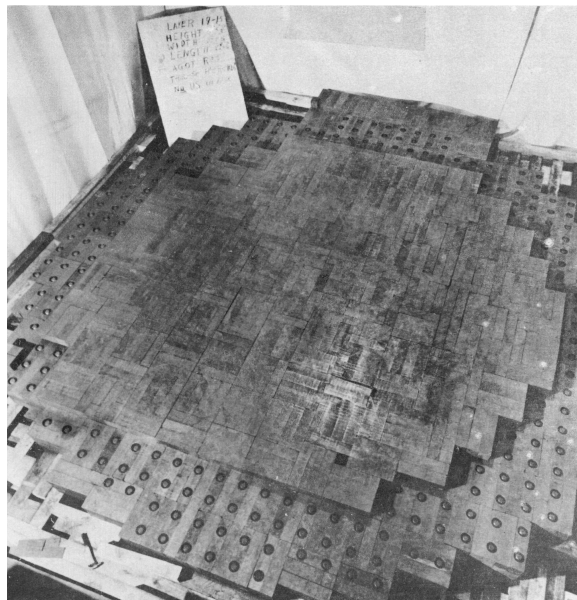
Using Fermi's slowing-down formula, equation 3.28, show that this analysis gives the same result as equation 3.64, but generalized for multiple species of nuclei.

- 3.4 Develop an equation for a putative ϵ' that takes into account (n, γ) depletion of the flux downwards in energy from the "fast" energy region.
- 3.5 Estimate the volume-average value of $\phi_F(E)$ at 1 MeV for an LWR. Estimate the volume-average value of $E\phi_I(E)$ ignoring resonant absorption. Estimate the volume-average value of $\phi_T(E)$ near its peak. Assume a 4m tall reactor, 1m in radius, producing 3 GW(th), with 25% of its power being produced by Pu fission. Ignore fission with fast neutrons.
- 3.6 Verify 2 rows, chosen at random, in each of tables 3.2, 3.3 and ???. You can download the tabular data and do your own averaging, or you can use the calculation feature at the bnl.gov website. In the latter case be careful that the limits of integration are set by the limits you place on the Plot Cart graphs. To weight a dataset by the Watt spectrum you can set the lower limit to some very low value, the upper limit to 10 MeV, and calculate using

$$y0*0.4865*\sinh(\sqrt{2*x/1.0e6})*\exp(-x/1.0e6)*10$$
where $y0$ is the data set that you want to weight. Then look at the average value displayed. Your result should be close to (but not equal to) the ^{252}Ca spectrum weighted average value that is provided automatically.
- 3.7 Consider, magically, that the thermal and fast reactors we considered in this chapter contained ^{233}U as their fissile component, rather than ^{235}U . Explain how this would affect each factor, ϵ, p, f , and η_T for the thermal reactor, and then ϵ, f , and η_{FR} for the fast reactor: higher, lower, or about the same? Illustrate your answer with cross-section figures where appropriate.
- 3.8 Four factors for graphite and/or heavy water reactors.
- 3.9 Fissile material production in LWRs. How about pure U-238 rods?

Chapter 4

Neutron Spatial Distribution



Chicago Pile 1, layers 1 - 18 plus partially completed layer 19. Note uranium slugs interspersed in graphite blocks.

Since only a small amount of metal (about six tons) was available and since our graphite was of various brands of different purity it had been planned originally to construct the pile in an approximately spherical shape, putting the best materials as near as possible to the center. ... During the construction as a matter of precaution, appreciably before reaching [the] critical layer, some cadmium strips were inserted in suitable slots. They were removed once every day with the proper precautions in order to check the approach to the critical conditions. The actual construction was carried in this way to the 57th layer, about one layer beyond the critical dimensions. When all the cadmium is removed the effective reproduction factor of the structure is about 1.0006.

Enrico Fermi, "Experimental Production of a Divergent Chain Reaction," AECD-3269, declassified Nov. 7, 1951

In Chapter 3 we discussed the slowing down of neutrons and their resulting distribution in energy. We ignored any spatial variation in the problem, effectively assuming an infinite, homogeneous system. We drove this calculation through to the evaluation of the neutron multiplication factor, appropriately called “ k_∞ ”. Here we will address the spatial motion of neutrons in a powerful approximation equivalent to treating them as gas of particles with only one speed – even though they collide only with the background nuclei, and not with each other like gas molecules. This will allow us to take into account the leakage of neutrons from the edges of a reactor and so evaluate the true multiplication factor in finite geometry, k , also sometimes called k_{eff} .

4.1 Neutrons as a one-speed gas

The neutron gas that we are about to consider is a bit of a peculiar one. We will assume that all of the neutrons have the same speed, v_n , and that they are everywhere close to isotropically distributed in direction. This means that the magnitude of the average flow of our neutron gas is much less than the neutron speed, or

$$|\langle \vec{v} \rangle| \ll v_n \quad (4.1)$$

The signature of a continuum theory of gases is that it develops equations for local quantities such as the number density, n , and the momentum density, $nm_n\langle \vec{v} \rangle$, based on the flows of particles and of momentum combined with any local sources or sinks of particles and momentum. For our case we will ignore the flow of energy, since are assuming a fixed one-speed system with little energy in the flow itself.

Consider now figure 4.2, where we depict a differential cube of volume $dxdydz$. If we are interested in the flow of neutrons into and out of this cube, we need to evaluate the flows of neutrons across its surfaces. Let us look first at the back shaded surface, whose four corners, progressing in the counter-clockwise direction, are located at (x, y, z) , $(x+dx, y, z)$, $(x+dx, y+dy, z)$ and $(x, y+dy, z)$. Now consider the time interval ∂t . We use partial derivatives in this analysis, since we are not evaluating time derivatives moving with the average neutron motion, but time derivatives in the lab frame. During this time interval we can consider that, in effect, a differential volume of particles, ∂V , moves across the surface we are considering. This volume is given by $\partial V = dxdy\langle v_z \rangle_{(x,y,z)}\partial t$, where the subscripted (x, y, z) here means “evaluated at.” We can ignore the random isotropic motion of neutrons and only consider the small average flow, since the random isotropic motion does

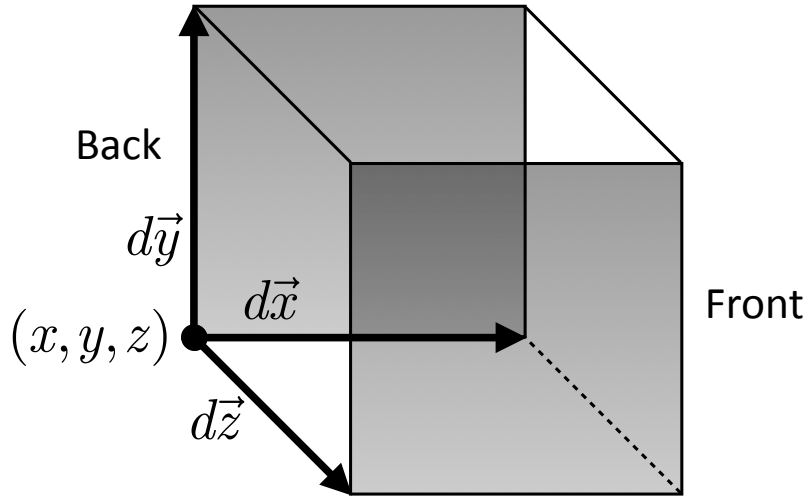


Figure 4.2 A differential cube with its left, lower, back corner located at (x, y, z) .

not result in a net neutron flow across the surface. The number of particles moving into our differential cube across the surface we are now considering is then

$$\partial N_{(x,y,z)} = (n\partial V)_{(x,y,z)} = dx dy (n\langle v_z \rangle)_{(x,y,z)} \partial t \quad (4.2)$$

where N here denotes a dimensionless number of neutrons, since it is a number density multiplied by a volume. Note that if $\langle v_z \rangle$ is negative, this corresponds to a negative number of particles moving into the cube, another way to say particles moving out.

Next look at the front shaded surface, whose four corners are located at $(x, y, z+dz)$, $(x+dx, y, z+dz)$, $(x+dx, y+dy, z+dz)$ and $(x, y+dy, z+dz)$. By the same logic as above, the number of particles moving into the differential volume across the surface is given by

$$\partial N_{(x,y,z+dz)} = -dx dy (n\langle v_z \rangle)_{(x,y,z+dz)} \partial t \quad (4.3)$$

where the minus sign arises from the fact that positive z velocity is *out* of the volume.

If we sum ∂N due to z -directed flows across these two surfaces we arrive at the total effect due to flow in the z direction, since flow in the z direction only affects the arrival of particles in the differential volume across the two surfaces we have considered so far, and both x and y flows are parallel to these surfaces, and so do not deliver (or extract) particles across our two

surfaces.

$$\frac{\partial N_{z\text{-}flow}}{\partial x \partial y \partial t} = (n\langle v_z \rangle)_{(x,y,z)} - (n\langle v_z \rangle)_{(x,y,z+dz)} \quad (4.4)$$

Recognizing that we are dealing with differential quantities we can simplify the right-hand side to give

$$\frac{\partial N_{z\text{-}flow}}{\partial x \partial y \partial t} = -dz \frac{\partial}{\partial z} n\langle v_z \rangle \quad (4.5)$$

Dividing both sides by dz and noting that $dV = dx dy dz$ we have

$$\frac{\partial n_{z\text{-}flow}}{\partial t} = -\frac{\partial}{\partial z} n\langle v_z \rangle \quad (4.6)$$

If we include the other two pairs of surfaces by analogy, we arrive at the final result that takes into account flows in all three directions, given by

$$\frac{\partial n}{\partial t} = -\frac{\partial}{\partial x} n\langle v_x \rangle - \frac{\partial}{\partial y} n\langle v_y \rangle - \frac{\partial}{\partial z} n\langle v_z \rangle = -\vec{\nabla} \cdot \langle \vec{v} \rangle n \quad (4.7)$$

In our situation where there can be sources and sinks of neutrons, not just effects from flows, we include any local volumetric source or sink, in units of number per second per unit volume, on the right-hand side.

$$\frac{\partial n}{\partial t} = -\vec{\nabla} \cdot n\langle \vec{v} \rangle + s \quad (4.8)$$

This is the particle conservation equation, commonly called the “continuity” equation. Perhaps not surprisingly, if the neutron flow “diverges” in the absence of a source of neutrons, the density of neutrons drops over time.

Now we come to something a bit more complex, the momentum conservation or force balance equation. Consider first the flow of z -directed momentum across the back surface of our differential cube. This momentum, of course, is carried by individual neutrons, each of which carries $m_n v_z$ of momentum. By analogy with equation 4.2, we can evaluate the neutron momentum crossing this surface in a differential time ∂t as

$$\partial(Nm_n v_z)_{(x,y,z)} = nm_n \langle v_z \partial V_{(x,y,z)} \rangle = dx dy (nm_n \langle v_z^2 \rangle)_{(x,y,z)} \partial t \quad (4.9)$$

The reason that we find $\langle v_z^2 \rangle$ coming into this equation is that in this case the depth of ∂V in the z direction is a function of the v_z of the individual neutrons not $\langle v_z \rangle$, the averaged flow speed. Here the random motion does deliver the quantity of interest, momentum, across the surface.

Question: Show that the flow of z -directed momentum in the z direction due to the average flow varies as $\langle v_z \rangle^2$ and so is quadratically smaller in $\langle v_z \rangle / v_n$ than the momentum flow due to random motion.

Taking into account the front surface we arrive at, in analogy to equation 4.6,

$$\frac{\partial(nm_nv_z)_{z\text{-flow}}}{\partial t} = -\frac{\partial}{\partial z}n\langle m_nv_z^2 \rangle \quad (4.10)$$

Recognizing that for our nearly isotropic velocity distribution

$$n\langle m_nv_x^2 \rangle = n\langle m_nv_y^2 \rangle = n\langle m_nv_z^2 \rangle = nm_nv_n^2/3 \quad (4.11)$$

We can sum over all of the surfaces to get

$$\frac{\partial nm_n \vec{v}}{\partial t} = -\frac{mv_n^2}{3} \vec{\nabla} n + \vec{s}_{mom} \quad (4.12)$$

where we have taken advantage of our assumption that v_n is constant over time and space. Note that in a Maxwellian gas $p = nm_n\langle v^2 \rangle/3$, so the first term on the right-hand side is analogous to ∇p , as we might expect. We have allowed for a local source or sink of momentum, indicated by s_{mom} , which has units of number density x mass per particle x velocity / unit time.

Question: Using the fact that $p = (2/3)U$, where U is the kinetic energy density, show that $p = nm_n\langle v^2 \rangle/3$.

Note that we have neglected the flow of momentum pointed in any direction other than that of the flow under consideration. For example when we examined momentum flow in the z direction, we neglected the z -directed flow of x -directed momentum. This follows from our assumption that the neutron velocity distribution is very nearly isotropic, since under this assumption $\langle v_i v_j \rangle$, which comes into the flow in the i direction of j -directed momentum, is much larger for $i = j$ than for $i \neq j$. We will see later in this chapter that the assumption of velocity isotropy breaks down when the neutron density varies significantly over a distance approaching the neutron mean free path, and how we can patch that up particularly at the edge of a fission system. In Chapter 11 we will study the conditions at the edge of fusion plasmas where flow speeds can be of the same order as the ion thermal speed, making the ion velocity distribution highly anisotropic.

4.2 The one-speed neutron diffusion equation

To make progress towards a closed form for neutron transport, let us consider the s_{mom} term in the force balance equation. If the neutron gas has some local average flow velocity, $\langle \vec{v} \rangle$, the flow will be dissipated by collisions with the nuclei that are present, which randomize the direction of motion of

the neutrons. Furthermore, momentum is of course lost by any form of neutron absorption, including fission. Since we are solving for the transport of neutrons in space, the mean free path for the dissipation of flow is denoted λ_{tr} , where the subscript “*tr*” stands for “transport.” The rate coefficient for momentum loss, with dimension 1/time, is then v_n/λ_{tr} . v_n comes into this rate coefficient rather than $|\langle \vec{v} \rangle|$ because it is v_n that determines the frequency with which neutrons encounter nuclei and undergo scattering or absorption. Of course we evaluate the cross-sections at the assumed neutron energy, so we get the correct rate coefficients for absorption processes that have $1/v$ effective cross-section. Thus we can write

$$s_{mom} = -nm_n \langle \vec{v} \rangle v_n / \lambda_{tr} \quad (4.13)$$

Now let us consider situations where the characteristic time over which the neutron momentum density changes, $nm\langle v \rangle / (\partial nm\langle v \rangle / \partial t)$ is long compared with the time scale for collisional dissipation, λ_{tr}/v_n . This allows us to neglect the left-hand side of equation 4.12, which represents neutron inertia, giving a balance between force and dissipation:

$$0 = \frac{v_n^2}{3} \vec{\nabla} n + \frac{n \langle \vec{v} \rangle v_n}{\lambda_{tr}} \quad (4.14)$$

which can be solved for the vector neutron flux, $n\langle \vec{v} \rangle$. In neutronics calculations, this is referred to as the “neutron current,” to distinguish it from the scalar neutron flux, $\phi \equiv nv_n$ in our one-speed approximation, and given the label \vec{J} .

$$\vec{J} \equiv n\langle \vec{v} \rangle = -\frac{v_n \lambda_{tr}}{3} \vec{\nabla} n \quad (4.15)$$

Equations of this form, where the flow of particles is down the density gradient and proportional to the strength of that gradient, are examples of “Fick’s Law.” Here we see how Fick’s Law arises in the context of neutron transport. It is worth noting that if the scale length of the density gradient, $n/|\vec{\nabla} n|$, approaches λ_{tr} the flow speed approaches v_n , which violates our original assumption of near isotropy.

Now we can take the step of combining equation 4.15 with the continuity equation, 4.8. This gives us

$$\frac{\partial n}{\partial t} = \vec{\nabla} \cdot \frac{v_n \lambda_{tr}}{3} \vec{\nabla} n + s \quad (4.16)$$

In conventional physics analysis, partial differential equations of this form are referred to as “diffusion” or “heat” equations, which have the generic

form

$$\frac{\partial f}{\partial t} = \vec{\nabla} \cdot D_{phys} \vec{\nabla} f + s \quad (4.17)$$

For our case we can identify $f = n$ and $D_{phys} = v_n \lambda_{tr}/3$. Note that the units of D_{phys} are length² / time.

In neutronics analysis, it is conventional to solve for $\phi \equiv nv_n$ and the neutron diffusion equation is cast as

$$\frac{1}{v_n} \frac{\partial \phi}{\partial t} = \vec{\nabla} \cdot D \vec{\nabla} \phi + s \quad (4.18)$$

with $D = \lambda_{tr}/3$. We will use this equation to define D , with $D_{phys} \equiv v_n D$.

To complete the development of the neutron diffusion equation, we need to look a little more deeply at λ_{tr} , the mean free path for momentum loss. Radiative absorption and absorption resulting in fission extract of the momentum from the incoming neutron. Elastic or inelastic scattering on heavy nuclei each extract, on average, essentially all of the momentum from a neutron. However elastic scattering on light nuclei may not. For example, a classical “head-on” collision of a neutron with a stationary proton transfers all of the neutron’s momentum to the proton. The proton proceeds with the original neutron velocity, and the neutron stops dead. However any other collision angle leaves the neutron with some forward velocity. Let us consider, then, the average loss of momentum in a collision with a nucleus of finite mass.

Let us assume, for this calculation, that we are considering elastic scattering that is isotropic in the center-of-mass frame. The absolute value of equation 3.3 gives us the speed of the neutron in the center-of-mass frame.

$$|\vec{v}_0 - \vec{v}_{CoM}| = \frac{Av_0}{A+1} \quad (4.19)$$

while equation 3.2 gave us

$$\vec{v}_{CoM} = \frac{\vec{v}_0}{A+1} \quad (4.20)$$

The remaining fraction of the velocity of the neutron in its original direction is then given by

$$\frac{\vec{v}_1 \cdot \vec{v}_0}{v_0^2} = \frac{A \cos(\theta) + 1}{A+1} \quad (4.21)$$

where θ is the scattering angle in the lab frame. For the case of no scattering, $\psi = 0$, we get the expected result of no change in the forward momentum of the neutron. For perfect backscattering, $\theta = \pi$, at $A = 1$ we have full

momentum transfer, and in the limit of high A we have reversal of the original momentum. Evidently if we were to average this over all scattering angles, assuming isotropy in the center-of-mass frame, we would get that the surviving fraction of the original neutron momentum would be $1/(A + 1)$. This is not, however, consistent with our assumption of a one-speed neutron distribution, since part of why the neutrons are losing momentum in these collisions is that they are losing speed.

To model a scattering event where energy is not lost, we note that equation 3.6 gives the energy and speed reduction at an elastic collision, as a function of θ . We can use this to “boost” the speeds of the lab-frame scattered neutrons back up to their original values by multiplying the surviving momentum, associated with the lab-frame final speed, v_1 , by v_0/v_1 , where v_0 is the lab-frame initial speed. For thermal neutrons, this could be due to gaining energy, on average, from the thermal motion of the target nuclei with which the neutrons are nearly in equilibrium. With this approach we get

$$\frac{\vec{v}_1 \cdot \vec{v}_0}{v_0^2} = \frac{A\cos(\theta) + 1}{\sqrt{A^2 + 2A\cos(\theta) + 1}} \quad (4.22)$$

Now we would like to average the fractional surviving momentum over scattering angle, assuming isotropy in the center-of-mass frame. This is given by

$$\begin{aligned} \langle \frac{\vec{v}_1 \cdot \vec{v}_0}{v_0^2} \rangle &= \frac{1}{4\pi} \int_0^{2\pi} d\phi \int_0^\pi \sin(\theta) d\theta \frac{A\cos(\theta) + 1}{\sqrt{A^2 + 2A\cos(\theta) + 1}} \\ &= \frac{1}{2} \int_{-1}^1 dx \frac{Ax + 1}{\sqrt{A^2 + 2Ax + 1}} = \frac{2}{3A} \end{aligned} \quad (4.23)$$

where a table of integrals or a computer algebra system helps with the last step. This is the conventional result. It is usually obtained, without discussion of the topic of energy loss, by averaging $\cos(\psi)$ over the isotropic center-of-mass scattering, where ψ is the lab-frame scattering angle.

We are now in a position to evaluate $\lambda_{tr} = 1/\overline{\Sigma_{tr}}$ where we remember that the overbar indicates a sum over all species of nuclei present, and Σ represents the macroscopic cross-section, $N\sigma$. As for any collisional effect, we need to add Σ s to sum up the various processes that extract momentum for the neutrons.

$$\lambda_{tr}^{-1} = \overline{\Sigma_{tr}} = \overline{\Sigma_\gamma} + \overline{\Sigma_f} + \overline{\Sigma_{(n,\alpha)}} + \overline{(\Sigma_e + \Sigma_{in})(1 - 2/(3A))} \quad (4.24)$$

where we have “boosted” all scattering events, both elastic and inelastic.

However at the energies of interest, inelastic scattering is essentially only a high-A phenomenon.

Finally, we may have a source or sink of neutrons in our system. In a system where neutron multiplication is taking place we can represent this as

$$s = (k_\infty - 1)(\overline{\Sigma_\gamma} + \overline{\Sigma_f} + \overline{\Sigma_{(n,\alpha)}})\phi = (k_\infty - 1)\overline{\Sigma_{abs}}\phi \quad (4.25)$$

since for each neutron absorbed k_∞ are produced. We are here ignoring any time delay between the production of these neutrons at high energy and their arrival at the energy under consideration. We are similarly ignoring spatial motion of the neutrons between birth and arrival at this energy. Also, you should remember that the basic derivation of the diffusion equation assumed that the neutron flow speed is much less than the random one-speed neutron motion and that the time rate of change of the average flow is much less than its rate of collisional dissipation. We showed as well that the requirement of flow speed much less than v_n implied that the scale length of the neutron density gradient, $n/|\vec{\nabla}n|$, had to be much greater than λ_{tr} . With these caveats, the reactor-analysis version of the neutron diffusion equation including sources and sinks is, finally,

$$\frac{1}{v_n} \frac{\partial \phi}{\partial t} = \vec{\nabla} \cdot \frac{\lambda_{tr}}{3} \vec{\nabla} \phi + (k_\infty - 1) \overline{\Sigma_{abs}} \phi \quad (4.26)$$

4.3 1-D δ -function initial condition without boundaries

In order to develop some physical intuition about neutron diffusion, it is helpful to consider the one-dimensional physics version of the one-speed diffusion equation, without sources or sinks, given by

$$\frac{\partial n}{\partial t} = \frac{\partial}{\partial x} D_{phys} \frac{\partial n}{\partial x} \quad (4.27)$$

with $D_{phys} = v_n \lambda_{tr}/3$.

Consider an initial condition of a δ -function of neutron density located at $x = 0$ and uniform vs. y and z at time $t = 0$, $n(t = 0) = \delta(x = 0)$. The solution to the time evolution of n vs. time and space is well known:

$$n(x, t) = \frac{1}{\sqrt{4\pi D_{phys} t}} \exp\left(\frac{-x^2}{4D_{phys} t}\right) = \frac{1}{\sqrt{2\pi\sigma_x^2(t)}} \exp\left(\frac{-x^2}{2\sigma_x^2(t)}\right) \quad (4.28)$$

where the last step comes from properties of the “normal” (or Gaussian) distribution. $\sigma_x(t)$ is the root mean square deviation of such a distribution from its mean value. You can show that this form solves equation 4.27 for

$t > 0$ by substitution. You can also show that its integral over all x is unity, independent of time. Figure 4.3 shows the solutions for various values of Dt .

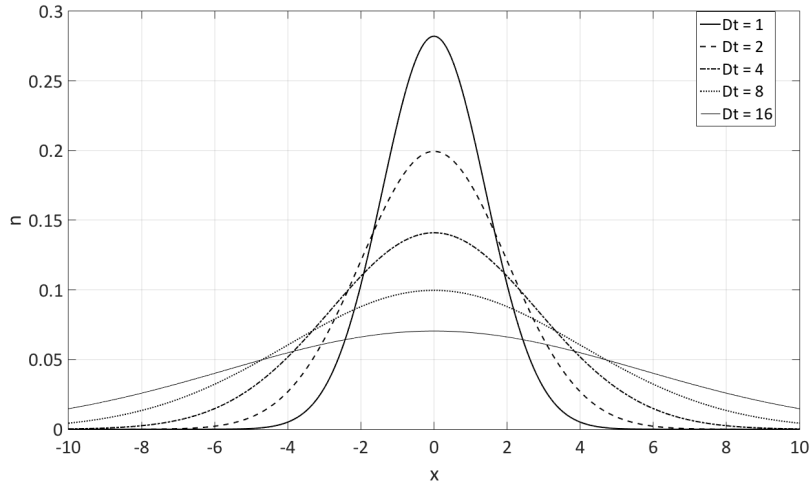


Figure 4.3 Evaluation of equation 4.28 for $Dt = 1, 2, 4, 8$, and 16 .

The major physics observation from this result is that the mean square deviation of the spatial distribution of neutrons grows linearly with time, $\sigma_x^2(t) = 2D_{phys}t$. This reflects a fundamental property of the diffusion equation, as you can see by dimensional analysis. In this equation time is fundamentally related to spatial scale length squared, divided by D_{phys} . If you have a steel rod that is twice longer than my steel rod, it takes heat four times longer to diffuse from one end to the other of your rod than mine. If, however, your longer rod is made of aluminum or copper (which have roughly four times the thermal diffusivity of steel), your diffusion time is reduced back down mine.

4.4 Statistical interpretation of the neutron diffusion equation

It is interesting to compare the above continuum result for a δ -function initial condition with a statistical analysis of the same problem. The Central Limit Theorem (CLT) of statistics considers a list of n uncorrelated random numbers, Δx_i for $i = 1 \dots n$, with mean value m and variance $\sigma^2 \equiv (1/n) \sum_1^n (\Delta x_i - m)^2$. The theorem states that the sum of this list approaches nm as $n \rightarrow \infty$,

$$x = \sum_{i=1}^n \Delta x_i \rightarrow nm \text{ as } n \rightarrow \infty \quad (4.29)$$

This should come as no surprise. The CLT further states, more interestingly, that if you perform this sum on many such lists, the variance from nm of the sums approaches $n\sigma^2$ for large n .

$$\langle(x - nm)^2\rangle \rightarrow n\sigma^2 \text{ as } n \rightarrow \infty \quad (4.30)$$

Thus, for large n , the variance of the sums grows linearly with the number of steps. It further states that for large n the probability distribution function of the sums will approach a “normal” (or Gaussian) distribution. Evidently the CLT is closely related to the solution of the generic diffusion equation given in equation 4.28.

Consider that after a decorrelation time of the neutron flight direction, τ_{decor} , a neutron lands a distance in x , Δx , away from its starting point. For a homogeneous medium and a random initial direction of motion, obviously the mean value of Δx , $\langle\Delta x\rangle$, equals 0 for any τ_{decor} . So for our case $m = 0$ in the CLT. But what is the decorrelation time, and what is the mean square value of the step $\langle\Delta x^2\rangle$ that corresponds to the CLT’s σ^2 ?

The mean decorrelation time of the neutron flight direction is $\tau_{decor} = \lambda_{tr}/v_n$, since v_n/λ_{tr} is the rate coefficient for momentum loss. (The CLT is not directly relevant to the case where neutrons are absorbed.) Thus for our case the number of steps, n , in the CLT is given by

$$n = t/\tau_{decor} = tv_n/\lambda_{tr} \quad (4.31)$$

If we say that the mean distance to decorrelation is λ_{tr} , we can evaluate the mean square distance to decorrelation by analogy with equation 2.3. Here we use s instead of x as the variable along the randomly-oriented original flight direction, and we average s^2 over the neutron decorrelation.

$$\frac{\int_0^{n_0} s^2 dn_b}{\int_0^{n_0} dn_b} = \overline{\Sigma_{tr}} \int_0^\infty s^2 e^{-s\overline{\Sigma_{tr}}} ds = \frac{1}{\overline{\Sigma_{tr}^2}} \int_0^\infty \tilde{s}^2 e^{-\tilde{s}} d\tilde{s} = 2\lambda_{tr}^2 \quad (4.32)$$

where the last step can be accomplished through two integrations by parts. Since this is the mean square step length to decorrelation and by isotropy $\langle\Delta x^2\rangle = \langle\Delta s^2\rangle/3$ we have $\langle\Delta x^2\rangle = 2\lambda_{tr}^2/3$. This is then the σ^2 for a single step that should appear in the CLT for our case. Let us now compare our diffusion equation result for the growth of the variance with time, equation 4.28, to the CLT result.

$$\begin{aligned} \sigma_x^2(t) &= 2D_{phys}t \text{ (generic diffusion equation)} \\ \sigma_x^2(t) &= 2n\lambda_{tr}^2/3 = 2tv_n\lambda_{tr}/3 \text{ (CLT)} \\ D_{phys} &= v_n\lambda_{tr}/3 \end{aligned} \quad (4.33)$$

Thus the value of D_{phys} we derive from the statistical CLT analysis is the

same as that we derived from our fluid neutron diffusion model. The CLT is equivalent to a very simple “kinetic” model that works directly from single particle motion. It provides an alternative and perhaps more intuitive sense for why diffusive neutron spreading grows as the square root of time. This is simply the way that random steps add, by summing their variance. Suppose steps have summed to progress in one direction. A subsequent step may add or subtract from that progress. This may seem like no progress, but if you want to get many step lengths from the starting point, you are more likely to get there with more random steps. This is also how statistical errors add. While errors may cancel, the overall breadth of uncertainty increases.

Note that the CLT is only valid for large values of n , the length of the list of random numbers. The width of the resulting Gaussian is much greater than the root mean square step size only for large n , so the criteria for validity of the CLT analysis and our diffusion analysis are the same - many step sizes over a gradient scale length. A weakness in the simple statistical analysis presented here is that we have not included absorption in our statistical picture. However in the fluid picture it is evident that absorption corresponds to momentum loss, and so must be included in λ_{tr} .

4.5 1-D δ -function steady source without boundaries

We can gain additional useful physical understanding by looking at another simple version of the unbounded diffusion equation. This time let us consider an infinite, homogeneous, net absorbing medium ($k_\infty < 1$), with a steady source of neutrons at $x = 0$. The one-dimensional time-independent neutronics-analysis diffusion equation for this case is

$$0 = \frac{\partial}{\partial x} \frac{\lambda_{tr}}{3} \frac{\partial}{\partial x} \phi + (k_\infty - 1) \overline{\Sigma_{abs}} \phi + S_2 \delta(x) \quad (4.34)$$

where S_2 indicates a two-dimensional (infinite in y and z) source of neutrons, in units of neutrons per second per meter². Second order differential equations in general have two solutions and the solutions of this equation are simple exponential growth or decay as a function of x . We should assume, in this net absorbing medium, that the solutions must go to zero at $x = \pm\infty$. Therefore we choose decay for $x > 0$ and growth for $x < 0$ (i.e., decay vs. $-x$). Matching the solutions at $x = 0$, since the problem is left-right

symmetric, we obtain

$$\begin{aligned}\phi &= \phi_0 \exp\left(\mp x \frac{\sqrt{1-k_\infty}}{L}\right) \\ L &\equiv \sqrt{\frac{\lambda_{tr}\lambda_{abs}}{3}} = \sqrt{\frac{D}{\Sigma_{abs}}}\end{aligned}\quad (4.35)$$

where the \mp is negative for $x > 0$ and positive for $x < 0$. L is the decay length due to the competition between diffusion and absorption, in the absence of fission. It is called the “diffusion length.” Note that the actual decay length of the neutron density in our case goes to infinity as k_∞ approaches unity, meaning that near-critical systems are tightly coupled spatially. Figure 4.4 shows the solution for various values of L for the case of $k_\infty = 0$.

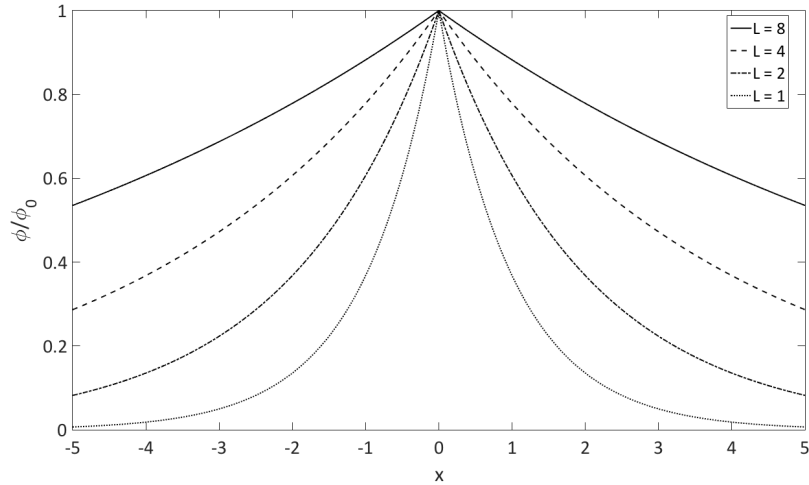


Figure 4.4 Evaluation of equation 4.35 for $k_\infty = 0$ and $L = 1, 2, 4$, and 8.

Let us evaluate ϕ_0 . To do this we look close to $x = 0$, choosing a point close enough that there cannot have been much multiplication of the source neutrons, so $x \ll \lambda_{abs}$, but where the diffusion equation should be applicable, $x \gg \lambda_{tr}$. While we are at it, let us choose $x \ll L/\sqrt{1-k_\infty}$. This means that one-half of S_2 must be flowing in each of the directions $\pm x$. Using equation 4.15, the one-speed neutron diffusion version of Fick’s Law, we have

$$S_2 = 2 \frac{\lambda_{tr}}{3} \frac{\partial}{\partial x} \phi = 2 \frac{\lambda_{tr}}{3} \phi_0 \frac{\sqrt{1-k_\infty}}{L} = 2\phi_0 \sqrt{1-k_\infty} \sqrt{\frac{\lambda_{tr}}{3\lambda_{abs}}} \quad (4.36)$$

so

$$\phi_0 = \frac{S_2}{2} \sqrt{\frac{3\lambda_{abs}}{\lambda_{tr}(1 - k_\infty)}} \quad (4.37)$$

Questions: Show that it is possible to chose an x , near $x = 0$, that meets all of the conditions we are imposing. You may assume $\lambda_{abs} \gg L \gg \lambda_{tr}$, so that diffusion is applicable in this case in the first place. Also, what shape does $\phi(x)$ take in the non-diffusive region $x < \lambda_{tr}$?

Now it is interesting to evaluate the total number of neutrons absorbed, per second per m^2 , from $x = -\infty$ to $+\infty$. Since, in this case, all of the neutrons produced are absorbed somewhere, the total number of neutrons absorbed must correspond to the sum of the source neutrons plus those produced from fission.

$$\begin{aligned} \int_{-\infty}^{\infty} \overline{\Sigma}_{abs} \phi dx &= \frac{S_2}{\lambda_{abs}} \sqrt{\frac{3\lambda_{abs}}{\lambda_{tr}(1 - k_\infty)}} \int_0^{\infty} \exp\left(\mp x \frac{\sqrt{1 - k_\infty}}{L}\right) dx \\ &= \frac{S_2}{L\sqrt{1 - k_\infty}} \frac{L}{\sqrt{1 - k_\infty}} = \frac{S_2}{1 - k_\infty} \end{aligned} \quad (4.38)$$

This result indicates that the total multiplication of the system is $1/(1 - k_\infty)$. This is exactly what we expect, since for S_2 source neutrons per second per meter² produced (and absorbed) there are $k_\infty S_2$ second generation neutrons produced (and absorbed) per second per meter², the third generation comprises $k_\infty^2 S_2$ per second per meter², and so on. And we know

$$S_2(1 + k_\infty + k_\infty^2 + k_\infty^3 + \dots) = S_2/(1 - k_\infty) \quad (4.39)$$

rather a satisfying result, with the correct limits as k_∞ goes to 0 and 1.

It is also interesting to know the mean distance at which a fission event at the origin induces a fission event elsewhere. Since we have a simple exponential fall-off of ϕ to the left and right of the source at $x = 0$, and a uniform medium, we can use the same calculation as that of the mean free path, equation 2.2, to get this mean distance. The result is $L/(1 - k_\infty)^{1/2}$.

4.6 Boundary conditions

Now we are interested in moving on to finite systems. To do this we need to set boundary conditions for the diffusion equation. Often fission reactors are surrounded by “reflectors” that bounce neutrons back into the reactor, in order to minimize neutron losses. In thermal reactors this is generally just a region of moderator without fuel assemblies. In fast “breeder” reactors that

are designed to produce net fissile material, a “blanket” of fuel assemblies with natural or depleted uranium reflects neutrons, but also absorbs them to produce ^{239}Pu . Alternatively, or in addition, a thick steel blanket can be used to minimize neutrons escaping from the core.

It is evident that ϕ must be continuous across the interface between dissimilar media. The diffusion equation cannot support a steep gradient in ϕ , even at a discontinuity in D . Calling the two sides of the discontinuity the + and - sides, we can express this as

$$\phi_+ = \phi_- \quad (4.40)$$

The diffusion equation also cannot support a discontinuity in the flow of neutrons, since this would constitute an infinite positive or negative local divergence of the flow. Thus we have another boundary condition at any interface,

$$\hat{n} \cdot D_+ \vec{\nabla} \phi_+ = \hat{n} \cdot D_- \vec{\nabla} \phi_- \quad (4.41)$$

where \hat{n} indicates a unit vector pointing directly across the interface.

There is a different kind of boundary condition at the edge of a nuclear system, say at an interface with air, where the neutron mean free path is long enough that a neutron is very unlikely ever to return when it crosses the interface. This means that within λ_{tr} of the edge the angular distribution of neutron velocities is highly anisotropic; there are very few inwards-directed neutrons. Such a physical condition violates the fundamental assumption of near-isotropy inherent in the one-speed diffusion equation.

As an approximation to this condition, let us assume that the angular distribution of neutrons at the edge of a nuclear system is hemispherically isotropic, meaning that for outgoing neutrons all elements of solid angle, $d\Omega$, are equally populated with neutrons, but there are no neutrons populating the incoming hemisphere. In this simple case it is easy to calculate the relationship between the outgoing neutron flux and the neutron density, particularly in our one-speed approximation. Taking \hat{n} to be the outgoing direction, and defining θ with respect to this \hat{n} direction, we need only average $\cos\theta$ over the populated hemisphere, recognizing that $d\Omega = \sin\theta d\theta d\varphi = -d\cos\theta d\varphi$, giving

$$n\langle v_{\hat{n}} \rangle = nv_n \langle \cos\theta \rangle = \phi \frac{\int_0^1 \cos\theta d\cos\theta}{\int_0^1 d\cos\theta} = \phi \int_0^1 x dx = \frac{\phi}{2} \quad (4.42)$$

This result illustrates the perhaps obvious fact that we cannot have a finite neutron flux across the outgoing interface without a finite neutron density

at that interface. Thus the boundary condition at the interface with long mean free path material, such as air, cannot be $\phi = 0$.

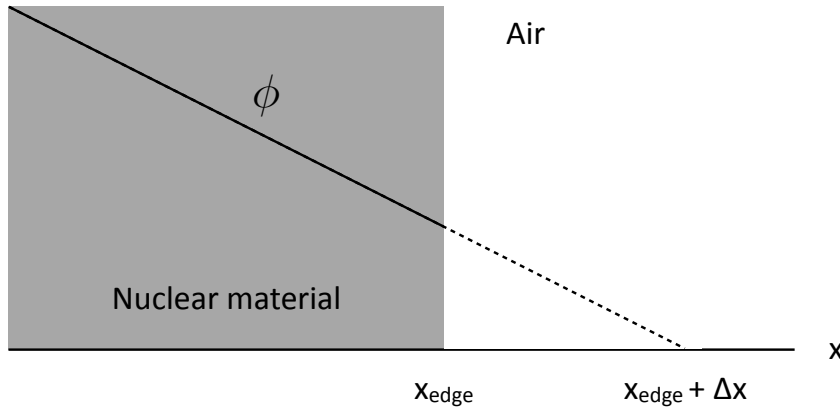


Figure 4.5 Linear extrapolation of ϕ from the edge of nuclear material

If we match the diffusive flux to this very simple “kinetic” edge calculation, we have, at the edge

$$\hat{n} \cdot \vec{\nabla}\phi = -\phi/2 \quad (4.43)$$

Now consider a boundary of some nuclear material at $x = x_{edge}$, as illustrated in figure 4.5. At the boundary of the material, but inside of it, we have $d\phi/dx = -\phi/(2D)$. If we extrapolate this gradient outside, we can find the distance at which the extrapolated line strikes $\phi = 0$.

$$\begin{aligned} \phi + \Delta x \frac{d\phi}{dx} &= \phi - \Delta x \frac{\phi}{2D} = 0 \\ \lambda_{ext} &= \Delta x = 2D = 2\lambda_{tr}/3 \end{aligned} \quad (4.44)$$

λ_{ext} is given the name “extrapolation length”. It is important to understand that this model for the edge is not accurate within a few λ_{tr} ’s of the edge within the material, and bears no relationship to the actual neutron flux outside of the material. However it does provide a reasonably good model for the effect that $\phi \neq 0$ at the boundary. Furthermore, it is important to remember that the edge of the material is at x_{edge} , not at $x_{edge} + \lambda_{ext}$. Finally, this procedure is only valid if ϕ is reasonably linear near the boundary.

As a final, final remark, full kinetic calculations for an infinite planar interface give $\lambda_{ext} = 0.7104\lambda_{tr}$.

4.7 Bounded Systems

Now we are in a position to solve the one-speed neutron diffusion equation in some informative geometries. We will simplify the problem by assuming that D_{reac} ($= \lambda_{tr}/3$), $\overline{\Sigma_{abs}}$, and k_∞ are constant across the reactor core. In practice burnable poisons can be distributed with a spatial profile, and the process by which fuel assemblies are replaced (typically 1/3 of the total every 18 months in commercial LWRs) and moved about, or “shuffled,” during the replacement process, means that this assumption is not really justified for practical cases. As we will see, the profiles we find are peaked, and operators prefer to have more nearly uniform burn-up of the nuclear fuel.

All that said, it is informative to solve the diffusion equation for uniform material properties. We are interested in a time-independent solution. Dividing equation 4.26 through by $D\phi$ we have

$$\frac{1}{D\phi v_n} \frac{\partial \phi}{\partial t} = 0 = \frac{1}{\phi} \nabla^2 \phi + (k_\infty - 1) \frac{\overline{\Sigma_{abs}}}{D} = \frac{1}{\phi} \nabla^2 \phi + \frac{k_\infty - 1}{L^2} \quad (4.45)$$

Note that we will need $k_\infty > 1$ to sustain a chain reaction, since neutrons will escape across the boundaries of this system. Reactor designers use some special “lingo” to describe the two terms on the far right of equation 4.45.

$$\begin{aligned} B_g^2 &\equiv -\frac{1}{\phi} \nabla^2 \phi \\ B_m^2 &\equiv \frac{k_\infty - 1}{L^2} \end{aligned} \quad (4.46)$$

B_g is called the “geometric buckling” which can be thought of as the degree to which ϕ is bent, or buckled, by the presence of the boundary conditions. If the boundaries are far away from the center of the system, the buckling is slight, but as they are moved inwards the buckling increases. The sign of the associated curvature means that $\nabla^2 \phi$ is everywhere negative, resulting in net outflow of neutrons from every volume element, and so the need for neutron production to compensate the outflow to sustain steady state. The neutron production is supplied by the “material buckling,” B_m . In this version of the neutron diffusion equation we have isolated all of the geometrical effects to the first term and all of the material effects to the second.

For steady operation, or criticality, we need $B_m = B_g$. If $B_m > B_g$, the system is supercritical and ϕ grows with time, while for $B_m < B_g$, the system is subcritical and ϕ decays with time. The dimension of both B_g and B_m is 1/length. It is interesting to note that $|1/B_m|$ is equal to the scale length of the solution to the one-dimensional unbounded case, equation 4.35.

However $\nabla^2\phi$ in that case is everywhere positive, since an inflow of neutrons is required to balance $k_\infty - 1 < 0$.

4.7.1 Cuboids

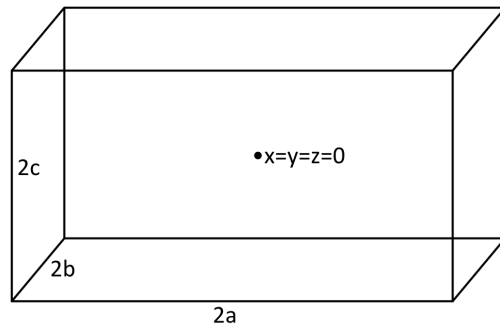


Figure 4.6 Cuboid reactor core.

Let us start by considering the simplest finite case, a cuboid-shaped reactor core. Formally this is a “right cuboid,” because we will assume that all of the intersections between the rectangular surfaces are at right angles. We will take the reactor core to occupy a volume defined by $|x| < a$, $|y| < b$, and $|z| < c$, as shown in figure 4.7. Using the approximation that $\phi = 0$ at the extrapolated boundaries, the boundary conditions for a solution are $\phi = 0$ at

$$\begin{aligned} x &= \pm(a + \lambda_{ext}) = \pm\tilde{a} \\ y &= \pm(b + \lambda_{ext}) = \pm\tilde{b} \\ z &= \pm(c + \lambda_{ext}) = \pm\tilde{c} \end{aligned} \tag{4.47}$$

where the meaning of a constant with a “tilde” is that it is represents an extrapolated boundary.

Now we will solve this equation by the method of “separation of variables.” This amounts to making the “anzats,” or assumption, that the solution will take the form

$$\phi(x, y, z) = \phi(x)\phi(y)\phi(z) \tag{4.48}$$

In rectilinear coordinates, equation 4.45 becomes

$$\frac{\nabla^2 [\phi(x)\phi(y)\phi(z)]}{\phi(x)\phi(y)\phi(z)} + B_m^2 = \frac{1}{\phi(x)} \frac{\partial^2 \phi(x)}{\partial x^2} + \frac{1}{\phi(y)} \frac{\partial^2 \phi(y)}{\partial y^2} + \frac{1}{\phi(z)} \frac{\partial^2 \phi(z)}{\partial z^2} + B_m^2 = 0 \quad (4.49)$$

Since we have assumed that B_m^2 is spatially uniform we need each of the other terms to be spatially uniform as well, since they cannot balance out any spatial variation in one another. The solution also needs to match our boundary conditions. The two potential solutions for this case, with $k_\infty - 1 > 0$, are sine and cosine. It is easy to see that if we use either a sine or cosine function for ϕ , the first three terms will be spatially uniform, but only cosine can match the boundary conditions. We conclude

$$\phi(x, y, z) = \phi_0 \cos\left(\frac{\pi x}{2\tilde{a}}\right) \cos\left(\frac{\pi y}{2\tilde{b}}\right) \cos\left(\frac{\pi z}{2\tilde{c}}\right) \quad (4.50)$$

and

$$B_g^2 = \left(\frac{\pi}{2\tilde{a}}\right)^2 + \left(\frac{\pi}{2\tilde{b}}\right)^2 + \left(\frac{\pi}{2\tilde{c}}\right)^2 \quad (4.51)$$

We require, furthermore, that $B_g^2 = B_m^2$ to achieve self-consistency between the neutron loss due to the finite system size (that drives B_g) and the excess of k_∞ above unity (that drives B_m). For a given B_m , the size of the reactor set by \tilde{a} , \tilde{b} , and \tilde{c} cannot be too small, or the chain reaction is quenched by neutron losses. By the same token the size cannot be too large, or the reaction runs away. For a cuboid reactor with one or more dimensions infinite (an infinite slab or infinite square-cross-section rod) the infinite dimensions play no role in determining B_g and therefore the necessary B_m . But if one dimension is too short, for example $\tilde{a} < \pi/(2B_m)$, it doesn't matter how long the others are made, the system will never achieve criticality. As a reminder, the physical reactor only extends to $x = \pm a$, $y = \pm b$, and $z = \pm c$, not to the extrapolated boundaries, \tilde{a} , \tilde{b} , and \tilde{c} .

Note that this type of analysis does not determine the absolute value of ϕ_0 and so, for example, the level of power production of a reactor. In practice the operating power of a reactor is set by the fact that k_∞ is a function of the temperature of the reactor. For example, a light water reactor should be designed to operate “under-moderated,” meaning that if there were more moderator present, k_∞ would increase, and by the same token less moderation reduces k_∞ . As a result, as the moderator temperature increases, and the water expands – reducing its density and so neutron moderation –

k_∞ decreases. Thus as the power level of a reactor is slowly brought up, and its temperature increases, k_∞ decreases. The equilibrium power of the reactor is where $k_\infty - 1$ just drops to the point where it balances the neutron losses. That point can be adjusted by inserting “control rods” that reduce k_∞ at any temperature, by absorbing neutrons.

Questions: $\phi_0 \cos [3\pi x/(2\tilde{a})]$ is a solution to the neutron diffusion equation that matches the required boundary conditions for slab infinite in the y and z directions. By what factor would $k_\infty - 1$ need to increase to support this solution? And why is this solution not physical anyway?

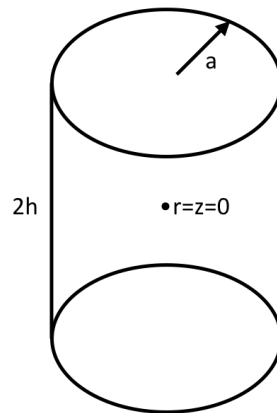


Figure 4.7 Cylindrical reactor core.

4.7.2 Cylinders

Now we move on to a more realistic case for a reactor, a right circular cylinder of finite length. Let the radius of the cylinder be a , and its height $2h$, the latter in violation of the conventional choice of h , but consistent with our practice here, making the named dimension half of the edge-to-edge distance. In cylindrical coordinates, and assuming cylindrical symmetry, equation 4.45 becomes

$$\frac{1}{\phi(r)r} \frac{\partial}{\partial r} r \frac{\partial}{\partial r} \phi(r) + \frac{1}{\phi(z)} \frac{\partial^2 \phi(z)}{\partial z^2} + B_m^2 = 0 \quad (4.52)$$

where we have already performed the separation of variables, as in equation 4.49. Again each term must be spatially uniform.

Starting from the first term on the left-hand side, we note that the 0'th

Bessel function of the first kind, J_0 , obeys the equation,

$$\frac{1}{J_0(\gamma r)} \frac{1}{r} \frac{d}{dr} r \frac{d}{dr} J_0(\gamma r) = -\gamma^2 \quad (4.53)$$

making this special function a candidate for our solution. The 0'th Bessel function of the second kind, Y_0 , is the other solution to this equation, but it diverges as r goes to zero, so we reject it.

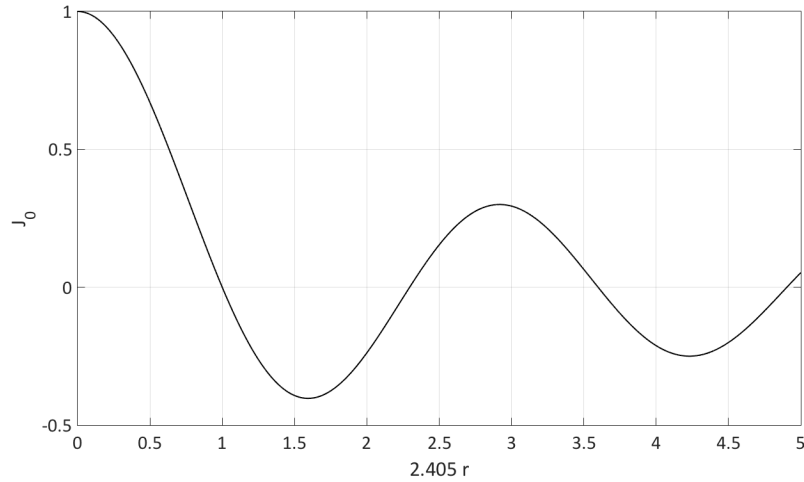


Figure 4.8 0'th Bessel Function of the first kind vs. γr for $\gamma = 2.405$

We can see from figure 4.8 that the 0'th Bessel function of the first kind has its first zero at $\gamma r = 2.405$. Thus to match our boundary condition $\phi = 0$ at $r = \tilde{a}$ we require

$$\begin{aligned} \gamma \tilde{a} &= 2.405 \\ \gamma &= 2.405/\tilde{a} \end{aligned} \quad (4.54)$$

Thus we have

$$\phi(r) \propto J_0(2.405r/\tilde{a}) \quad (4.55)$$

and γ^2 is the contribution to B_g^2 from this term.

The second term of equation 4.53 is familiar from the cuboid solution. Its solution, taking into account the boundary conditions at $\pm \tilde{h}$, is

$$\phi(z) \propto \cos\left(\frac{\pi z}{2 \tilde{h}}\right) \quad (4.56)$$

Bringing these together we have

$$\phi(r, z) = \phi_0 J_0 \left(\frac{2.405r}{\tilde{a}} \right) \cos \left(\frac{\pi z}{2 \tilde{h}} \right) \quad (4.57)$$

and

$$B_g^2 = \left(\frac{2.405}{\tilde{a}} \right)^2 + \left(\frac{\pi}{2 \tilde{h}} \right)^2 \quad (4.58)$$

4.7.3 Spheres

Finally we consider a spherical reactor, with extrapolated radius \tilde{a} . This is the configuration that reaches criticality, for given B_m , with the least mass of material. Thus it is a reasonable guess for the shape of the fissile material in a nuclear weapon. Equation 4.45 in spherical coordinates, assuming spherical symmetry, is

$$\frac{1}{\phi r^2} \frac{\partial}{\partial r} r^2 \frac{\partial}{\partial r} \phi + B_m^2 = 0 \quad (4.59)$$

Now we try a substitution, $\phi = \psi/r$.

$$\begin{aligned} \frac{r}{\psi r^2} \frac{\partial}{\partial r} r^2 \frac{\partial}{\partial r} \left(\frac{\psi}{r} \right) + B_m^2 &= 0 \\ \frac{1}{\psi r} \frac{\partial}{\partial r} \left(r \frac{\partial \psi}{\partial r} - \psi \right) + B_m^2 &= 0 \\ \frac{1}{\psi r} \left(\frac{\partial \psi}{\partial r} + r \frac{\partial^2 \psi}{\partial r^2} - \frac{\partial \psi}{\partial r} \right) + B_m^2 &= 0 \\ \frac{1}{\psi} \frac{\partial^2 \psi}{\partial r^2} + B_m^2 &= 0 \end{aligned} \quad (4.60)$$

Question: Give a plausibility argument, in terms of volume and surface area, for why the sphere might be the most efficient shape for achieving criticality with a fixed amount of fissile material.

This is the same equation that we solved for the cuboid reactor, but in this case the variable is ψ , not ϕ . Furthermore the boundary conditions are different. We know that sine and cosine are valid solutions to the equation for ψ , but now we must reject cosine, because if ψ takes on a cosine variation ϕ goes to infinity at the origin, which is non-physical. Thus we need a sine solution for ψ , and we require $\phi = 0$ and therefore $\psi = 0$ at \tilde{a} . This leaves us with

$$\phi = \phi_0 \left(\frac{\tilde{a}}{\pi} \right) \frac{\sin(\pi r/\tilde{a})}{r} \quad (4.61)$$

giving

$$B_g^2 = \frac{1}{\psi} \frac{\partial^2 \psi}{\partial r^2} = \left(\frac{\pi}{\tilde{a}} \right)^2 \quad (4.62)$$

and again we require that $B_g^2 = B_m^2$, setting the self-consistency between the neutron loss and the excess of k_∞ above unity.

Questions: Why does the factor \tilde{a}/π appear in the equation for ϕ ? What is $\partial\phi/\partial r$ at the origin, and why is this necessary?

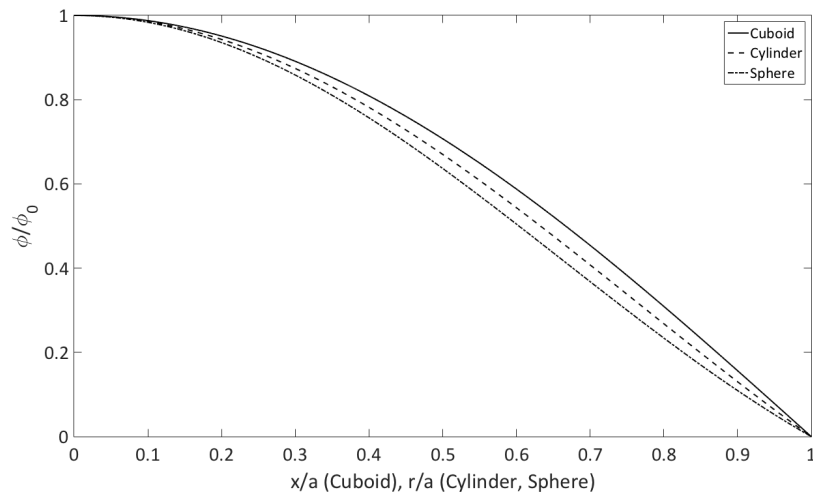


Figure 4.9 Profiles of neutron flux for cuboid, cylindrical, and spherical geometries.

Figure 4.9 shows the spatial profiles of neutrons for the three cases we have considered here. Evidently they are quite similar, but the cuboid is flattest, the cylinder slightly less flat and the sphere most peaked. This is because surface losses affect the outer part of the profile most strongly in the case where the surface curves around the outer part in two dimensions, the sphere, less in the case where the surface curves around the outer part in only one dimension, the cylinder, and least in the case of a planar surface, with no curvature.

4.7.4 Reflectors

Nuclear reactor cores are generally surrounded by neutron “reflectors,” as discussed at the beginning of this section, 4.7, on bounded systems. Their purpose is to use inexpensive non-fuel material to reduce neutron loss from

the reactor core by “reflecting” escaping neutrons back into the core. As we will see momentarily, this reduction in neutron loss shows up as a decrease in *linear dimension* $\cdot B_g$, so for fixed material buckling, B_m , the system can be made smaller. Alternatively, for fixed linear dimension B_m can be reduced, so a lower k_∞ is required for criticality. Furthermore, the flux profile is flattened, giving more uniform fuel burn.

For simplicity, let us consider a planar reactor, confined in the region $|x| < a$, with reflectors in the regions $|x| > a$. If the reflectors were to extend to $\pm\infty$, the flux profile in the reflectors would be the same as that for a planar source in a net absorbing medium, given in equation 4.35 with $k_\infty = 0$. Covering both $x < 0$ and $x > 0$ we have, for ϕ in the reflectors,

$$\phi_r = \phi_a \exp\left(-\frac{|x| - a}{L_r}\right) \quad (4.63)$$

where ϕ_a is the neutron flux at the interfaces between the reactor core and the reflectors, $x = \pm a$, and L_r represents the neutron “diffusion length” in the reflectors. In a realistic case, of course, the reflectors do not extend to $\pm\infty$, but if they extend for a distance much greater than L_r they act largely as if they did. To get a feel for the maximum effects of reflectors, with a minimum of mathematics, let us consider this infinite case.

The left-right symmetric one-dimensional solution for ϕ in the core region is

$$\phi_c(x) = \phi_0 \cos(xB_g) \quad (4.64)$$

by the definition of B_g , equation 4.46. The boundary conditions (equations 4.40 and 4.41) that will determine B_g in this case are given, first, by matching ϕ , at the core-reflector interfaces,

$$\phi_c(a, -a) = \phi_0 \cos(aB_g) = \phi_r(a, -a) = \phi_a \quad (4.65)$$

Next we must match the neutron flow out of the core at $\pm a$ with that into the reflector at $\pm a$, giving

$$\begin{aligned} -D_c \frac{d\phi_c}{dx} \Big|_{a,-a} &= \pm D_c \phi_0 B_g \sin(aB_g) = \\ -D_r \frac{d\phi_r}{dx} \Big|_{a,-a} &= \pm D_r \phi_a / L_r = \pm D_r \phi_0 \cos(xB_g) / L_r \end{aligned} \quad (4.66)$$

giving us

$$B_g \tan(aB_g) = D_r / (L_r D_c) \quad (4.67)$$

If we multiply both sides by a we arrive at

$$aB_g \tan(aB_g) = aD_r/(L_r D_c) \quad (4.68)$$

Transcendental equations of this type (and *much* more complicated) are endemic to calculations about reflectors. They can be solved for quantities like aB_g using numerical root finders, or for graphic display the problem can sometimes be made easier by evaluating quantities like $aD_r/(L_r D_c)$ as a function of aB_g , but then plotting $aD_r/(L_r D_c)$ on the x axis. Figure 4.10 shows the solution to this equation, including $\phi_a/\phi_0 = \cos(aB_g)$, a measure of the degree of the flattening within the core provided by reflection. aB_g is divided by $\pi/2$, to allow direct comparison with the no-reflector case without consideration of an extrapolation length.

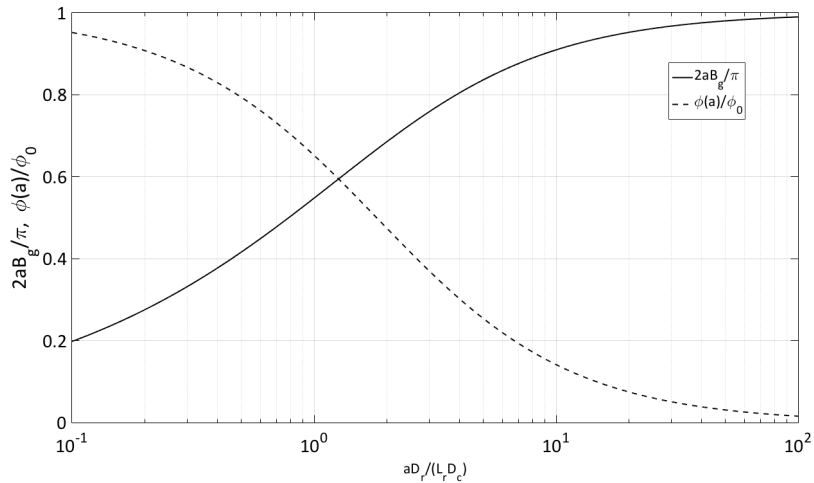


Figure 4.10 Normalized geometric buckling and profile flattening as functions of normalized diffusion length, in a slab reactor

There is valuable physical insight to be gained from figure 4.10. Assuming that $D_r/D_c \approx 1$, low values of a/L_r correspond to little absorption in the reflector over a length comparable to the reactor dimension. This gives rise to high values of aB_g , meaning that the profile from $-a$ to a is significantly flattened, as can also be seen by the value of $\phi(a)/\phi_0$. On the other hand, high values of a/L_r correspond to a very small diffusion length compared to the reactor dimension and so essentially immediate absorption of neutrons leaving the core. In this limit the solution converges to the no-reflector case with zero extrapolation length.

Question: L must be greater than the mean free path for momentum loss,

λ_{tr} , for the diffusion model to be valid, so a small L implies an even smaller λ_{ext} . Show that this implies that $\lambda_{abs} > \lambda_{tr}$, and why this is a reasonable assumption.

Table 4.1 gives λ_{tr} , L and v_n for the nominal reactor cores we considered in sections 3.5 through 3.8 (thermal reactors) and section 3.9 (fast reactors), and for some representative reflector materials. The nominal fast reactor blanket is assumed to have the same configuration as the core, but the uranium is pure ^{238}U . The last four lines anticipate a calculation we will do in Chapter 7 on nuclear weapons and nuclear proliferation.

Table 4.1 *Mean free paths for momentum loss and absorption, diffusion length, neutron speed for various media. Fast reactor speed corresponds to 300 keV. Watt spectrum speed is for mean energy of 2 MeV.*

Medium	λ_{tr}	λ_{abs}	L	v_n	Spectrum
Nominal LWR Core	—	—	—	$2.2 \cdot 10^3$	Thermal
$^{235}\text{UO}_2$	—	—	—	$2.2 \cdot 10^3$	Thermal
$^{238}\text{UO}_2$	—	—	—	$2.2 \cdot 10^3$	Thermal
H_2O	0.0128	0.457	0.0442	$2.2 \cdot 10^3$	Thermal
H_2O	0.0128	0.457	0.0442	$2.2 \cdot 10^3$	Thermal
D_2O	0.0360	28.2	0.582	$2.2 \cdot 10^3$	Thermal
Graphite	0.0338	22.7	0.506	$2.2 \cdot 10^3$	Thermal
Nominal FR Core	—	—	—	$7.58 \cdot 10^6$	Fast
Nominal FR Core	—	—	—	$1.96 \cdot 10^7$	Watt
Nominal FR Blanket	—	—	—	$7.58 \cdot 10^6$	Fast
Nominal FR Blanket	—	—	—	$1.96 \cdot 10^7$	Watt
Natural Iron metal	0.0322	19.5	0.458	$7.58 \cdot 10^6$	Fast
Natural Iron metal	0.0366	38.5	0.685	$1.96 \cdot 10^7$	Watt
^{235}U metal	0.0213	0.136	0.0311	$7.58 \cdot 10^6$	Fast
^{235}U metal	0.0271	0.156	0.0376	$1.96 \cdot 10^7$	Watt
^{238}U metal	0.0210	1.71	0.109	$7.58 \cdot 10^6$	Fast
^{238}U metal	0.0265	0.553	0.0699	$1.96 \cdot 10^7$	Watt

4.8 Non-leakage probability

Now we are interested to know the probability that a neutron born in a bounded volume is absorbed in that volume, rather than lost across its boundary. As it turns out, Gauss's theorem performs magic for us. Let us evaluate the rate of neutron loss, in neutrons/s, across the boundary of the system:

$$\begin{aligned} \int_A n\langle\vec{v}\rangle \cdot d\vec{A} &= \int_V \vec{\nabla} \cdot n\langle\vec{v}\rangle dV = \int_V -\vec{\nabla} \cdot D\vec{\nabla}\phi dV \\ &= \int_V DB_g^2 \phi dV = DB_g^2 \int_V \phi dV \end{aligned} \quad (4.69)$$

where A represents the surface area of the bounded volume, and V its volume. We have used the definition $B_g^2 \equiv -\nabla^2\phi/\phi$. Because B_g and D are assumed to be spatially uniform, each element of volume, on net, loses neutrons in proportion to its local value of ϕ , and the total neutron loss per second across the boundary can be evaluated quite simply using Gauss's theorem.

Conveniently, the local absorption rate is also proportional to the local neutron flux, ϕ , because we have assumed that the macroscopic cross-section for absorption is spatially uniform. So we can evaluate the total absorption rate, in neutrons/sec, very easily:

$$\int_V \overline{\Sigma_{abs}} \phi dV = \overline{\Sigma_{abs}} \int_V \phi dV \quad (4.70)$$

Thus the probability that a neutron is *not* lost across the boundary, and so is ultimately absorbed, the non-loss probability, is given by

$$P_{nl} = \frac{\text{neutrons absorbed/s}}{\text{neutrons absorbed/s} + \text{neutrons lost/s}} = \frac{\overline{\Sigma_{abs}}}{\overline{\Sigma_{abs}} + DB_g^2} \quad (4.71)$$

Now we use equation 4.35 to write $D = L^2\overline{\Sigma_{abs}}$ and we divide out $\overline{\Sigma_{abs}}$ from top and bottom, giving

$$P_{nl} = \frac{1}{1 + L^2 B_g^2} \quad (4.72)$$

for any reactor with homogeneous materials.

Returning to the steady-state one-speed neutron diffusion equation, equation 4.45, we can extract

$$0 = \frac{1}{\phi} \nabla^2 \phi + \frac{k_\infty - 1}{L^2} \quad (4.73)$$

from which we can see that for an infinite, homogeneous medium we require

$k_\infty = 1$, or criticality, to meet the requirement of time independence. For a bounded system, we can use the definition of B_g^2 (but not invoking B_m^2) to write

$$\begin{aligned} B_g^2 &= \frac{k_\infty - 1}{L^2} \\ 1 + L^2 B_g^2 &= k_\infty \\ \frac{k_\infty}{1 + L^2 B_g^2} &= 1 \end{aligned} \tag{4.74}$$

Thus we can define a k such that

$$k \equiv P_{nl} k_\infty = P_{nl} \epsilon p f \eta_T = 1 \tag{4.75}$$

is required for time independence, nicely consistent with our derivation of P_{nl} . This is Fermi's five-factor formula, taking into account spatial losses in the one-speed approximation. Sometimes $P_{nl} k_\infty$ is also denoted k_{eff} .

4.9 Spatial diffusion in thermal reactors

We just determined the effect of the boundary on a very simple one-speed diffusion model for a fission reactor. Let us consider now, one by one, the three energy regions that we discussed in the last chapter: Fast, Intermediate, and Thermal. We will see if we can improve those calculations by taking into account a finite medium.

The goal of our calculation in the Fast energy region was to evaluate ϵ , the fast fission multiplication factor, that enhances the number of number of neutrons slowing down into the Intermediate energy region, compared to those produced from thermal fission. This situation is far from diffusive, however, because slowing down out of this energy region due to collisions with the moderator is very rapid. Thus the one-speed diffusion model does not handle this energy region well in the case of thermal reactors. There will be some loss of Watt-spectrum fast neutrons from the edge of the reactor, but the fission rate is depressed at the edge compared with the volume average, so this is a small effect on what, after all, proved to be a small multiplication effect (for thermal reactors) in the first place. So we will neglect finite medium effects on ϵ .

The Intermediate energy region at first does not seem to be amenable to treatment by our one-speed model, since the neutrons are anything but mono-energetic. They are spread out over some six orders of magnitude in energy, or a factor of fourteen in lethargy. However we can take advantage

of the insight we have gained from the diffusion model to consider the loss of neutrons during slowing down.

During a differential time period, dt , neutrons slow down by an amount of energy

$$dt = dE \left(\frac{dE}{dt} \right)^{-1} \approx \frac{-dE}{v\xi\Sigma_e E} \quad (4.76)$$

where we have used Fermi's continuous slowing-down approximation, equation 3.28. Now during this time dt we expect the differential increment in the mean-square spreading of the neutrons in any direction, for example x , to be given by

$$\frac{d\langle(\Delta x)^2\rangle}{2} = D_{phys}dt = \frac{-\lambda_{tr}dE}{3\xi\Sigma_e E} \quad (4.77)$$

Integrating over the Intermediate range of energy traversed by neutrons, from 500 keV to 0.5 eV (so dE itself is negative), we have quite simply

$$\frac{\langle(\Delta x)^2\rangle}{2} = \int_{0.5\text{eV}}^{500\text{keV}} \frac{\lambda_{tr}}{3\xi\Sigma_e E} dE \approx \frac{\lambda_{tr}}{3\xi\Sigma_e} \ln 10^6 = 4.6 \frac{\lambda_{tr}}{\xi\Sigma_e} \equiv \tau_{Fermi} \quad (4.78)$$

where we have used the approximation of energy-independent cross-sections across the full energy range. This spreading, with dimension equal to length², is called the "Fermi Age," τ_{Fermi} . It is hard to find a logic for this nomenclature. It is Fermi's calculation – but why call it an "age"? In any event this spreading is analogous to L^2 . The time-dependence of the expected spreading in the one-speed diffusion equation, equation 4.28, is

$$\frac{\langle(\Delta x)^2\rangle}{2} = \frac{\sigma^2}{2} = D_{phys}t = \frac{D_{phys}}{\Sigma_{abs}v_n} = \frac{D}{\Sigma_{abs}} = L^2 \quad (4.79)$$

where we have identified t with the mean time to absorption. The analogy is that the neutrons in the Intermediate energy region are "lost" when they slow down to thermal energies.

With some trepidation, we can take the point of view that if a group of neutrons in the Intermediate energy region spreads spatially in any one dimension by a mean-square distance of τ_{Fermi} during slowing down, while a one-speed group of neutron spreads spatially in any one dimension by a mean-square distance of L^2 in the time it takes be absorbed, then the non-loss probability of neutrons traversing the Intermediate energy range should be given by

$$P_{I,nl} = \frac{1}{1 + \tau_{Fermi}B_{I,g}^2} \quad (4.80)$$

Note that this rough approximation is on top of the approximation of assuming continuous slowing down, even when collisions with hydrogen play the dominant role.

Finally we come to the thermal distribution, where our one-speed model is most reasonably applicable. Here we evaluate L using thermal cross-sections, to give

$$P_{T,nl} = \frac{1}{1 + L_T^2 B_{T,g}^2} \quad (4.81)$$

This gives a six-factor formula for criticality

$$k = P_{I,nl} P_{T,nl} \epsilon p f \eta_T = 1 \quad (4.82)$$

In the cases where $\tau_{Fermi} B_{I,g}^2$ and $L_T^2 B_{T,g}^2$ are both much less than unity, and the difference between the Intermediate and Thermal values for B_g is negligible, we multiple together $P_{I,nl} P_{T,nl}$ to get

$$P_{nl} = P_{I,nl} P_{T,nl} = \frac{1}{(1 + \tau_{Fermi} B_{I,g}^2)(1 + L_T^2 B_{T,g}^2)} \approx \frac{1}{1 + M^2 B_g^2} \quad (4.83)$$

where $M^2 = \tau_{Fermi} + L^2$. M in this context is called the “migration length.” This brings us back to the alliterative one-speed Fermi five-factor formula, equation 4.75, but with a different definition of P_{nl} , with M substituted for L . For our model light water reactor, $\tau_{Fermi} = abc$, $L = xyz$ and $M = lmn$.

It is interesting that while spatial loss is a minor correction to the neutron economy in a light water reactor, spatial diffusion is still very important; it governs the flux profile within the reactor. For spatially uniform material properties, the neutron sink at the edge results in a much lower total power production than would be obtained with a flat flux profile equal to the peak value.

4.10 Spatial diffusion in fast reactors

In Chapter 3 we developed a model for fast-spectrum reactors involving two energy regions. The higher region, characterized by a Watt spectrum, was analogous to the Fast region for thermal reactors, with neutron energy above about 0.5 MeV. However because of the weak moderation by the coolant in fast reactors, ϵ , the fast multiplication factor is much higher. The second region we called the Fast Reactor, *FR*, region, between about 100 and 500 keV.

We can marginally apply the diffusion model in the Fast region, because the elastic scattering cross-section is somewhat higher than the absorption

cross-sections in this region. Inelastic scattering is absorption in this picture, since it transfers neutrons to the lower, Fast Reactor, energy region. Radiative capture is very small. In this energy range, we can consider the fission cross-section to be a form of scattering, plus, of course, a source term. This gives us

4.11 Integrated numerical modeling

NEED to fill in the table in this section.

NEED to evaluate tau Fermi and L for a thermal reactor

NEED to figure out about whether we can do the solution inside a fuel rod.

Review

Resources

Exercises

- 4.1 show that the solution for momentum loss for finite-A is also consistent with just considering the average of the cos of the scattering angle in the lab frame
- 4.2 show that if you use equation 4.43 for the boundary condition in a slab reactor you get the same result for $\lambda_{tr} \ll x_0$.
- 4.3 Show that for a cuboid reactor, the highest k
- 4.4 Spherical reflector
- 4.5 Finite size reflector

Chapter 5

Safety

Neutrons can go wild.

5.1 The neutron “kinetic” equation

5.2 Including delayed neutrons

5.2.1 *Finding τ 's that solve the equation*

5.3 Consequences for reactor stability

5.4 Behavior over longer time scales

5.5 Chernobyl

5.6 Fukushima

5.7 Regulatory response

5.8 Effects of radiation on human health

5.9 Impacts of Chernobyl and Fukushima

Review

Resources

Exercises

5.1 Jumping jacks

5.2 Pushups

5.3 Running in place

Chapter 6

The Nuclear Fuel Cycle

Digging it up, burning it, and burying it.

6.1 Mining

6.2 Enrichment

6.3 Burnup

6.4 Interim storage

6.5 Geological repository

6.6 Reprocessing for thermal reactors

6.7 Fast reactors and reprocessing

Review

Resources

Exercises

6.1 Jumping jacks

6.2 Pushups

6.3 Running in place

Chapter 7

Nuclear Weapons and Nuclear Proliferation



I am become death, the destroyer of worlds.

J. Robert Oppenheimer at the Trinity test, 1945

7.1 How nuclear weapons work

7.2 History of nuclear proliferation

7.3 Proliferation risks going forward

7.4 Means to manage risks

Review

Resources

Exercises

7.1 Pushups

7.2 Running in place

7.3 General Groves, who managed the Manhattan Project, commissioned Princeton Professor Henry DeWolf Smyth to write a report about the basic principles employed in the construction of nuclear weapons. Stalin had the report translated and distributed to his nuclear scientists. Arguably, while it did not release details, it indicated which paths had been pursued in the Manhattan project, and which had succeeded. Much later, Edward Teller argued that ideas developed in the U.S. inevitably leaked to the Soviet Union within about six months. Remarkably, he used this to argue against hiding the basic ideas behind advances in nuclear weapons, while accelerating nuclear weapons R&D. There are websites that purport to discuss the science and technology of nuclear weapons. What do you think about secrecy in nuclear weapons development?

Chapter 8

Advanced Reactors

Trying to address the issues of safety, waste and nuclear proliferation.

8.1 Generation III and III+ reactors

8.2 Generation IV reactors

8.3 Thorium cycle

8.4 Breed and burn in Place

Review

Resources

Exercises

8.1 Jumping jacks

8.2 Pushups

8.3 Running in place

PART TWO

FUSION

Chapter 9

Power and Particle Balance

Need enough power and not too much helium.

9.1 Fusion reactions

9.2 Plasma heating

9.3 Heat loss

9.4 Energy gain!

9.5 Particle balance

Review

Resources

Exercises

9.1 Jumping jacks

9.2 Pushups

9.3 Running in place

Chapter 10

Particle Motion

Combining general drifts and torus. Should I do the polarization drift and correct radial acceleration?

10.1 Uniform electric and magnetic fields

10.2 Curved magnetic field

10.3 Perpendicular gradient in magnetic field strength

10.4 Parallel gradient in magnetic field strength

10.5 Drifts in toroidal magnetic field

10.6 Passing particle orbits

10.7 Trapped particle orbits

10.8 Bootstrap current

Review

Resources

Exercises

10.1 Jumping jacks

10.2 Pushups

10.3 Running in place

Chapter 11

Plasmas as Fluids

Reference neutron fluid derivation of diffusion.

11.1 Plasmas as fluids?

11.2 Equilibrium in a cylinder

11.3 Plasma control

11.4 Stellarators

11.5 2-fluid model and parallel force balance

Review

Resources

Exercises

11.1 Jumping jacks

11.2 Pushups

11.3 Running in place

Chapter 12

Macroscopic Stability

Should we dig a little deeper into Troyon scaling?

12.1 Ideal MHD stability

12.2 Interchange and ballooning modes

12.3 Kink modes

12.4 Plasma shaping

12.5 Stellarators

Review

Resources

Exercises

12.1 Jumping jacks

12.2 Pushups

12.3 Running in place

Chapter 13

Collisions and their Effects

Should we include ion-electron thermal equilibration? NRL formulary?

13.1 Coulomb collisions

13.2 Debye shielding

13.3 Small-angle scattering

13.4 Collisional cross-field transport

13.5 Other collisional effects

Review

Resources

Exercises

13.1 Jumping jacks

13.2 Pushups

13.3 Running in place

Chapter 14

Turbulent Transport

Need better intuitive derivation of drift waves.

14.1 Bohm and GyroBohm

14.2 Turbulence and flows – simulation

14.3 Turbulence and flows – measurement

14.4 Transport barriers

14.5 Global scaling

Review

Resources

Exercises

14.1 Jumping jacks

14.2 Pushups

14.3 Running in place

Chapter 15

Divertors, Scrape-off layers, and Plasma-Facing Components

Get into the vapor box?

15.1 Divertors

15.2 Scrape-off layers

15.3 Transient events

15.4 Plasma-facing components

Review

Resources

Exercises

15.1 Jumping jacks

15.2 Pushups

15.3 Running in place

Chapter 16

Neutron Interactive Materials, Blankets; Safety, Waste and Proliferation

Text to allow proper formatting.

16.1 Neutron interactive materials

16.2 Blanket designs

16.3 Safety

16.4 Waste

16.5 Nuclear proliferation

Review

Resources

Exercises

16.1 Jumping jacks

16.2 Pushups

16.3 Running in place

Chapter 17

Inertial Fusion Energy

17.1 Vision and status

17.2 Batch burn vs. hot-spot ignition

17.3 Drivers

17.4 Targets and chambers

Review

Resources

Exercises

17.1 Jumping jacks

17.2 Pushups

17.3 Running in place

Chapter 18

Power Plant Concepts, Development Path and Deployment

$$\begin{aligned} q_{\parallel} &= \kappa_e, \parallel \frac{dT_e}{d\ell}; \quad \frac{dq_{\parallel}}{d\ell} = n_e^2 c_z L_z \\ \frac{1}{2} \frac{dq_{\parallel}^2}{d\ell} &= n_e^2 T_e^2 F_z \kappa_0 T_e^{1/2} L_z \frac{dT_e}{d\ell} \\ q_{\parallel, det} &= n_{e, sep} T_{e, sep} \sqrt{2 \int_{T_{e, det}}^{T_{e, sep}} F_z \kappa_0 T_e^{1/2} L_z dT_e} \end{aligned} \quad eq.1$$

18.1 Power plant concepts

18.2 Development path

18.3 Deployment

Review

Resources

Exercises

18.1 Jumping jacks

18.2 Pushups

18.3 Running in place